Polymer electrolyte membrane fuel cell degradation in ships
Review of degradation mechanisms and research gaps

Broer, Annabel; Polinder, Henk; van Biert, Lindert

DOI
10.1016/j.jpowsour.2025.236678

Publication date
2025

Document Version
Final published version

Published in
Journal of Power Sources

Citation (APA)
Broer, A., Polinder, H., & van Biert, L. (2025). Polymer electrolyte membrane fuel cell degradation in ships: Review of degradation mechanisms and research gaps. *Journal of Power Sources*, *640*, Article 236678. https://doi.org/10.1016/j.jpowsour.2025.236678

Journal of Power Sources 640 (2025) 236678

Contents lists available at ScienceDirect

Journal of Power Sources

journal homepage: www.elsevier.com/locate/jpowsour

Review article

Polymer electrolyte membrane fuel cell degradation in ships — Review of degradation mechanisms and research gaps

Annabel Broer *, Henk Polinder, Lindert van Biert

Delft University of Technology, Mekelweg 2, Delft, 2628CD, Zuid-Holland, The Netherlands

GRAPHICAL ABSTRACT

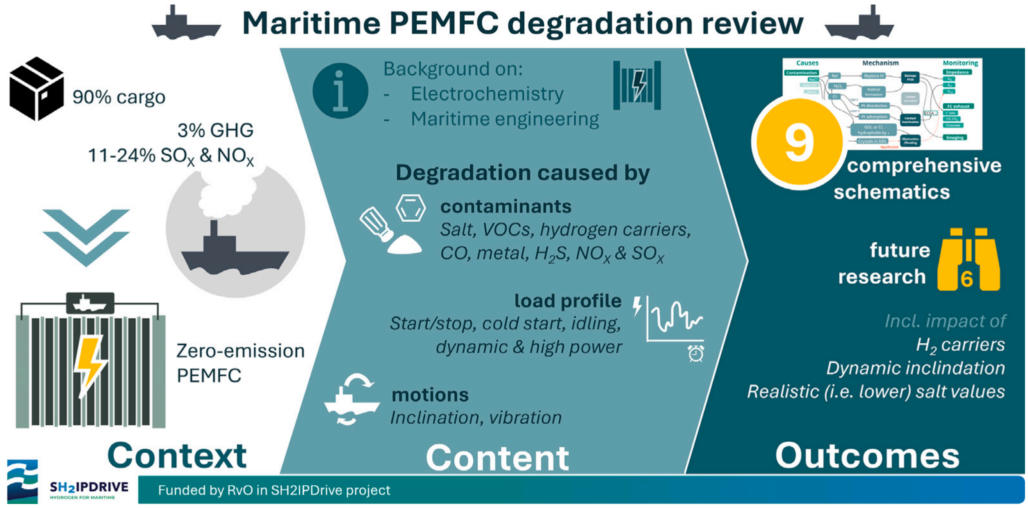

HIGHLIGHTS

- PEMFC degradation in the novel field of maritime environments.
- Maritime-specific stressors incl. load cycles, ship motions and coastal contaminants.
- Insightful schematic to foster insight into maritime degradation.
- Six knowledge gaps identified incl. air salinity and hydrogen carrier contamination.

ARTICLE INFO

Dataset link: https://doi.org/10.4121/c56334c8-31ae-43eb-9b74-e02805c20ed2

Keywords:
PEMFCs
Maritime degradation

ABSTRACT

Sustainability regulations urge the maritime sector to implement green technologies. The integration of polymer electrolyte membrane fuel cell (PEMFC) systems is a promising solution to cut emissions. However, their degradation in maritime environments is rarely addressed, while the environment differs significantly from land-based or automotive contexts and can greatly affect the type and extent of damage. Research in this field

---

* Corresponding author.
E-mail addresses: a.broer@tudelft.nl (A. Broer), h.polinder@tudelft.nl (H. Polinder), l.vanbiert@tudelft.nl (L. van Biert).
URLs: https://www.tudelft.nl/staff/a.broer/ (A. Broer), https://www.tudelft.nl/staff/h.polinder/ (H. Polinder), https://www.tudelft.nl/staff/l.vanbiert/ (L. van Biert).

https://doi.org/10.1016/j.jpowsour.2025.236678
Received 18 November 2024; Received in revised form 10 February 2025; Accepted 27 February 2025

Contamination
Air salinity
Load-based degradation
Ship motions
Schematics

is especially relevant as ships often operate in isolated areas and require durable and reliable power propulsion systems.

This work collects the insights from existing PEMFC durability research and analyzes degradation mechanisms specifically relevant for the maritime field. We consider air and fuel contamination, maritime load profiles, and vessel motions as potential causes. Insightful schematics summarize the content by linking these causes to damage indicators. Moreover, we identify various areas for further research including degradation from interconnected effects of maritime drive cycles, marine air salinity, hydrogen-carriers and their residues, long term maritime vibrations, and dynamic inclination.

The overview of existing literature combines insights from electrochemistry and maritime research while the knowledge gaps help to prioritize future research. Together, these elements promote collaboration in this multidisciplinary field, advancing mitigation strategies and improving cell, stack, and ship design and operation. Such improvements encourage PEMFCs application in ships and support the move towards zero-emission shipping.

Abbreviations

AFC	Alkaline fuel cell
AST	Accelerated stress test
BP	Bipolar plate
BoP	Balance of plant
CAPEX	Capital expenditure
CC	Current collector
CL	Catalyst layer
COR	Carbon oxidation reaction
CV	Cyclic Voltammetry
DOE	Department of Energy (USA)
ECSA	Electrochemical surface area
EIS	Electrochemical impedance spectroscopy
EoL	End of life
GDL	Gas diffusion layer
GHG	Greenhouse gas
HER	Hydrogen evolution reaction
HFO	Heavy fuel oil
HOR	Hydrogen oxidation reaction
IMO	International maritime organization
LEL	Lower explosion limit
LNG	Liquified natural gas
LOHC	Liquid organic hydrogen carrier
MCFC	Molton carbonate fuel cell
MDO	Marine diesel oil
MEA	Membrane electrode assembly
OCV	Open circuit voltage
OER	Oxygen evolution reaction
OPEX	Operational expenditures
ORR	Oxygen reduction reaction
PAFC	Phosphoric acid fuel cells
PEMFC	Polymer electrolyte fuel cell
PFSA	Perfluorosulfonic acid (membrane component)
RH	Relative humidity
SOFC	Solid oxide fuel cell
TPB	Triple phase boundary
VOC	Volatile organic compound

1. Introduction

The maritime industry is of vital importance to the global economy. About 90% of all international trade is carried on board of vessels and vessel transport is still expected to grow in the coming decades [1–3]. Unfortunately, the industry still relies heavily on fossil fuels such as marine diesel oil (MDO) and heavy fuel oil (HFO). As a consequence, 13.5% of all transport-related greenhouse gasses (GHGs) in Europe are released by the maritime sector. On a global scale, shipping is responsible for 3% of all anthropogenic GHG emissions [2,4]. These values are comparable to the emissions of the aviation industry. Moreover, the industry contributes to other forms of pollution: CO, particulate matter, volatile organic compounds (VOCs) and especially NOx and SOx. In Europe, 11% of all sulfur oxides and 19% of all nitrogen oxides can be traced back to domestic and international shipping [5].

In the light of these fact, both national and international governing bodies aim at reducing the impact of the maritime sector. The International Maritime Organization (IMO) adopted a new emission reduction strategy in July 2023, increasing their ambitions compared to the 2020 strategy [2]. They now aim to reduce the CO_2 emissions per transported cargo wit 40% by 2030 and to have net zero GHG emissions around 2050 [6]. Introduction of fuel cells running on green hydrogen can help to reach these goals.

1.1. Focus on PEMFCs

There are various types of FCs: polymer electrolyte membrane fuel cells (PEMFCs, also known as proton exchange membrane fuel cells.[1]); alkaline fuel cells (AFCs); molton carbonate fuel cells (MCFCs); phosphoric acid fuel cells (PAFCs); and solid oxide fuel cells (SOFCs) [8] All have their own challenges and advantages. For maritime applications, PEMFCs and SOFCs seem to be the most promising candidates [9,10, 10–12].

To limit the scope, this review focuses on PEMFCs. In the past decades, they have been studied more extensively compared to SOFCs, resulting in a higher maturity and commercial availability of the technology [9,12,13]. While the high temperature of SOFCs allows for heat recovery (and thus higher system efficiency) and fuel flexibility (besides H_2, they can also operate on liquid natural gas and methanol), it also means SOFCs are relatively slow in starting up, shutting down and responding to load changes. In contrast, PEMFCs operate at lower temperatures (generally 60-80 °Celsius), allowing for faster response on load changes and quicker start-ups. Moreover, PEMFCs have relatively high power density and decent energy efficiency [11,12,14]. The main issues for further (maritime) implementation include limited lifetime, the requirement for very pure H_2 and high costs for the materials, especially the platinum catalyst and membrane [15,16]. These problems are all rooted in durability issues. The PEMFC lifetime is directly linked to the overall degradation rate, the pure fuel feed is set as a standard

---

[1] All fuel cell types are categorized by their unique electrolyte material. For example phosphoric acid FCs or solid oxide FCs. Most texts state that PEM refers to “proton exchange membrane”, which could be confusing as the electrolyte in phosphoric acid FCs also transports protons. In this work we therefore stick to the definition of polymer electrolyte fuel cells to refer to low temperature fuel cells with PFSA membranes.[7]

to prevent contamination issues (see Section 3) and the Pt catalyst is needed because non-noble catalysts are unstable in the harsh corrosive environment of the cell [14,17]. Given the importance of durability, it is essential to improve our understanding PEMFCs degradation.

PEMFC durability has been subject of research for a couple of decades. Various reviews have analyzed degradation from a wide range of causes, including design choices, operation set points (such as temperature and humidification), load profile and contamination. Some publications focus on degradation of specific components, other consider degradation in the context of a specific application.

The application of PEMFCs in the maritime industry is yet to be considered. Up to now, they were mostly studied in automotive context, which differs significantly from the maritime environment. Durability is arguably even more important in ships, as they often operate in remote areas and thus need to be robust and reliable. Moreover, maritime load profiles vary more strongly and consist of more operational hours, at least in comparison to passenger cars. A review on maritime PEMFC degradation can help to shape and prioritize the required research.

1.2. Aim, method and structure

Various good degradation publications have been written, including [13,15,18–21]. In contrast to these previous reviews, this work focusses on maritime applications and aims to (i) provide a comprehensive overview PEMFC degradation causes relevant in a maritime context, (ii) identify the fundamental degradation mechanisms related to the different causes and (iii) point out research gaps in the field of maritime PEMFC degradation.

The initial literature database is selected with the Scopus search engine. We entered six different search terms: PEMFC, degradation, maritime, modeling, NaCl and inclination. Of each term, also synonyms, related terms and abbreviations were considered in the search. For example, the term PEMFC was entered as: *PEFC OR PEMFC OR "Polymer electrolyte membrane fuel cell" OR "Proton exchange membrane fuel cell" OR "PEM fuel cell"*.

Various different combinations of the terms were entered to obtain relevant publications. When Scopus returned more than 100 results, additional search criteria were added. These criteria were availability of the full paper; specifying the work needed to be a review; or only including publications from 2012 onward. In all cases, the list of literature was scanned, and based on the title and abstracts a final selection was made.

The selection process resulted in a literature database of 49 works. Additional references were added to place the original set of publications into context. The additions include studies cited in the original database, environmental reports, user manuals and conference proceedings.

First we provide some fundamental information on PEMFC design and its electrochemical processes (Section 2). In this chapter we also show how scaling up from individual cells to stacks brings additional challenges (Section 2.5). The three following chapters elaborate on how contamination, load profile and PEMFC movement cause damage (Sections 3–5). Thermal stress is included in the sections on load-related stress: cold-starts (Section 4.5) and dynamic loads Section 4.6. More fundamental reflection on thermal resistance of PEMFC materials is beyond the scope of this review, but can be found in other publications such as Wu et al. [21]. Sections 3–5 are all concluded with schematic overviews that link the causes, via their respective degradation mechanisms, to specific degradation indicators. Section 6 summarizes the insights that these schematics give, if considered all together. Finally, Section 7 concludes on the most important degradation mechanisms for maritime PEMFCs and highlights several knowledge gaps that require further research.

2. Background — PEM fuel cell characteristics

This review aims to attract both scientists in the field of fuel cell research and maritime engineers. The objective of this section is to provide a comprehensive background for readers that are not acquainted with electrochemistry or the maritime field. Such a section is essential to improve the readability of a multi-disciplinary review such as this one. Later sections (Section 3 to 5) will use the concepts and techniques discussed here, addressing:

1. PEMFC components (Section 2.1);
2. The essential electrochemical reactions (Section 2.2);
3. How performance losses can be monitored (Section 2.3);
4. Trade-offs between performance and durability (Section 2.4);
5. Scaling up from cells to stacks (Section 2.5); and
6. Stress testing, reversibility and PEMFC lifetime (Section 2.6)

Of these sub-sections, the first three are focused on basic electrochemistry, while the latter three define various important concepts and when applicable, specify them for maritime applications.

2.1. PEMFC components

A schematic overview of a fuel cell is shown in the supplementary information, fig. A.1. The polymer electrolyte membrane (PEM), i.e. the (solid) electrolyte, is located in the center of the cell [22]. It consists of hydrophobic perfluorinated back-bones and hydrophilic sulfonated side-chains [14] that facilitate the proton transport. Most PEMFCs use Nafion™, a perfluorosulfonic acid (PFSA) based membrane, for its adequate stability and good proton conductivity [14].

The membrane is flanked by an anodic and cathodic catalyst layer (CL). They are referred to as electrodes, as the electrochemical reactions occur here [23]. Together with the membrane, the cathodic and anodic CL form the membrane electrode assembly (MEA). Each CL contains catalyst particles, a catalyst support and ionomer [22]. The ionomer (usually Nafion™) gives structural support and facilitates proton transport towards and from the membrane. The catalyst particles are essential in facilitating the chemical reaction at moderate temperatures (usually $< 80\,^{\circ}$Celsius) [14]. Platinum (Pt) is the conventional catalyst material for PEMFCs, both for the anode and cathode. Yet the cathode often has a higher loading of Pt, as the oxygen reduction reaction (ORR) is the rate limiting reaction [17,23,24]. The catalysts in the CL are often mounted on top of carbon, the catalyst support, to increase electrochemical surface area (ECSA).

A subset of PEMFC research is dedicated to increase the ECSA, while retaining a stable catalyst layer. Scientists also develop catalysts other than Pt. They aim to reduce costs, improve catalyst activity or increase material availability while the material still has sufficient stability in the harsh acidic PEMFC environment [14,25].

Reactants and products are transported to and from the CLs via the pores in the gas diffusion layer (GDL, also known as (gas) diffusion media), while electrons can exchange via its solid strands. Carbon-based materials are often used, although metal GDLs are also available. The latter can be thinner than carbon GDLs, while carbon is more corrosion resistant [14,23,26]. The GDL is often covered with a hydrophobic layer such as PTFE (poly(tetrafluoroethylene) to reduce the risk of water blocking the pores.

The current collectors (CC, also referred to as flow plates) serve three main functions: conducting electrons to the external circuit, transporting reactants and products to and from the cell and providing structural support [27]. The layout of the flow-field impacts cell performance significantly. Several designs have been developed, including pin-type, straight and serpentine, all aiming to distribute the reactants evenly over the cell. The regions directly facing the flow fields are called channel regions while the regions under to the ribs of the flow field are referred to as land regions. Finally, the cell is enclosed with two end plates, which compress the stack together and distribute the pressure.

If the cell is part of a stack, the flow plates are referred to as bipolar plates (BPs) as it has both an anodic and cathodic ‘pole’. Heat management becomes more important in stacks, as each cell releases heat. Therefore, cooling liquid channels are often added to the BPs to keep the stacks at a desired temperature. Section 2.5 will elaborate further on the challenges of scaling up from single cells to cell stacks.

In commercial applications, the stacks are integrated in a lager PEMFC system. The additional components, referred to as the balance of plant (BoP), ensure that the stacks can operate smoothly. Components include humidifiers, condensers, fuel re-circulation, cooling system and various sensors. These make sure that the reactants are supplied conditions while the exhausts are taken out in the right way (e.g. by taking out condensation water to prevent system flooding). The size of the system as a whole is significantly larger than the stack [28]. Especially for ships that have both high robustness requirements and limited space, BoP engineers should strike a balance between making it elaborate enough to promote durability while limiting the sizing to keep a decent system energy density.

2.2. Chemistry

As mentioned in Section 2.1, the chemical reactions occur in the CL. More specifically, they occur at the triple phase boundary (TPB) where the ionomer, catalyst surface and void space for reactant and product transport meet. Hydrogen enters at the anode side of the cell and passes through the GDL to the CL. The catalyst particles enable the hydrogen oxidation reaction (HOR, Eq. (1)). The electrons are conducted through the solid part of the GDL towards the current collector and the external circuit. Simultaneously, the produced protons move through the PEM towards the cathode in the form of H_3O^+ as shown in Eq. (2) [29]. This process, in which the protons drag water molecules from the anode to the cathode, is called electro-osmosis [15,30]. At the cathode the protons combine with the electrons and oxygen in the oxygen reduction reaction (ORR, Eq. (3)). Water is formed, which will exit the cell through the cathode outlet. The chemical reactions, including the overall reaction (Eq. (4)) are therefore

$$2\,H_2 \longrightarrow 4\,H^+ + 4\,e^-, \tag{1}$$

$$4\,H^+ + 4\,H_2O(\mathrm{an}) \longrightarrow 4\,H_3O^+(\mathrm{mem}) \longrightarrow 4\,H^+ + 4\,H_2O(\mathrm{cath}), \tag{2}$$

$$4\,H^+ + 4\,e^- + O_2 \longrightarrow 2\,H_2O, \tag{3}$$

$$2\,H_2 + O_2 \longrightarrow 2\,H_2O. \tag{4}$$

2.3. Monitoring performance losses

Cyclic voltammetry (CV), polarization curves, power curves, and electrochemical impedance spectroscopy (EIS) are standard electrochemical analysis techniques to monitor PEMFC performance [23]. All four will be discussed below in more detail.

Cyclyc voltammetry can be used to characterize the catalyst layer. For instance, scholars apply it to quantify the ECSA and monitor platinum oxidation [31,32]. Because the ORR is the rate limiting reaction, it is often applied to analyze the cathode [31–33]. The typical data plot (cyclic voltammogram) is obtained by sweeping the potential at a constant rate up (the forward scan) and down again (the backward scan) while recording the current [33,34]. The distinctive peaks in the plot represent adsorption and desorption of electrochemically active species (such as protons) or the reduction and oxidation of e.g. platinum. Scientists can monitor the height of the peaks and the potentials at which they occur to draw conclusions about the electrode reactions.

Polarization curves plot the cell potential versus current density (see Fig. 1). Current is normalized to the geometric area of the MEA ($\mathrm{mA\,cm^{-2}}$), so that different cells and stacks can be compared to one another. Various losses are visible in the plot. Phase I in Fig. 1 shows the first and unavoidable voltage drop from the theoretical open circuit voltage (OCV, which is 1.2 V at standard conditions) to the measured OCV (about 1.0 V at standard conditions). This drop results from H_2 crossover and simultaneous side reactions such as platinum surface oxidation [22]. In the second phase, at low current densities, activation losses are prominent. These relate to the speed at which electrochemical reactions can occur and are minimized using effective catalysts. The third phase is associated with ohmic losses, which arise from resistance against ionic current through the ionomer and membrane as well as electronic current through the GDL, CC and outer circuit. In this region, voltage loss is often near-linear [28]. Finally, at high current densities (phase IV in Fig. 1) mass transfer resistance becomes significant. Here, the reaction products cannot cross the GDL to the reaction sites quick enough to keep up with the high demand [23].

The power density, represented by the orange line in Fig. 1, can be generated by multiplying the current density and cell potential. The power density steadily goes up when the current increases. However, at some point the increase in current density does not outweigh the increase in the combined resistances, resulting in a power output drop. Therefore the maximum power is not achieved when the maximum current is applied, but rather at an intermediate current density as shown in the orange curve of Fig. 1.

When the cell ages, the path of the polarization curve and power curve will change. The cell potential at a specific current density will lower, and the maximum power also reduces and peaks at an earlier current density. Polarization curves are used in many experimental studies to access the performance of the PEMFC, for instance in the contamination review by Cheng et al. [18] where various curves are plotted to show the impact of different contaminants. However, polarization curves fail to differentiate between loss-inducing processes that occur simultaneously in the PEMFC [23]. In order to distinguish those, impedance measurements are often applied.

EIS is a non-invasive, in-situ analytical technique to measure the impedance of a system. For an EIS measurement, a small mono-frequency sinusoidal voltage (in potentiostatic mode) or current (in galvanostatic mode) is applied to the system. The resulting output, current or voltage respectively, is measured. A phase difference between the voltage and current arises — that is, the current wave is not synchronized with the voltage wave. The deviation between the curves is represented by the phase angle. For a full EIS analysis, measurement of the phase angle and resulting current or voltage are repeated at different perturbation frequencies. Because the PEMFC processes have different time constants, the full EIS measurement can deconvolute processes that occur simultaneously [23]. Fast processes such as charge transfer can be studied at the high frequencies while slow ones, such as mass transport, appear at low frequencies. To interpret the EIS data, equivalent electrical circuits are used. These circuits are simplified models of the more complex electrochemical cell. The appropriate selection of the circuit elements is a research field on its own, and will not be discussed in detail here as it is beyond the scope of this work. When an applicable circuit is chosen, it can help to quantify the activation, ohmic and mass transfer losses.

In Sections 3–5 we refer to the three main losses: charge transfer (R_{ct} also known as activation losses), ohmic (R_{Ω}) and mass transfer (R_{mt}). Yet, due to the interdisciplinary nature of fuel cell research, various other terms are used for these main losses as well [28]. Within this review, the following terms are considered equivalent:

1. Activation losses, relating to the charge transfer at the catalyst sites, are to charge transfer losses or charge transfer resistance [23,35,36] and activation overvoltage or overpotential [23,37];
2. Ohmic losses represent the ionic resistance (proton transport through the ionomer and membrane), electronic resistance (both in the CL, GDL and external circuit) and contact resistance. They are also known as electric resistance [23], electrolyte resistance ([38]), ohmic overpotential [39], and internal resistance [40];

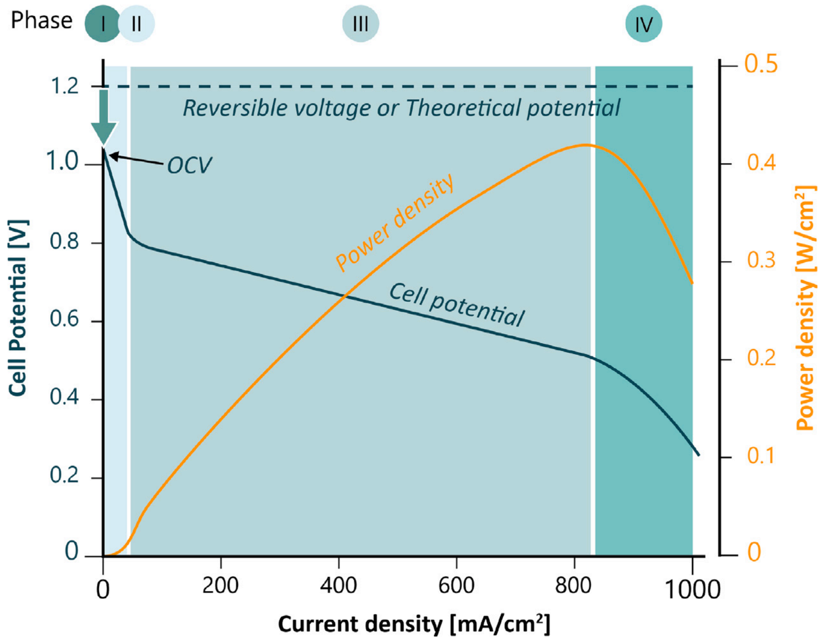

Fig. 1. Schematic representation of the polarization curve of a PEMFC (dark blue, left y-axis) and the generated power density (orange — right y-axis). The reversible voltage or theoretical potential is also shown in dark blue. The shaded areas indicate various phases in which a specific type of polarization losses is dominant: OCV drop (I), activation losses (II), ohmic losses (III) and mass transfer losses (IV). Image based on figure 3.1 in the book by Larminie and Dicks [28] and figure 1.27 and 1.28 from [23].

3. Mass transfer losses relate to the transport of reactants to, and products away from the reaction site. These losses are also referred to as concentration overvoltage [37] and mass transport overpotential or resistance [39]

Finally, in the work by Lee et al. [41] the activation losses and mass transfer losses are grouped as polarization resistance. Polarization is also used as general term for drawing current or to refer to the difference between the theoretical and measured OCV [28]. It is clear that close attention is needed to avoid mixing up terms when reading PEMFC literature.

2.4. Balancing durability, performance and costs

The PEMFC materials and the operational conditions have a strong impact on its performance, durability and costs. There are often trade-offs within parameters such as the choice of material (1), reactant stoichiometry (2), membrane thickness (3), cell temperature (4), reactant humidification (5), operational set-points (6), and system design (7). The choices are often already made in the design phase of a system, and each PEMFC supplier strives to find a good balance for their specific fuel cell. It is however good to note that all these choices affect the durability of the cell.

(1) Material choice: On the one hand, material costs should be reduced while the quality of the materials should still be of sufficient quality to meet durability standards. The PEMFC materials are exposed to harsh conditions due to the acidic environment and potential differences between the two electrodes. Therefore, they need to be sufficiently corrosion resistant. This is one of the reasons why platinum is still the default catalyst material even though it is a costly and rare metal [14,15]. Another important reason to opt for Pt-catalysts is the high catalytic activity of Pt and Pt-based catalysts [14,22]. Beside the catalyst, also the GDL and BP materials should be corrosion resistant. PEMFC manufacturers consider metal bipolar plates as they are easier to mass-produce. The metal BPs can also be thinner than graphite ones, resulting in a lower ohmic resistance and a higher power output [15]. However, metal bipolar plates corrode more easily and contribute to the formation of radical species which reduces the cell lifetime [42]. Section 3.6 describes the radical formation process in more detail.

(3) Membrane thickness: The thickness of the PEM membrane should be carefully chosen. Just like for the BPs, a thinner membrane results in a lower ohmic resistance because the protons have to be transported over a shorter distance. In addition, thin membranes help to reduce flooding risk. While water is transported from anode to cathode via electro-osmotic drag (as discussed in Section 2.2), back-transport is easier in a thinner membrane [15]. Yet, these are also more prone to damage such as chemical degradation and mechanically caused defects. Additionally, a thinner membrane allows for more gas crossover. This is in itself again worsens degradation due to heat release from H_2 combustion and increase in chemical degradation [43].

(4) Temperature: PEMFCs are operated between 60 °Celsius and 80 °Celsius [42]. When choosing the operational temperature, one should consider that higher temperatures speed up the red-ox reactions at the cathode. The activation energy is lower, resulting in a lower overall charge transfer resistance. Yet, at higher temperatures, more water is turned into vapor. The vaporization is partially compensated by the cathodic H_2O formation, but especially towards 80 °Celsius, membrane dehydration occurs. This compromises proton transport as the membrane needs to contain liquid water for the formation of H_3O^+ ions [29,30]. As a result, the ohmic resistance increases and the cell performance drops.

(5) Reactant humidification: To counteract membrane drying, the fuel and air stream are humidified. When selecting the relative humidity (RH) of the gasses one must strike an intricate balance between membrane drying and flooding of the (cathode) catalyst layer. When the relative humidity is too high, towards 100%, liquid water accumulates in the CL, GDL and flow channels. This impedes the transport of reactants towards the catalyst surface and lowers the output voltage. On the other hand, when the relative humidity is too low, the membrane will dry out [15,44]. The operational pressure is also an important factor. At higher pressures, the air can contain less water and thus the risk of membrane drying increases.

(6) Operational set-point: The current or voltage set-point dictates if the cell is operated towards high efficiency or maximum power. From the polarization curve (Fig. 1) one can see that the voltage losses increase with the current density [15,28]. When one aims to have a high energy efficiency, i.e. convert most of the chemical energy stored in the H_2 molecules, the cell should be operated at low current densities. Yet, the maximum power of the cell is delivered when the cell operates at high current densities. In practice, ship designers have to ensure that the vessel's maximum power requirements fall safely within the margins of the power plant (including other power sources such as engines and batteries). Due to the great variety in ships, balancing the trade-off between efficiency and maximum power will be different for each vessel. Section 4 will explore the power demands of vessels and how they impact PEMFC degradation in more detail.

(7) System design: A more elaborate BoP can help to keep the operational conditions within a narrow bandwidth which allows for a longer PEMFC lifetime. However, more elaborate BoPs also often require more space and power, lowering the volumetric power density. For instance, when applying PEMFCs in drones, durability is a major issue because the BoP needs to be kept to the bare minimum to allow the vehicle to fly [45]. In other applications, system engineers also clearly strike a balance between durability and practical use. In stationary PEMFC heat and power plants the BoP takes up the majority of the volume. In more compact automotive PEMFC systems, it still takes up over half the space [28].

2.5. Stack testing

Most PEMFC research centers around single fuel cells rather than cell stacks. This lowers material costs and reduces complexity of the experiments. However, when PEMFCs are applied for power generation, for instance in a ship, requirements are significantly higher than what a single cell can deliver. To accomplish this the cells are combined into a stack. This adds additional durability challenges, beside the mechanisms that will be addressed in Sections 3–5.

The thermal management differs considerably between single cells and stacks. Even though the chemical reactions are exothermic, they do not provide sufficient heat to bring single cells to the desired temperature (usually between 65 and 80°C [42]). Experimental single cells therefore require a heating system. In contrast, industrial applications such as the ones required for maritime PEMFC applications require cooling. Smaller systems $<2\,\mathrm{kW}$ can still use air cooling, while higher power systems require a liquid cooling systems [28,46]. Liquid cooling systems allow for a more stable temperature profile along the stack and require less space [28].

As mentioned in Section 2.1, cells are generally mounted in series, separated by bipolar plates. That is, the electronic flow is in series, causing the same current to pass from the first to the final cell of the stack. The reactant and coolant flow are, however, in parallel. When these media flow in the same direction as the current it is said to be a concurrent flow (or parallel flow), in contrast to the counter current flow where the media and current flow in opposite directions. In some cases, the stack is designed with a dead end anode to increase fuel utilization [47]. These could be more suitable for small, air cooled power systems ($<2\,\mathrm{kW}$) [48].

Regardless the exact flow type, small differences in reactant and coolant flow will arise along the stack. Because of this, and because of slight variations in operational conditions from cell to cell, no cell in the stack has exactly the same voltage even though they carry the same current [42]. Degradation will therefore also be different for every cell, and might be worse in individual cells due to positive feedback loops while others are still fine. This is an issue because the lifetime of the stack is determined by the weakest cell rather than the average degradation of all cells combined [42,49,50]. The following experimental studies have tested degradation on stack level and show how degradation can differ between cells.

Lamard et al. [51] conducted part of their NaCl contamination experiments on short stacks. In the two experiments they conducted, cell failure was caused by one or two out of the five cells. The authors did not comment on the significance of the cell location in relation to the cell failure. Yet, they observed a significant increase in the mass transfer resistance and found corrosion marks on the MEA and BP in the post-mortem analysis.

Pei et al. [52] showed that degradation was non-homogeneously distributed over the 100 cells in their stack. After a 500-h load-based degradation test, the first fourteen cells of the stack degraded significantly more than the cells further along the stack. The average voltage and OCV dropped while the internal resistance increased. The worst cell had an OCV of 0.7 V (in contrast to 0.96 V of the best performing cell) and with a value of 200 mA/cm2 the maximum current was one sixth compared to the best cell. In addition, catalyst particles agglomerated resulting in a twofold increase in the average particle diameter. Degradation varied not only between cells, but also within individual cells. It was especially strong near the air-outlet, followed by the H_2-outlet while the region near the H_2-inlet was least affected. The latter is in line with segmented single cell studies, such as conducted by Reshetenko [53], where data showed that in an air contamination test, the cell inlet was more affected than the outlet.

Similar to Pei et al. [52], Hou et al. [49] noticed the cells in front of the stack degraded faster than the ones near the end. A stack of 90 cells was tested in their $150\,\mathrm{h}$ vibration experiment. The most probable reason for the front-end degradation distinction was the lack of shock absorption in the front, whereas a rubber cushion was located between the last current collector and the end plate. These experiments highlight the importance of proper stack design and cell-to-cell testing.

2.6. Stress testing, reversibility and lifetime

Accellerated stress test

As it would be costly and time-consuming to test new cell designs or concepts for thousands of hours, researchers often apply accelerated stress tests (ASTs, also known as accelerated degradation tests, accelerated durability test or accelerated lifetime test). Here, the stressor is increased significantly to bring about signs of degradation in a shorter time frame. For instance, the experiments by Pei et al. [52] cycled the load from idling, to dynamic, to high power and to start stop quickly instead of simulating these loads at the actual duration they would last in an automotive use-case. Other ways to create more harsh conditions are increasing the contamination concentration or the amplitude and frequency of vibrations [54,55]. The data generated from an AST can be extrapolated to estimate the system lifetime in practice.

Reversibility

Some forms of degradation are reversible while in other cases the performance loss cannot be recovered. The reversibility of degradation highly depends on the mechanism. For instance, adsorption of a chemical on the catalyst surface can often be reversed with appropriate recovery procedures such as removing the contaminant [56]. Oxidation of platinum catalysts or GDL flooding are other examples of reversible performance loss [19]. Yet, when the structure of the PEMFC components is damaged, for instance due to volume cycling caused by dynamic load profiles [57], degradation is often lasting.

Lifetime

Both the application context and the end of life (EoL) definition are important to determine the total lifetime of a system. When operated in steady state PEMFCs can already last thousands of hours [13,58]. Yet, when the load is varied and/or when other harmful conditions apply, the lifetime reduces. The impact of those conditions will be addressed in detail in Sections 3–5. In 2022, the Department of Energy (DOE) of the USA set a 8000 h durability target for FC electric vehicles [59]. While there are no generally accepted lifetime targets for maritime PEMFCs, it is reasonable to expect these to be higher as ships compared to passenger cars. Ships are operated for longer durations and, depending on their mission, might need to be robust and reliable in isolated areas.

The boundary conditions for when a system considered dysfunctional are referred to as the EoL criteria. In other words, the boundaries of the “operating window” where the fuel cell is stably operated [15]. Most PEMFC experiments use a 10% reduction of the cell voltage at rated current (i.e. 10% reduction in rated power) as their EoL criterion. This metric is prescribed by the DOE of the USA for automotive applications, yet it is used in many other fields of research [59–62]. Yet, this EoL criteria is quite arbitrary, as the FCs still provide power at the EoL point. Instead, the EoL criteria should be based on a more holistic consideration of the use case and safety aspects. The use case consideration strongly connect to cost optimization of the capital expenditures (CAPEX, buying or replacing the fuel cell system), operational expenditures (OPEX, fuel costs) and (loss of) revenue. The more a PEMFC system ages, the lower the power output at any current density set point. Overall efficiency also drops, not only due to the lower electrochemical efficiency, but also because BoP components require more energy in a degraded system (e.g. fuel cell cooling demand is proportional to internal resistances [63]). Ship designers have to balance between two extremes:

- Oversize the system, ensuring it can provide sufficient power even in a far degraded state — more time passes before system needs replacement, higher OPEX (system becomes less efficient), more loss of revenue (more deck space needed for system and fuel).
- Keep the system small, reach EoL in shorter duration — system replacement needed within shorter time period, lower OPEX (system runs more efficiently), less loss of revenue (less deck space required for system and fuel).

Even though most experimental work sticks to the 10% rated power reduction target, some degradation studies have defined their own cut off values. For instance Benesch and Jacksier [64], who stopped testing after voltages dropped below 0.3 V (> 50% of the initial voltage). Other scholars went beyond using voltage to determine EoL. For instance, Cleghorn et al. [58] based it on H_2 crossover which they monitored via sensors. Even though the authors state that the cut off at a H_2-crossover current density of $10\,\mathrm{mA\,cm^{-2}}$ to $15\,\mathrm{mA\,cm^{-2}}$ is an arbitrary value, such an EoL boundary does relate more strongly to safety than using the cell voltage or power as a reference.

All in all, the varieties in the use and environmental factors and the lack of a maritime EoL definition, make it challenging to give an exact definition of fuel cell lifetime in a maritime application. It is beyond the scope this review to determine more specific EoL criteria. Instead this review will address the impact of fuel and air contamination (Section 3), applied load profile (Section 4), and inclination and vibration of the PEMFC (Section 5) in the following sections.

3. Contamination

3.1. Maritime contaminants in air and fuel

Contamination or poisoning is the infiltration and counterproductive binding or reacting of unwanted species. The impurities can enter via the anode (fuel) or cathode (air or oxygen) inlets. Table 1 indicates which contaminants will be considered relevant for PEMFCs in ships, as elaborated on below. Note that metal impurities, VOCs and H_2S will be considered for both anode and cathode. Various great resources such as Borup et al. [13],Madhav et al. [65],Li et al. [66] give a more detailed insight in contamination. The aim of this section is to cluster the maritime relevant contaminants and give an overview of mechanisms involved. Furthermore, the sub-sections are grouped by shared contamination mechanism, rather than entry side.

Table 1
Maritime contaminant origins and entry side.

Contaminant	Side	Maritime origin
CO, CO_2	Anode (fuel)	On-board reforming of hydrocarbons
NOx, SOx	Cathode (air)	Marine exhaust gasses
H_2S	Anode (fuel) Cathode (air)	On-board reforming of crude oil/LNG Sea-bed disruption during dredging
VOCs	Anode (fuel) Cathode (air)	On-board reforming of hydrocarbon fuels Fossil fuel storage and combustion Specific solvents, warefare chemicals (navy)
Salt (ions)	Cathode (air)	Sea air (for sea going vessels)
H_2 carriers	Anode (fuel)	On-board reforming/de-hydrogenation
Metal (ions)	Anode (fuel) Cathode (air)	Metal system components

Air impurities

On board of a ship, unfiltered engine room air may contain exhaust gasses, volatile organic compounds (VOCs) and – especially important for (short) sea and international shipping – salt particles originating from saline waters. The maritime industry emits significant amounts of sulfur compounds and nitrogen oxides (NOx). Data gathered in 2018 and 2019 for the European Environmental Agency shows that inland and international shipping combined is responsible for 11 to 24% of European NOx and sulfur oxide (SOx) pollution [4,5]. Shipping routes can even be visualized through tracking e.g. NOx emissions with models or satellites [67]. Besides these oxides, hydrogen sulfide (H_2S) is present in significant concentrations at dredging sites. The gas is generated from anaerobic decomposition of organic material, and it accumulates in within the sea bed [68]. As dredging vessels disturb the sea-bed, stored H_2S is released in the atmosphere.

As for VOCs, only a few have to be considered for maritime PEMFCs. VOCs carbon-based molecules that are volatile at standard atmospheric temperatures and pressures. Because it is a broad group, and because the concentration strongly depends on the distance from the source, they are not always included in PEMFC contamination reviews [18,69]. Nevertheless, benzene, toluene ($C_6H_5CH_3$) and naphthalene ($C_{10}H_8$) can all be harmful to PEMFCs [65,70–72]. They originate from various sources, including fossil fuels through sublimination or their combustion. The former might raise VOC concentrations in engine rooms where traditional ICEs are combined with PEMFCs in the transition period towards sustainable sailing. Other studies show that various battlefield contaminants such as cyanogen chloride CNCl and hydrogen cyanide (HCN) can have devastating effects on fuel cells, although it is highly unlikely that a vessel would encounter these chemicals [66,73].

Considering the last two paragraphs, ship environments at standard sailing routes, and even more so around (industrialized) harbors and during dredging operations, contain various PEMFC contaminants. Surprisingly, there is no publicly available database on the composition and concentration of contaminants inside engine rooms. Our upcoming research will address this knowledge gap [74], to access which of the impurities reach harmful concentrations. In absence of such data, the following sections aim to provide insights into the mechanisms and harmful concentrations of the maritime-relevant air contaminants. Carbon oxides (CO and CO_2), nitrogen oxides and sulfur compounds are analyzed in Section 3.2, VOCs in Section 3.3 and salts in Section 3.4. Because the latter has only be studied to a limited extent, and is of specific interest to maritime applications, Section 3.4 quite thoroughly examines existing studies to discover which direction further research should go.

It should be noted that air filters can reduce contamination risks. Still, filter installment leads to a larger, less efficient and more complex system. The systems can be bulky and expensive, components need to be replaced periodically and pump energy demand will increase to overcome the pressure drop over the filter [75,76]. More importantly, it would not fully resolve contamination issues. Contaminants can still remain because filters only clear the air to a certain threshold and cleaning systems can fail and contaminants [42]. Therefore, even if filters are applied, these should be selected with care ensuring the right contaminants are filtered out to a sufficient extent.

Fuel impurities

It is still undecided how hydrogen will be stored on board of vessels. On the one hand PEMFC companies prescribe the use of very pure hydrogen (e.g. 99.99% or higher percentages of H_2) to reduce contamination risks [77,78]. On the other, ships require fuels with a sufficiently high volumetric and gravimetric energy density, limiting the volume and weight of the H_2-based power plant. When storing hydrogen in a material based way, the molecules are captured within a material or chemically bound to a different molecule [79]. Various hydrogen carriers can reach energy densities significantly higher than using the current standard of (cryo)compressing. Van Rheenen et al. [79] assessed hydrogen storage techniques for maritime applications, based on their energy density, technology readiness level (TRL), safety, recyclability and dehydrogenation process. They concluded that liquid organic hydrogen carriers (LOHCs) and borohydrides are the most interesting for marine applications. Specifically sodium borohydride ($NaBH_4$), dibenzyl toluene ($C_{21}H_{20}$) and ammonia borane (H_3NBH_3) seem to be promising. Both $NaBH_4$ and H_3NBH_3 have the advantage that in hydrogen release reactions, not only the H_2 bound to the molecule is released, but also the hydrogen from the water that is required for the reaction. The authors did not recommend ammonia itself (NH_3) for safety reasons, nor methanol (CH_3OH) and formic acid (HCOOH) as these are not zero-emission fuels. Nonetheless, these fuels will be addressed in this review as they are frequently mentioned as low-carbon fuels [3,80–85]. The 2023 UN report by Sirimanne [3] states that methanol is attractive because of its relatively high technology readiness level while ammonia can be interesting as it is expected to have the lowest total cost of operation between zero-emission (well-to-wake) fuels.

Hydrogen carriers also introduce contamination risks. Non-H_2 components could end up in the PEMFC, including the carrier molecule itself, by-products or the spent fuel (chemical product that remains after hydrogen is extracted). Unfortunately, to the best of our knowledge, there is no literature available on the impact of sodium borohydride or dibenzyl toluene on PEMFC durability. As these carriers could become important for green shipping in the future it is an interesting field to explore. Nonetheless, Section 3.5 describes degradation mechanisms from NH_3 (aside from being a fuel also a by-product from ammonia borane), methanol and formic acid. When reforming hydrocarbon fuels such as liquified natural gas (LNG) or methanol, the product stream (i.e. the reformat) also contains CO_2, CO, H_2S and VOCs [13,18,65,86]. Their contamination mechanisms will be addressed in Sections 3.2 and 3.3.

Metal ions, recovery and schematics

This contamination section ends with metal impurities (Section 3.6), recovery procedures (Section 3.7) and lastly schematic overviews of the relation between contaminants, degradation mechanisms and monitoring (Section 3.8). While metal ion contamination is not necessarily a specific risk for maritime PEMFCs, it is included in this review. Also in marine PEMFC systems, metal impurities could originate from metallic system components such as BPs piping. Especially as demineralized water is often used for humidification and possibly as coolant, which also promotes corrosion [15]. The chemical degradation pathways promoted by metal ions occur in other degradation pathways too (e.g. NaCl degradation, idle operation), showing the overlap between various mechanisms.

3.2. Carbon oxides, nitrogen oxides and sulfur compounds

CO and CO_2

CO and CO_2 contamination studies generally pollute the system via the fuel rather than the air inlet. CO_2 is an indirect contaminant. It can prevent H_2 from reaching the catalyst sites and, more importantly, it can convert to CO via the electrochemical CO_2 reduction [66,87]

$$2\,Pt + H_2 \longrightarrow 2\,Pt{-}H_{ads}, \tag{5}$$

$$CO_2 + 2\,Pt{-}H_{ads} \longrightarrow Pt{-}CO_{ads} + H_2O + Pt, \tag{6}$$

or via the reverse water-gas-shift reaction [18,66,69,88]

$$CO_2 + H_2 \longrightarrow H_2O + CO. \tag{7}$$

The performance loss resulting from carbon dioxide intrusion is higher when more CO is formed. This happens when the cell temperature or water content at the anode is low, or when the cell operates at high current [18,66]. The harm caused by CO_2 poisoning strongly depends on the amount of formed CO. In the experiments by Rajalakshmi et al. [87], the power output of the PEMFC stack only dropped with 9% when the fuel stream consisted of 50% CO_2 and 50% H_2. After operating on pure hydrogen, the system recovered to original output within seconds. The researchers concluded the performance reduction was mostly caused by the decrease in H_2 partial pressure rather than CO formation in the reverse water-gas-shift-reaction. Direct CO contamination causes significant harm. CO binds strongly to catalyst sites causing ECSA reduction and a drop in cell potential [18]. In 2005 Benesch and Jacksier [64] showed that low concentrations of 10 ppm in the fuel stream could cause voltage drops larger than 0.4 V within 10 h of operation. Even contamination with 5 ppm induced a steady state with a significantly lower cell potential. The review by Cheng et al. [18] points out that CO poisoning is aggravated by lower operational temperatures and especially during high current density operation, just like CO_2 poisoning. These results are in line with the elaborate work by Ohi et al. [89]. Qi et al. [90] showed that CO can also cross over to the cathode, especially when the membrane is dehydrated, and bind to the catalyst particles there.

Nitrogen oxides

NO and NO_2 are both forms of NOx which can enter the FC via the air inlet. In presence of platinum, NO_2 molecules are split into NO and oxygen, while NO adsorbs to the cathode catalyst particles [91]. NO_2 can also adsorb directly on the catalyst surface area, although this is a weaker connection and thus less harmful than NO adsorption [92]. Low concentrations of just 1.0×10^{-1}-1.5×10^{-1} ppm are sufficient to lower the output potential [20,23]. Yet, in contrast to other pollutants, this decay can most likely be fully recovered after operation on clean air.

Sulfur compounds

Sulfur compounds (SOx and H_2S) are even more detrimental for fuel cell operation than carbon or nitrogen oxides [20,89,93]. For instance Büchi et al. [42] state that CO can be harmful in ppm levels while H_2S is already harmful at ppb levels. This is due to the strong adsorption of sulfur on the catalyst surface, which occurs both when the sulfur compounds enter via the anodic or cathodic inlet. In addition, this strong adsorption complicates recovery. For example in the experiments by Zhang [23],Jing et al. [93], just 1-2 ppm of SOx in the airflow during 100 h caused a cell potential drop of 35%. After operation on pure air, only 84% of the original voltage could be recovered. Similarly, Schmid et al. [20] show that SO_2 concentrations above 30 ppb cause voltage losses that ar irrecoverable on clean air. The work by Reshetenko [53] showed that repetitive CV cycles or several purges with N_2 followed by O_2 result in better recovery. Poisoning damage increases, just like for CO, with operation at lower temperatures around 30-40 °Celsius or with higher current densities [23,53]. In addition, Ohi et al. [89] show that low RH also results in higher losses.

3.3. Volatile organic compounds

When benzene, toluene or naphthalene are introduced at the anode, the effects seem to be negligible [86,94]. In contrast, cathode contamination does results in voltage loss [70,71]. In comparative studies naphthalene seems to be the most harmful out of the three VOCs [71,95]. St-Pierre et al. [95] showed that contamination with 20 ppm resulted in a voltage drop of over 80% within an hour. Also lower concentrations up to 1.4 ppm have been tested and resulted in voltage drops of 25% [96].

The publication by Moore et al. [73] shows that benzene is more damaging at high current densities. After introducing 50 ppm, the cell potential reduced by 5% and 28% when operating on $50\,\mathrm{mA\,cm^{-2}}$ and $200\,\mathrm{mA\,cm^{-2}}$ respectively. The authors hypothesized that adsorption of benzene to the catalyst sites is responsible for the voltage drop. The performance was almost fully recovered after operating on clean air and keeping the cell at OCV for 1 min.

3.4. Sea salt: HCl and NaCl

Sea salt can contaminate the PEMFC via the cathode inlet. The salt is suspended into the air in the form of sea salt aerosols as a result of an interplay between sea water and wind [97,98]. As 85 to 90% of sea salt is NaCl [99], most maritime related degradation studies apply this as a contaminant rather than the more complex mixture of various salts. In contrast to the gaseous contaminants discussed earlier, salt contamination comes with additional complexity, it can be carried in the air both dissolved in water droplets as well as in the form of salt crystals of various sizes. In addition, the type of air treatment in the PEMFC system will most likely affect the concentration and form (dissolved or crystalline) as well. For instance, a water column humidifier will most likely dissolve a significant proportion of the salt while membrane humidifiers could change the way the salt aerosols are formed.

Several researchers investigated impact of NaCl on PEMFC operation [44,50,51,54,100–111]. This section also includes some works on HCl contamination, in addition to the NaCl references. These HCl publications can help to understand NaCl degradation mechanisms because HCl-induced harm is mostly ascribed to Cl^- ions, which also become available when NaCl enters the cell. HCl contamination is interesting because it is a common contaminant when H_2 is sourced from the chlor-alkali industry. Currently, this industry is one of the major ways to obtain hydrogen with a low carbon footprint [112]. Below we first discuss the observations from our salt contamination database as a whole and present an overview of the degradation mechanisms. Thereafter a few interesting studies will be reviewed in more detail.

General observations

Tables 2 and 3 give an overview of the experimental parameters and results of HCl, NaCl and sea water degradation studies. They show clearly that the experiments have a short duration — only a few authors tested longer than 50 h [51,54,64,105]. This is relatively short considering fuel cells should last for a few thousand to several ten thousands of hours. As mentioned in Section 2.6, it is common to set up accelerated stress tests with a relatively short duration by increasing the stressors (salt concentration in this case).

A second observation from Tables 2 and 3 is that the experimental salt-flows vary significantly. To compare the flows of different publications, we normalized them to the MEA surface area. This area specific NaCl flow ranges from 1.2×10^{-6} [111] to $1.4 \times 10^{-1}\,\mathrm{g/h/cm^2}$ [54]. Fig. 2 depicts both these NaCl values and the HCl data. Reference values for actual salt concentration in sea air are hard to find. Tallgren and Ihonen [113] use a concentration of $10\,\mathrm{ug/m^3}$[2] in their MARANDA project, although the publication does not provide a reference or explanation on how and where the value was obtained. Our upcoming publication will report air salinity of sea air as well as of engine room air of sea going vessels. In absence of this data, the MARANDA [113] value is used as air salinity reference in the remainder of this review.

To assess how the experimental results relate to this sea air salinity value, we calculate the commercial system salt intake and normalize it to the MEA surface area. First the maximum area specific air flow of a commercial system ($Q_{AsAf.com.max}$ in $\mathrm{l/h/cm^2}$) is computed via

$$Q_{AsAf.com.max} = \frac{I_{PEM} * V_m * \lambda_{air} * 3600}{F * e_{O2} * Fr_{O2}}. \tag{8}$$

I_{PEM} is the current density of the PEMFC, assumed to be a maximum of $1\,\mathrm{A/cm^2}$ for a commercial system [77]; V_m is the molar volume of an ideal gas which is $24.06\,\mathrm{L/mol}$ at 20 °Celsius and atmospheric pressure; λ_{air} is the air stoichiometry in the system, assumed to be 2; the factor 3600 converts the unit of $\mathrm{l/s/cm^2}$ to $\mathrm{l/h/cm^2}$; F is Faraday's constant of $96\,485.33\,\mathrm{C/mol}$; e_{O2} is the number of electrons transferred per molecule in an electrochemical reaction, which is 4 in the case of O_2 and finally Fr_{O2} is equal to 0.21, representing the fraction of O_2 in air. As all factors in Eq. (8) are known or defined, $Q_{AsAf.com.max}$ is $2.137\,\mathrm{l/h/cm^2}$. It can be used to calculate the area specific salt flow of a commercial system ($Q_{AsSf.com}$ in $\mathrm{g/h/cm^2}$) with

$$Q_{AsSf.com} = \frac{C_{salt} * Q_{AsAf.com.max}}{1.0 * 10^6}. \tag{9}$$

Here C_{salt} is the salt concentration in $\mathrm{\mu g/dm^3}$, which is 0.01 in the MARANDA reference [113]; and the factor $1.0 * 10^6$ is used to convert the unit from $\mathrm{\mu g/h/cm^2}$ to $\mathrm{g/h/cm^2}$. $Q_{AsSf.com}$ is equal to $2.137 \times 10^{-8}\,\mathrm{g/h/cm^2}$ and is shown as the reference in Fig. 2. Experimental studies introduced, on average, 9.97×10^5 times more salt in the test systems compared to the MARANDA reference. Even though the published experiments are ASTs, and therefore the contaminant concentration should be high, the discrepancy between experimental values and realistic exposure is too large to judge if PEMFCs can withstand salt contamination. Therefore, it is unknown if PEMFC can tolerate air salinity. To study this, scholars should expose PEMFCs to lower, realistic concentrations of salt for a longer duration. The current experimental literature is still valuable and provides insight in degradation mechanisms. Besides, it is challenging to generate sea air in a laboratory setting, because the salt concentration is relatively low. It can be introduced via a saline solution, yet a careful balance must be found to keep the relative humidity such that the cell does not dry out and does not flood.

Salt-induced degradation mechanisms

Even though the current studies are not tolerance studies, they can give insight into degradation mechanisms at play during salt contamination. We sub-divided the principles based on the harmful component: Cl^-, Na^+ and NaCl. Both NaCl and HCl literature suggests Cl^- can have a strong negative impact on operation of PEMFCS. It adsorbs to catalyst particles, induces Pt dissolution, reduces hydrophobicity of the CL and GDL and favors H_2O_2 formation over the ORR [44,50,54,101,105,106,108–111,114]. The latter will lead to further radical formation and PFSA damage and increases the ohmic resistance. The Cl^- adhesion and Pt dissolution can lower the ECSA and increase the charge transfer resistance. Kitahara and Nakajima [44] pointed out that even though all voltage losses increased, the increase in charge transfer resistance was most significant. This suggests that the lowering of ECSA was the main cause of the overall voltage decay in their experiments. Lastly, Cl^- ions can pose a threat to metal components of the cell as corrosion will be induced when they are in contact with salt [50,51,103].

In the experiments by Mikkola et al. [54], Na^+ ions instead of Cl^- ions seemed to cause the voltage drop. The ohmic resistance increased, which was contributed to replacement of H^+ in the membrane by Na^+. In fact, the membrane sulfonate sites have a stronger affinity for most

---

[2] This would be $2.1\,\mathrm{g/h/cm^2}$ in a PEMFC system with a current density of $1\,\mathrm{A/cm^2}$ and an air stoichiometry of 2

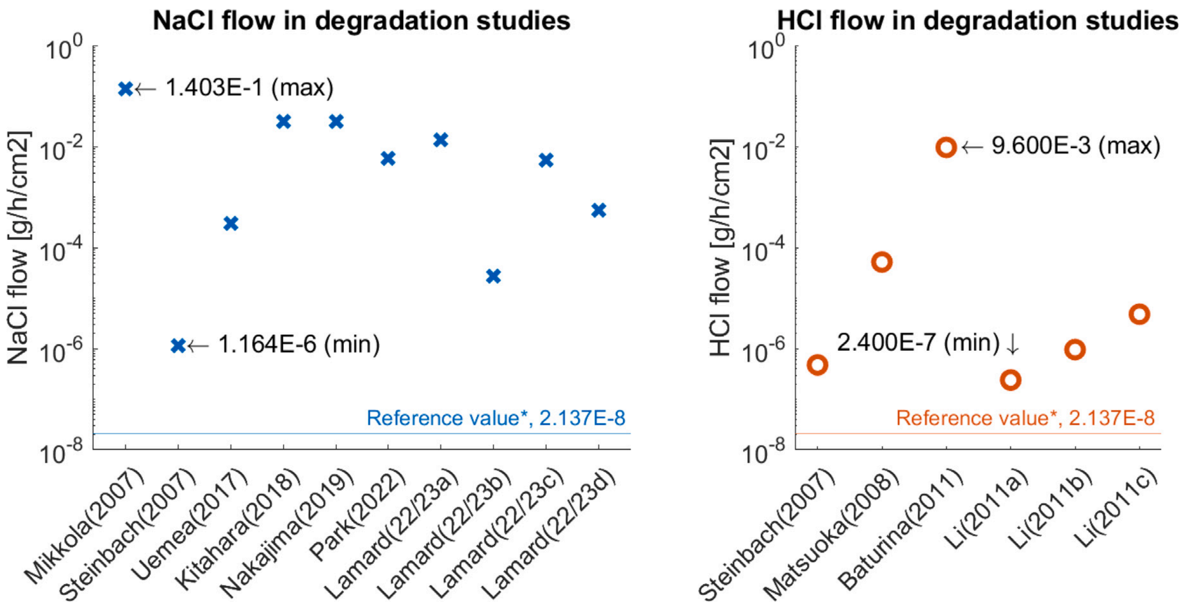

Fig. 2. Area specific NaCl flow (left) and area specific HCl flow (right) in literature compared to reference value of 6.23×10^{-9} mmol/min/cm^2. Literature data points were taken from [44,50,51,54,100,101,109,111] for the NaCl and [104,105,108,111] for the HCl. Some references are included multiple times (indicated with the suffix a, b and c) if various concentrations were tested in the same study. *Reference value is calculated via Eq. (9) using [77,113] and represents the salt intake of a maritime PEMFC system operating at 1 A/cm^2 and an air stoichiometry of 2.

Table 2
Table of HCl degradation experiments analyzed in this review.

Publication details			Degradation signs	Experimental details					Recovery?
Author (year)	Ref	Range*		Component	Insertion	Flow [g/h/cm^2]	Duration [h]	Total salt [g/cm^2]	
Schmidt (2001)	[110]		- Up to 14% H_2O_2 formation at 0.6 V; - <0.2 V H_2O_2 formation independent of Cl^-;	Cath CL in RRDE	Injection in electrolyte	N/A	N.i.	N/A	N.i.
Steinbach (2007)	[111]		- Current density decay rate >×higher than control; - Performance loss of 70% within 20 h followed by steady state;	PEMFC	Cathode and anode humidifier	3.3E−7	20	9.6E−6	N.i.
Matsuoka (2008)	[108]		- Voltage drop and 30% loss of ECSA; - Pt dissolution at inlet and Pt band in membrane;	PEMFC	Anode injection	5.2E−5	50	2.6E−3	N.i.
Baturina (2011)	[115]		- Cl^- inhibits ORR and probably reduces hydrophobicity of GDL - ECSA loss mainly due to Ostwald ripening - Cl ions remain retained in cell after Pt desorption, repetitive exposure to low potentials required for removal	PEMFC	Cathode air mixing	9.6E−3	20	1.9E−1	Repetitive OCV in N_2 after H_2 treatment
Li (2011)	[105]	Low	- Onset 'sudden drop' earlier with high HCl and anode insertion; - Severity increased with high HCl and high current density - Increase in overpotential, dominated by Rct - ECSA cath. reduction higher regardless of injection side - At low HCl performance recoverable	PEMFC	Cathode and anode injection	2.4E−7	210	5.1E−5	Pure water in humidifier
		High				4.8E−6	200	9.8E−4	
Lam (2012)	[106]	Low	- 40% ECSA loss due to Cl^- adsorption to catalyst and Pt dissolution	Cl ex situ	CL submerged	N/A	N.i.	N/A	N.i.
		High	- 60% ECSA loss						

cations over protons [15]. The authors compared cyclic voltammetry data of individual P/C electrodes with fuel cell data to assess the impact of Cl^-. In absence of the characteristic peak changes associated with Cl^- coverage, Mikkola et al. conclude that the chloride ions contributed little to the performance loss in their experiments. Also Madhav et al. [107] found H^+ replacement by Na^+ and showed the rate of substitution increased with temperature. Nakajima et al. [109] suggested that Na^+ could even cause hydrophobicity loss of the CL and GDL, increasing flooding risks and mass transfer issues.

Uemura et al. [100] conducted experiments with small diameter dehydrated salt aerosols. The polarized microscopy images revealed presence of NaCl crystals in the GDL, mostly beneath the flow field channels. For the short duration of the experiment (50 min) these crystals did not seem to block pores. Longer term experiments with salt crystals would be interesting, especially to test if the salt particles would grow over time, or rather be removed with the produced water vapor. The Uemura et al. [100] publication also highlights our lack of understanding of how salt enters fuel cells. It might be in dissolved state, as mimicked with a nebulizer, but could also be as crystals, like in the Uemura experiments.

Interesting publications

In the elaborate work by Steinbach et al. [111], both HCl and NaCl (among other contaminants) were introduced via the reactant humidifiers. The data shows that NaCl increased the decay rate by threefold compared to desalinated water. Yet, the impact of HCl and Na_2S contamination was significantly stronger resulting in decay rates 5 to over 120 times higher than the control.

Sasank et al. [102] have been the only authors working with actual sea water contamination. They used an open-cathode fuel cell, in which

Table 3

Table of NaCl and sea water degradation experiments ∗ Some researchers tested a range of concentrations (low and high) or tested at different voltages. If applicable, it is specified in this column.

Publication details			Degradation signs	Experimental details					Recovery?
Author (year)	Ref	Range*		Component	Insertion	Flow [g/h/cm^2]	Duration [h]	Total salt [g/cm^2]	
Mikkola (2007)	[54]		- 33% reduction current density; - increase in ohmic resistance of MEA;	PEMFC	NaCl cathode injection	1.4E−1	100	1.4E1	Run with clean air
Steinbach (2007)	[111]		- Current density decay rate >3×higher than control;	PEMFC	NaCl in cathode & anode humidifier	1.2E−6	N.i.	N.i.	SD/SU with thermal cycling
Cui (2016)	[103]		- BP surface corrosion	BP submerged	Solution of 0.01M NaCl	N/A	4	N/A	N.i.
Sasank (2016)	[102]		- 65% power loss; - 90% recovery after washing	PEMFC stack	Sea water mist in cathode	N.i	48	N.i.	Pure water washing
Uemura (2017)	[100]		- NaCl particles in GLD under channel - ECSA decreased by 22.6%, possibly caused by Cl^- catalyst adsorption	PEMFC	µm size NaCl crystal injection via cathode	3.0E−4	0.8	2.5E−4	N.i.
Kitahara (2018)	[44]		- Increase in overpotential, mainly R_ct - 10% V reduction	PEMFC	NaCl cathode injection	3.1E−2	2	6.3E−2	
Nakajima (2019)	[109]		- Cell voltage drops of 4%, 22%, and 41% after 2.5, 5 and 10 h respectively - V recovery 80%–96%	PEMFC	NaCl solution nebulized at cathode inlet	3.1E−2	2.5	7.8E−2	2 h pure water in humidifier
Lamard (2022, 2023)	[51] [50]	Short	- 10 mg/m^3 did not trigger performance loss - 5000 mg/m^3 caused sudden drop from 0.36 V to 0.1 V (old MEA) and gradual drop from 0.65 V to 0.55 V (new MEA) - Delamination, corrosion at current collector		NaCl mist from ultrasonic vibrator at cathode inlet	1.4E−2	0.5	6.8E−3	Pure water in humidifier
		Long	- Old MEA tested 24 h, 24 mV/h voltage drop, 68% recovery - New MEA tested 165 h, 3.3 mV/h voltage drop, 80% recovery - New MEA with graphite CC tested 122 h, 2.2 mV/h voltage drop, cell failure after OCV	PEMFC with different MEAs Old with 0.5 mg/cm2 Pt, new with 0.4 mg/cm2 CC from stainless steel and graphite		2.7E−5	24 – 165	- 4.5E−3	Pure water in humidifier, 30 min N_2 rinsing
		Short	- After 3 h voltage oscillations, sharp V drop of 4th cell (NaCl and corroded stainless steel in effluent) - 95% recovery after characterization cycle			5.4E−3	10	5.4E−2	
		Long	- Cell 5 unstable after 10 h, sharp drop after 30 h likely due to high R_mt, 96% recovery - Cell 5 unstable after re-starting, test halted after 13 h due to failure cell 5 and 1, 95% recovery	PEMFC stack		5.4E−4	43	2.3E−2	Characterization cycles with pure water humidification
Park (2022)	[101]	0.6 V	- 21% ECSA loss, high R_ct - Cause Cl^- adsorption to Pt	PEMFC	NaCl solution nebulized at cathode inlet	5.8E−3	1	5.8E−3	Oxidation Cl^- at 1.3 V
		0.9 V	- 32% ECSA loss, high R_ct - Cause Cl^- induced Pt dissolution						
Madhav (2023)	[65]		- PEM mass increase at high temp - H+replaced by Na+ - Degradation worsens with higher temperature and to a lesser extend due to increase in NaCl	PEM submerged	Solution of 0.17M NaCl	N/A	24	N/A	N.i.

the air steam is not humidified and the RH cannot be controlled. These type of fuel cells are often applied in unmanned aerial vehicles, that are highly weight limited [116]. In the study [102], saline water was evaporated with a heat lamp and fed to the cathode with a fan. The FC output power decreased by 40 W (64 % lower than control) after 48 h of operation. After washing with distilled water, 87 % of the original power was recovered. While the authors suggest that both 'electrode surface occupation' and 'loss in proton conductivity' reduce the performance, it remains unclear if that is true. No distinction is made between the two mechanisms and there is no evidence (e.g. in the form of an increased charge transfer resistance or ohmic resistance) to clarify if either or both occur. In addition, the salinity of the air entering the fuel cell was not measured so that it is unknown if the test set-up is representative for operation of PEMFCs in sea air. Specifically for maritime applications, it is fair to assume that PEMFCs will not be of the open cathode type, as weight is less of a concern compared to durability.

More systematic research was conducted by Lamard et al. [50,51]. A short term (ca. 30 min) exploratory study was followed by a longer term (up to 165 h) degradation test, characterized with in-situ and post-mortem analysis techniques. Their work highlights the importance of selecting the right PEMFC materials. Compared to the cells with graphite CCs, the cells with metallic ones degraded eight times faster. In stack tests with copper BPs, the authors observed corrosion in line with stainless steel BP research by Cui et al. [103]. The increase in mass transport resistance was attributed to corroded particles clogging the reactant transport routes. Possibly, mass transport was also limited due to a loss of GDL hydrophobicity caused by Cl^- ions and consequential flooding. Additionally, Lamard et al. report on post-mortem analysis of a PEMFC stack that ran for 50 h on a ship in 2015 (seven years before the publication was made). The BPs showed corrosion near the air inlet and metal impurities were present in the GDL and cathode CL.

Lastly, interesting work by Park et al. [101] shows that the impact and degradation mechanisms induced by NaCl depend strongly on the operating cell voltage. At 0.6 V, Cl^- adsorption on catalyst particles was seen as the main degrading mechanism while at 0.9 V, Pt dissolution was seen as the main cause of performance loss. The authors differentiated between the different degradation mechanisms by applying 1.3 V to the cathode, which promotes the oxidation of the adsorbed chloride ions to Cl_2 and serves as a recovery procedure. Yet when NaCl poisoned cells were operated at 0.9 V, this recovery procedure could not fully recover the performance, indicating that irreversible Pt dissolution took place. The HCl contamination experiments by [114] also show a dependency of Cl^- contamination on potential differences. Chloride ions remain present in the fuel cell, even after they desorbed from the catalyst sites. Repetitive exposure to low potentials is required to remove the ions from the cell.

Insights

In summary, the existing research is valuable as it gives insight in possible degradation mechanisms related to NaCl, Na^+ and Cl^- contamination. This knowledge is important for development of marine PEMFCs, yet further research is needed to assess the impact of marine air on fuel cells. Currently, it is unknown if PEMFCs can tolerate sea air. Even the publications by Sasank et al. [102] and Lamard et al. [50,51], that tested with sea water, are not representative of actual marine air conditions. The first [102] had a limited a characterization procedure and did not report the salt concentration. Because the saline water was heated and manipulated with a high air flow, one cannot judge if the amount of salt was similar compared to marine environments. Lamard [51] analyzed their samples more elaborately. One part of their study characterizes a stack that operated at sea years earlier. Their post-mortem analysis points out that metal BPs corroded. Yet, there is little information available on how the stack was used and if other stressors might have contributed to its decay as well. Because no representative studies exist, and because experimental salt concentrations are significantly too high (see “General observations” above) follow-up experiments should be of longer duration contaminate the air-stream with lower amounts of salt.

3.5. *Hydrogen carriers and their residues*

Ammonia/ammonia borane

Ammonia borane (H_3NBH_3) can release hydrogen via hydrolysis, in which ammonia is released as a by-product. Both H_3NBH_3 and NH_3 have a relatively high hydrogen content [79], but when ammonia enters the cell (e.g. when purifying equipment fails) it strongly affects the power output. Rajalakshmi et al. [87] found that concentrations beyond 20 ppm caused irreversible voltage drops. The work by Ohi et al. [89] shows that just 2 ppm already leads to degradation five times higher than the baseline in a >400 hr test. Their recovery procedure of 50 h operating on clean hydrogen had minimal effects. The US DOE therefore advices to keep NH_3 content < 0.1 ppm.

The contamination mechanism is still up for discussion. In line with other studies [23,117], [118] suggest that NH_3 adsorbs to the anode platinum catalyst. If it crosses the membrane, even the cathode catalyst could be affected. However, other researchers state that NH_3 and $NH_4{}^+$ do not adsorb to the catalyst surface [23]. In any case, ammonium ions ($NH_4{}^+$) can be formed at the anode, that can binds to the ionomer and membrane and catalyst layer. Here they replace H^+, leading to a higher ohmic resistance [89]. The negative impact of ammonia seems to be independent of the injection side [20,117]. Airborne ammonia should therefore also be considered as a contamination risk.

Methanol

Methanol is a promising hydrogen carrier as it has a lower hydrogen: carbon ratio compared to other carbon based carriers (propane, ethane, isopropanol) and low reaction temperature (200-300 °Celsius) [85]. Moreover, it is relatively easy to transport, handle and store, and is abundantly available. This allows for easier implementation in the existing infrastructure, and makes it attractive for a large scale industry such as shipping. As mentioned in Section 3.2, the main risk of using methanol as hydrogen carrier, is the CO and CO_2 that are produced along with the H_2 in the reforming process. While some studies focus on removing the CO from the exhaust gas, for instance with a preferential oxidation reactor [85], this does not resolve the issues with CO_2 contamination.

Formic acid

Similar to methanol, formic acid is a liquid at room temperature and thus also has the advantage of easy handling. In contrast, it is non-toxic and less flammable, which makes it even safer to transport and use [80]. When used as hydrogen carrier, CO and CO_2 are released as by-product. Without proper treatment these can poison the catalyst layer as discussed in Section 3.2. Whit partial post-treatment, where CO is removed, but CO_2 remains, damage is less severe. This is in line with results of Czaun et al. [119] who decomposed formic acid and fed the resulting a mixture of H_2 and CO_2 into a PEMFC. The cell voltage did not decrease during the 14 h experiment. However, the duration was short and current density low ($0.04\ \mathrm{A/cm^2}$). The gas stream from formic acid decomposition contains up to 50% CO_2 [80], considered to be harmful on the long run according to Rajalakshmi et al. [87] (discussed in Section 3.2). Additionally, HCOOH itself can also contaminate the PEMFC, if the concentration is high enough. Zhang et al. [120] showed that introduction of 100 ppm resulted in strong voltage drops, which were especially high in the first 20 h of the test (800 μV/h) compared to the remaining 80 h (only 257 μV/h, more similar to the reference degradation rate of 231 μV/h). CV and EIS data showed that HCOOH and reaction species including CO, adsorb on the anode catalysts, but also the cathode catalyst after the contaminant crosses the membrane. A last finding in the Zhang et al. [120] experiments is that beside the charge transfer resistance, also mass transfer resistance increased. The authors assume the formic acid blocks reactant access to the CL, although no clear explanation was provided on the mechanism. Wang et al. [94] tested formic acid both as single contaminant and in a mixture with other impurities. They introduced only 2 ppm of pure (HCOOH) in the hydrogen stream and in a different experiment about 2.5 ppm of the mixture. In both cases, no significant degradation was observed within 204 h and 440 h respectively.

Overall, the H_2-carrier degradation studies highlight the importance of proper fuel treatment and monitoring systems to prevent contamination. Which carriers will be adopted in the maritime sector is still unclear. Van Rheenen et al. [79] do not regard ammonia, methanol or formic acid as viable future hydrogen carriers. The ammonia is dismissed due to its toxicity, safety issues and because it cannot be recycled. Formic acid and methanol are both based on CO_2, which they will release when the hydrogen is extracted. Both carriers can therefore not be seen as zero-emission fuels. At best they are carbon-neutral, if a carbon capture and storage plant is installed on board.

3.6. *Metal ions*

Metal ions are known to reduce proton transport by replacing H^+ in the membrane, resulting in a higher membrane resistance [65,121]. Yet, their ability to induce chemical degradation is even more detrimental and therefore widely studied. The metal ions catalyze the formation of radicals, which are atoms, molecules or ions with one or more unpaired electrons in the outer shell. This makes them highly reactive. Inside the PEMFC these radicals damage both the side-chains and backbone of PFSA of the membrane and ionomer. Of the various radicals, $OH^{\bullet}$ is considered to be most harmful [19,122,123].

The damage manifests as membrane thinning, increase in surface roughness and the formation of cracks and pinholes in the membrane. These defects can all be visualized with imaging techniques. In addition, fluoride (F^-) and sulphonate ions ($SO_3{}^-$) are emitted during PFSA breakdown. These can be detected in the fuel cell outflow as an indication of chemical degradation [124].

In chemical equations, radicals are denoted with a dot directly after the chemical formula. In PEMFCs they are formed via the Fenton reactions (where X^{2+} and X^{3+} represent the metal ions):

$$H_2O_2 + X^{2+} \longrightarrow OH^{\bullet} + X^{3+} + OH^-, \tag{10}$$

$$H_2O_2 + X^{3+} \longrightarrow OOH^{\bullet} + X^{2+} + H^+, \tag{11}$$

$$H_2O_2 + OH^{\bullet} \longrightarrow OOH^{\bullet} + H_2O, \tag{12}$$

$$H_2 + OH^{\bullet} \longrightarrow H^{\bullet} + H_2O, \tag{13}$$

$$H_2 + O_2 \longrightarrow 2\,OH^{\bullet}, \tag{14}$$

and

$$O_2 + 2\,H^+ + 2\,e^- \longrightarrow H_2O_2. \tag{15}$$

Eq. (10)–(12) show that hydrogen peroxide (H_2O_2) is often involved. The H_2O_2 is formed within the PEMFC via an anodic oxygen reduction reaction Eq. (15) [19]. In order to occur, O_2 must cross the membrane. This is why thinner membranes or membranes with cracks and pinholes experience higher levels of chemical degradation. The increased gas crossover worsens chemical degradation [125].

3.7. Damage mitigation and recovery procedures

Damage to the PEMFCs can be mitigated by selecting the right materials. For instance, Cheng et al. [18] review various CO-tolerant electrodes, formed by alloying the catalyst to other metals. Two different mechanisms are hypothesized be responsible for the effect — the metal alloy either promotes CO oxidation to CO_2 (bifunctional mechanism) or it reduces the CO bond stability relative to the hydrogen bond strength (intrinsic mechanism). It is still unclear which of the mechanisms mainly takes place. In any case alloying does not seem to mitigate the damage caused by sulfur compounds [56]. Another example is the use of graphite bipolar plates rather than metal ones, to prevent metal corrosion and metal ion induced degradation [15].

Alternatively, when the cell is contaminated, a recovery procedures could restore (part of) the cell performance. For salt contamination, the applied recovery procedures are summarized in Tables 2 and 3. The table shows that recovery is mostly the removal of the contaminant. Mohtadi et al. [56] also applies this strategy to resolve cathodic NO_2 contamination, similar to the elaborate investigation by Misz et al. [72] in which all 27 tests were ended with clean air operation of 1 h to check for reversibility.

Other scholars have applied more elaborate procedures, in which both the contamination was stopped and operational parameters were altered. For instance, Mohtadi et al. [126] observed that cathodic H_2S or SO_2 poisoning could not be restored by operating the system on clean air for 24 h. Interestingly, near-complete recovery was achieved by applying CV to the poisoned cathode. This is caused by the oxidation of the tightly adsorbed sulfur species. Zhang et al. [118] applied three different recovery procedures in their ammonia fuel contamination experiments. They stopped the contaminant flow and (1) kept the temperature and RH constant; (2) lowered the fuel cell temperature to room temperature and back up again while keeping the RH at 49%; and (3) increased the RH to 100% and kept the temperature constant at 65 °Celsius. The characterization with CV and EIS showed that removing the contaminant in combination with a high RH operation resulted in near-full recovery of the catalyst layer. However, membrane resistance remained higher than before NH_3 contamination.

In all of these recovery procedures, the contaminant is removed from the inlet. This is a viable strategy for PEMFC suppliers and power system technicians when they have to do maintenance of the fuel cells. They could operate the PEMFCs in a clean environment, apply recovery procedures by changing RH, temperature or conduct CVs and restore the power output. However, these strategies are no solution during ship operation. If a vessel sails in a saline environment, or when a fuel treatment system fails and hydrogen carriers enter the system, removing the contaminant flow is not possible. The most viable alternative will therefore be to use air intake (quartz) filters and cleaning procedures [18]. Alternatively, a backup tank with clean compressed air or oxygen could be carried on board. Still, in order to keep systems as efficient as possible the mitigation measures should be sufficient to guarantee reliable PEMFC performance, but not too much to reduce BoP costs and energy use. Contaminant tolerance thresholds are essential to find this balance.

3.8. Contamination schematics

Below, we summarized the contents of this section on contamination in schematics, as we will do for the following two sections as well. Section 6 elaborates further on the overall impact and use of the nine schematics included in this review. In each, we sub-divide the mechanisms based on the degradation location and process: (i) radical damage to the PFSA in the membrane or ionomer, (ii) carbon corrosion in the CL or GDL, (iii) catalyst inactivation in the CL, and (iv) obstruction or pores in the CL and GDL. These mechanisms are used to connect the causes of degradation (contamination, load, and movement stressors) to various damage monitoring options (impedance measurements, exhaust analysis and imaging techniques). R_{Ω}, R_{ct} and R_{mt} link to ohmic, charge transfer and mass transfer resistances, as introduced in Section 2.3. Orange broken lines indicate links that we deem likely, yet that are not stated in the cited literature.

The overviews show that most degradation mechanisms relate to the membrane and catalyst layer. Only Cl^- ion interactions with the GDL seem to lead to obstruction and flooding Fig. 3(a). In extension of that, impedance analysis will mostly show contamination effects in the ohmic and charge transfer resistance values.

4. Load induced degradation

The characteristics of the load profile demanded from the PEMFC has a great impact on its durability. In general, constant loads, at a moderate current will result in a long lifetime [127]. In contrast, idling (Section 4.2), dynamic operation (Section 4.6), high load operation (Section 4.3) or start-up and shut-down cycles (Section 4.4) will cause degradation. When the PEMFC starts up at temperatures below 0 °Celsius (i.e. a freeze start) it is specifically harmful and therefore addressed separately (Section 4.5). Most of the load related research focuses on one specific type of load, rather than drive cycles. If drive cycles are considered, they are generally automotive ones such as buses ([128,129]) and electric vehicles ([19,61,130–133]). Even though this does give some insight into the complex interconnected effect of combined load modes (such as start ups and high load operation), ship drive cycles will be significantly different as will be addressed in Section 4.1. Finally, also this section is concluded with four schematics linking the load characteristics to degradation mechanisms and monitoring Section 4.7.

4.1. Maritime FC power demand

Maritime load profiles vary widely depending on the ship's purpose and external factors such as sea state and amount of cargo. For instance, a tugboat (vessel that maneuvers large ships) has a highly fluctuating profile, while for container vessels it is relatively constant. The power that the FC system has to provide depends on the design of the power plant as a whole and its energy management system. Most maritime engineers pair PEMFC systems with short term energy storage systems such as batteries or super capacitors. This allows for a more compact and efficient energy system, combining the superior response time and energy efficiency of batteries or super capacitors with the higher energy density of FCs [134,135]. An energy management system controls the power plant, determining how many stacks should be used, at what moment in time and which power should be delivered. Considering the above, the type of load-based degradation taking place depends on the vessel type, power plant and energy management system. There are no specific maritime drive-cycle degradation studies so far, a field which should be explored.

4.2. Idle operation

In idle operation the PEMFC system only supplies power for its own BoP and some auxiliary users. The power output drops below 1 % of the maximum power and a low flow of current $<100\,\mathrm{mA\,cm^{-2}}$ is sustained [19,136]. In experimental setting, idling is commonly mimicked by keeping the cell at OCV [19,137]. In these conditions, the cathode potential increases, facilitating (severe) chemical membrane degradation and catalyst particle breakdown.

Radical formation is discussed in more detail in Section 3.6. Under idle conditions, gas crossover increases. This is because (i) the membrane dries out as there is little to no water production, increasing gas permeation, (ii) the dry conditions lower the electro-osmotic drag that opposes O_2 migration towards the anode and (iii) no gasses are consumed, increasing their partial pressure. As a result, the O_2 concentration at the cathode rises and more H_2O_2 can form via Eq. (15).

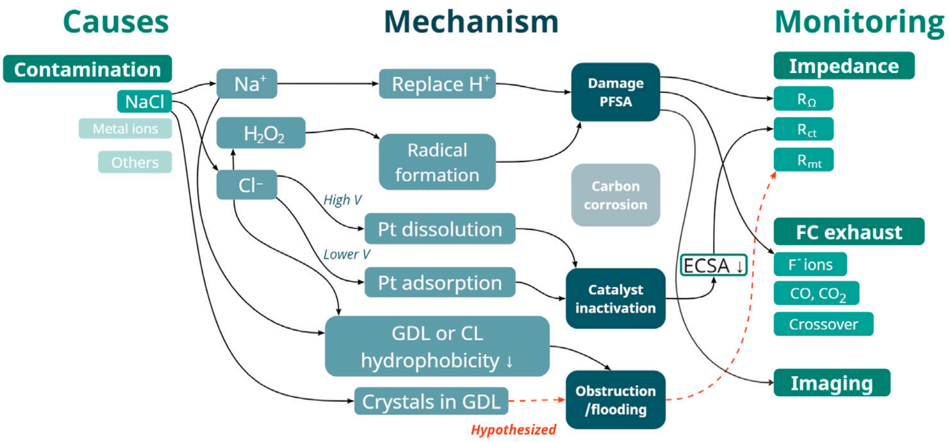

(a) NaCl induced degradation

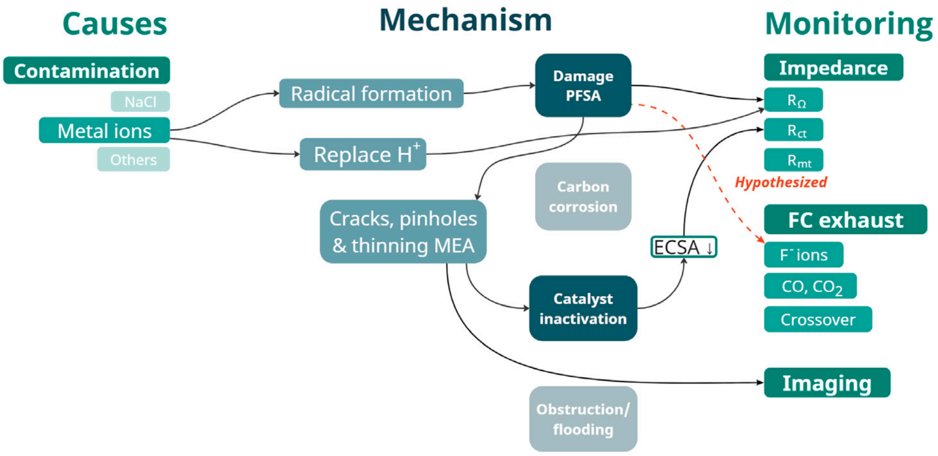

(b) Metal ion induced degradation

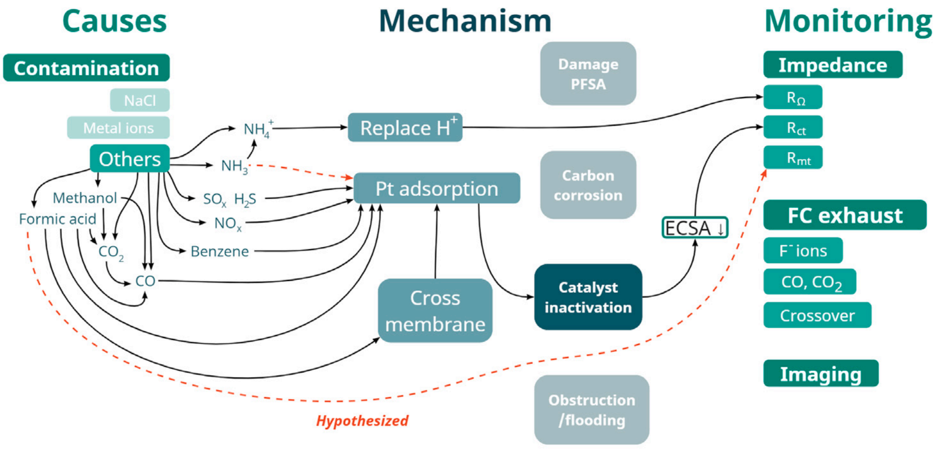

(c) Degradation due to CO, CO_2, NO_x, NH_3, benzene, methanol, formic acid or sulfur compounds

Fig. 3. Schematics of contamination degradation mechanisms and possible monitoring options. Orange broken lines indicate that the relation has not been reported in the referenced publication, but is still hypothesized to occur. ECSA stands for membrane electrode assembly, CL for catalyst layer and MEA for membrane electrode assembly. (For interpretation of the references to colour in this figure legend, the reader is referred to the web version of this article.)

Furthermore, the high cathode potential promotes Fe^{2+} migration in the membrane which catalyze the Fenton reactions Eq. (10)–(14) [138]. Together the O_2 crossover and high cathode potential worsen the radical damage, affecting the membrane and ionomer.

Gas crossover can also cause the formation of hot spots — areas where the released heat is much higher than the heat dissipation rate of the cell [21,139]. In idle/OCV operation, H_2 can reach the anode combust with O_2 at the catalyst surface, while releasing significant heat. The high temperature will facilitate thermal catalyst and polymer (i.e. membrane) decomposition [133,139,140]. Especially when the membrane has pinholes, either from chemical degradation or from manufacturing defects, a positive feedback loop can occur, where the

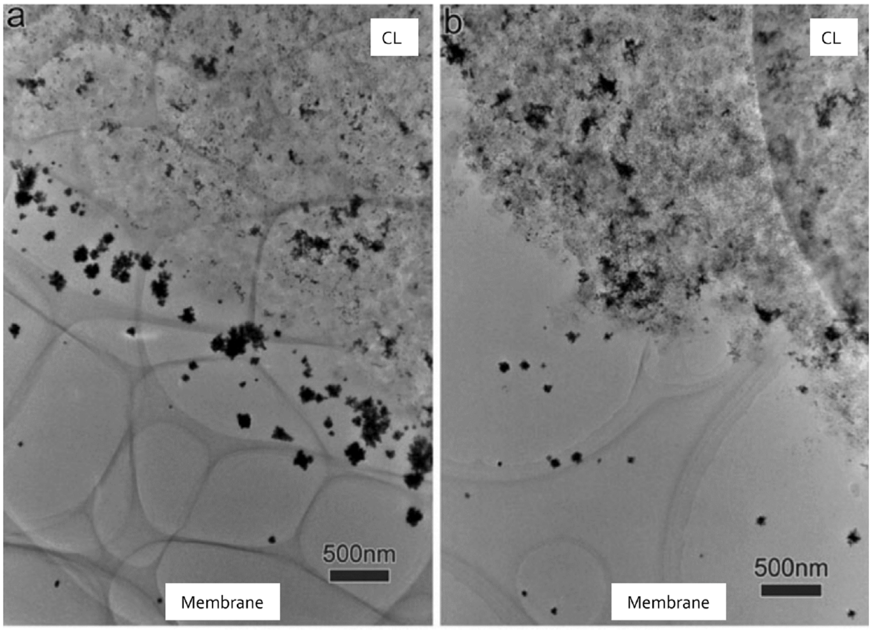

Fig. 4. TEM images from Yasuda et al. [142] of a Pt band in the membrane (bottom left area) after two different potential cycling tests. Figure a has a more defined Pt band (black particles), indicative of the harsher conditions during the test. The potential was cycled 500 times between 0.1–1.2 V (a) and 0.1–1.0 V (b). The Pt particles originate from the cathode CL (top right area). (For interpretation of the references to colour in this figure legend, the reader is referred to the web version of this article.)

pinholes promote gas crossover, and that results in hot spots and widening of the holes [133].

Even without hotspots, carbon corrosion increases due to the high cathode potentials (see for more details Section 4.4). The structural integrity of the CL deceases, leading to detachment of catalyst particles. Additionally, more Pt particles dissolve at high cathode potentials. This stimulates Pt-membrane deposition and Ostwald ripening. The latter is a phenomenon often seen in crystal formation. It entails that particles of small crystals tend to dissolve in the surrounding solution and redeposit on larger crystals. These mechanisms are two out of the four commonly described catalyst degradation mechanisms, shown in fig. A.2 in the supplementary information [141].

PEMFC catalysts can undergo electrochemical Ostwald ripening, also known as electrochemical coarsening [141]. In this case the Pt particles dissolve to form $Pt_2{}^+$ and $Pt_4{}^+$. Simultaneously the electrons transport via the carbon support and are recombined when the Pt ions precipitate on a growing Pt particle. As a result the available Pt surface area decreases.

Instead of depositing onto a growing Pt particle, the dissolved Pt ions can migrate towards the membrane. As the catalyst mostly dissolves from the cathode, a concentration gradient builds up over the membrane. This drives the ions to diffuse towards the anode. Crossover hydrogen gas from the anode facilitates the Pt-ion reduction to atomic Pt [137,142]. Subsequently other catalyst ions can precipitate on its surface, eventually forming a so-called Pt-band as shown in Fig. 4. This image is from a dynamic load AST, and will be addressed in more detail in Section 4.6.

All these catalyst degradation mechanisms decrease the ECSA. When the average Pt particle size grows due to Ostwald ripening, the surface-to-catalyst ratio reduces. The dissolution and membrane precipitation also lowers the available Pt. These mechanisms are not exclusive to idle/OCV operation. As we will discuss in Section 4.6, Pt dissolution is also an issue at dynamic loads. However, the effects are most excessive in OCV/idle mode due to the high cathode potential. Yasuda et al. [143] applied this knowledge and held their PEMFCs at the high potential of 1 V in order to study Pt band formation.

4.3. *High power and high current operation*

The high power condition refers to PEMFCs operating at, or close to their rated power. The rated power is the maximum continuouspower output for which a system is designed. In several studies that compare degradation rates of various drive cycle modes, high power operation is one of the most damaging modes [60–62,144,145]. Only in the study by Hu et al. [62], high power is clearly defined, in their case as a power equal or larger than 80% of the rated power.

Hu et al. [62] report a degradation rate at high power of $10.00\,\mu V\,h^{-1}$, significantly higher than the other modes (idle operation and load changes with degradation rates of $8.66\,\mu V\,h^{-1}$ and $0.04\,\mu V\,kW^{-1}$ respectively). This is in line with the degradation rates reported in the review by Lorenzo et al. [127]. Still, in the works by Pucheng Pei, the overall contribution of high power related damage to the overall degradation was limited to $5.8\,\%$. This is probably because high power operation does not occur often and does not last long in an average automotive drive cycle [61,144].

High powers are paired with high current densities. When they are too high, the output power will lower due to mass transfer issues (as shown in Fig. 1), and starvation could take place [145]. Ren et al. [19] illustrate its various forms, both local and overall starvation form either oxygen or hydrogen. Hydrogen starvation is accompanied by carbon oxidation,

$$C + 2\,H_2O \longrightarrow CO_2 + 4\,H^+ + 4\,e^-, \tag{16}$$

and

$$C + H_2O \longrightarrow CO + 2\,H^+ + 2\,e^-. \tag{17}$$

The CO is thermodynamically unstable and reacts on to form CO_2

$$CO + H_2O \longrightarrow CO_2 + 2\,H^+ + 2\,e^-. \tag{18}$$

Therefore only trace amounts of CO can be found in the cathode exhaust [146]. The carbon is sourced from the catalyst supports. Also the GDL can corrode, although at a lower rate due to the absence of Pt particles to catalyze the reaction [145–147]. As the catalyst support degrades, the Pt particles are dislocated or agglomerated. The ECSA lowers and the PEMFC performance drops [19,136,145]. Carbon corrosion can be accelerated when hot spots are formed, which also occurs at high currents [133]. Beside high currents, freeze-starts (Section 4.5) and dynamic operation (Section 4.6) can trigger gas starvation and carbon corrosion as well.

Finally, flooding can be an issue at high current operation. For example, the experiments by He et al. [148] in 2003 show that above $0.55\,\mathrm{mA\,cm^{-2}}$ the cell voltage decreases drastically. When the PEMFC floods, liquid water accumulates in the pores of the CL and GDL. This obstructs the flow of reactants towards the catalysts while products linger in the CL, eventually leading to gas starvation. Even though flooding can occur on both sides of the cell, cathodic flooding is more common because the water is generated here and the electro-osmotic drag takes water from the anode to the cathode [149]. Flooding itself is not necessarily a form of degradation. Cell voltage can be fully recovered when the pores are opened up again. Yet, flooding can promote other forms of degradation via gas starvation as reactants cannot reach the catalyst cites anymore and reaction products accumulate at the CL.

4.4. Start up and shut down

Startups and shutdowns have a significant impact on PEMFC degradation. This is mainly caused by the abrupt air-hydrogen boundary at the anode [19,42]. In case of start-up, H_2 enters the anode flow field where O_2 is still present, and during shut-down, oxygen diffuses from the cathode or anode outlet into the anode. The anode areas with hydrogen will still perform the HOR (Eq. (1)), generating electrons. These move in-plane to anode areas with air, and take part in the oxygen reduction reaction (Eq. (3)), which would normally only occur at the cathode. The cathode areas facing the oxygen rich anode areas experience a temperature increase and, more detrimental, increased cathodic inter-facial potential differences [19,150].

Both the potential peak and the high temperature favor carbon oxidation reactions (CORs) Eq. (16)–(18). As described in Section 4.3, the corrosion lowers the ECSA and PEMFC performance. The mass transfer resistance increases as the porosity of the CL is altered [151] and the charge transfer resistance increases when the ECSA reduces. The carbon corrosion also thins out the CL, some researchers observed ionomer accumulation in the direction of the GDL, again reducing porosity and increasing mass transfer resistance. Carbon corrosion can be studied ex-situ via imaging techniques revealing the physical damage to the CL. In-situ, ECSA decrease and the increase in mass transfer resistance can be an indication of carbon corrosion, although these signs can also be linked to other types of damage. A more clear proof of COR activity is the detection of CO and CO_2 in the PEMFC exhaust.

4.5. Freeze start

Cold start is a specific case of start-up and therefore has similar degradation mechanisms. However, the sub-zero temperatures add the complexity of water freezing [19]. This introduces two new forms of damage: volume changes and overall starvation. The former is the result of freezing and thawing of the residual water present in PEMFC components while the latter is caused by severe blockage of pores by the ice.

The volume changes affect different layers in the PEMFC. In the GDL, the porous structure is damaged and the hydrophobicity reduces [152]. Mass transfer is complicated and the flooding risk increases as a result. At the level of the MEA, other types of damage occur, some examples are shown in Fig. 5. The defects include pinholes in the membrane and interface separation in the GDL-CL or CL-PEM boundary (delamination). The latter is accompanied with higher contact resistance, hampering the transport of electrons. If the MEA has pre-existing cracks, which can arise during the manufacturing process, these are likely to deepen as liquid water tends to accumulate in them. Finally, the ECSA can irreversibly reduce as ice patches detach the ionomer from the catalyst particles [19,153].

Beside the mechanical damage, fuel starvation leads to more positive anode potentials. When large scale H_2 shortage perseveres this can result in cell reversal [154]. The cell voltage becomes negative and instead of the HOR the electrons are sourced from either COR (Eq. (16) and (17)) or from the oxygen evolution reaction (OER),

$$2\,H_2O \longrightarrow O_2 + 4\,H^+ + 4\,e^-. \tag{19}$$

Even though the COR is thermodynamically more favorable, at lower anode potentials the OER is dominant due to its faster kinetics. Carbon oxidation slowly takes over as the anode potential rises, leading to more mechanical damage. Some damage mitigation strategies therefore aim to steer the fuel starvation reactions towards the OER [154].

4.6. Dynamic operation

Dynamic load operation results in similar damage as cold starts (Section 4.5) even though the cause is different. During dynamic operation, swift changes in the load can lead to mechanical damage and a shortage of fuel and oxygen supply, which causes gas starvation and catalyst defects.

At high loads, electrode reactions are enhanced and thus more water is produced. However, as potential is cycled, humidity of the ionomer and membrane changes as well, resulting in shrinking (drying) and swelling (wetting). These volume changes cause mechanical defects including cracks, pinholes and delamination. The top figure of Fig. 5 illustrates this with scanning electron microscope images of Alavijeh et al. [57] after an extreme cycling test, varying the relative humidity between 0% and 100% RH within minutes. Severe damage is visible, and cathode cracks coincide with membrane ones. In addition, te ohmic resistance increases significantly at low RH, as the membrane needs water molecules to transport protons (as seen in Eq. (2)).

Load changes can also lead to gas starvation when the O_2 or H_2 supply lags behind on the requested current. Fuel starvation occurs more often because H_2 is supplied in a lower stoichiometric excess compared to oxygen. The fuel starvation process described in Section 4.5 is essentially overall H_2 starvation, a sub-category of gas starvation. The broader concept of gas starvation concerns to both local and overall shortage of reactant gasses, and either oxygen or fuel can be lacking.

Overall air starvation may result in cell reversal, just like overall H_2 starvation (Section 4.5). When O_2 is locally depleted, the ORR (Eq. (3)) is replaced by the hydrogen evolution reaction (HER),

$$2\,H^+ + 2\,e^- \longrightarrow H_2, \tag{20}$$

in order to deposit the electrons. As a result, the cathode potential lowers and the overall cell potential decreases. In adjacent areas with sufficient O_2, the H_2 can react directly according to Eq. (4). Significant heat is produced in the process and hot spots are formed. In affected areas Pt particles agglomerate more easily and the chemical membrane degradation is facilitated [155]. Interestingly, when air starvation occurs only for a short period of time, performance can improve because not only the protons are reduced, but also the platinum oxides, making the platinum particles available again. This was shown in work by Bodner et al. [156], who conducted an AST where the cell's power density improved after 100 h. They reduced the air stoichiometry from 2 to 0.9 for 10 s every hour. The authors do however expect that on the long term, performance will reduce because Pt agglomeration and dissolution outweighs the platinum oxide reduction, eventually lowering the ECSA.

When H_2 is locally lacking, the consequences differ from the case of overall fuel shortage. In their elaborate review, Ren et al. [19] state that local depletion is accompanied by carbon corrosion at the cathode side directly facing the anodic H_2 shortage region. With overall shortage, the anodic CL is predominantly corroded.

Finally, load changes affect the catalyst particles. As mentioned before in Section 4.2, Ostwald ripening and Pt migration are also enhanced in dynamic load conditions. The experiments by Yasuda et al.

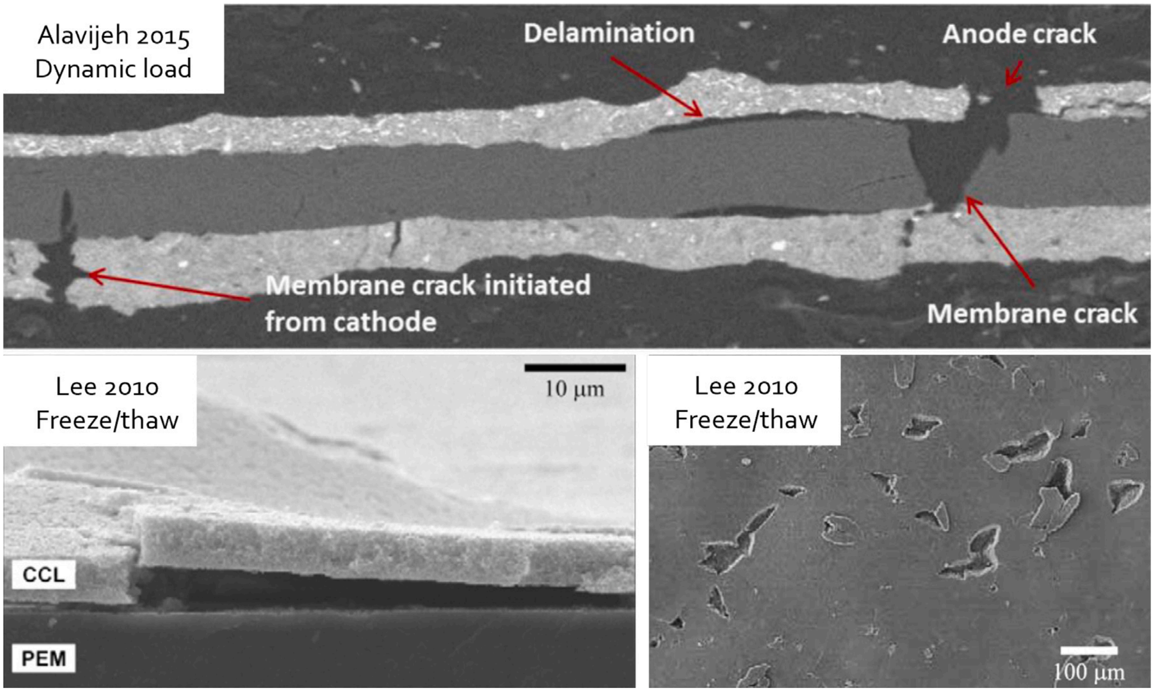

Fig. 5. SEM images copied from Alavijeh et al. [57] (top) and Lee et al. [153] (bottom) showing different types of mechanical damage to the MEA. The top picture shows delamination and cracks resulting from an aggressive wet–dry cycling accelerated stress test. The bottom two images show the result of a freeze/thawing experiment causing cracks, delamination and pinholes.

[142] clearly show this. In their experiments, potential was cycled with an upper limit of 1 or 1.2 V vs RHE. In both cases a Pt-band was visible in the membrane. The effects were most severe in the test with an upper voltage of 1.2 V vs RHE as can be seen in Fig. 4. This is probably caused by the aggravated Pt dissolution at higher cathode potentials.

4.7. Load degradation schematics

Just like in the contamination section, this load section concludes with a set of degradation schematics. Section 3.8 includes a more detailed description of how they are set-up. Figs. 6(a) to 6(d) show that load based degradation occurs via many different routes. Fuel and air fluctuation, cycling of humidity and significant increases in temperature or (local) cell potential lead to various forms of chemical and mechanical damage within the cell structures. Simultaneously, Fig. 6(d) also shows that especially high power or high load operation could be studied in more detail (at least based on the literature collection used in Section 4).

5. Motion-based degradation

This chapter deals with two types of motion-based degradation triggers — vibration and inclined operation. Ships move with six degrees of freedom (as shown in fig. A.3 in the supplementary information): heaving (up or down movement); surging (forward and backward); swaying (from left to right); yawing (turning around the vertical axis); rolling (turning around the forward axis); and pitching (turning around the sideways axis). Combined, these movements can lead to various inclinations. The Class Societies, who set the safety standards for maritime components, determine the requirements to which maritime PEMFC have to comply. For instance, Lloyd's Register (one of the big Class societies) states that the fuel cells need to operate normally at an angle of 22.5°. To prove this, PEMFC manufacturers are required to perform both a dynamic test of over 15 min and a static test [157].

The extent of vibrations to which the PEMFC will be exposed, depends on both internal and external factors. Internal factors include the type of machinery in the engine room, such as gear boxes, engines and generators, as well as the type of propeller that is used. External factors include slamming of the ship hull on the water surface, impact of waves and, in heavy sea states, impact of 'green water' (flow of water on the deck of the ship) [158,159]. Generally speaking, larger ships have larger engines and propellers and direct drives, resulting in lower vibration frequencies [159]. Ship designers have to control the level of vibration and remain below specific threshold, both to prevent equipment damage as well as prevent harm to human passengers [160]. Typical vibration spectra include vibrations up to 100 Hz [160]. This is reflected in the Class Society vibration requirements; for instance, the test protocols by Register [157] prescribe a series of tests with frequencies starting at 2-5 Hz up to 100 Hz, and displacements up to 1.6 mm.

5.1. Inclined operation

In contrast to higher temperature fuel cells, PEMFCS deal with multi-phase flows in which liquid water exists alongside water vapor, oxygen and hydrogen. Depending on the orientation, gravity will pull more strongly on the liquid water, potentially leading to problems in operation. It is therefore surprising that only a few inclined operation studies have been carried out [37,39,161,162].

In extreme cases, faulty stack orientation can lead to stack failure. Ejiri and Yamada [37] tested performance of a dead-end PEMFC stack in which the cells were oriented in three different positions: horizontally with the anode-side up; vertical (e.g. as depicted in fig. A.1, the common way to position a cell); and horizontally with the cathode side up. In both horizontal orientations, the PEMFC broke down within an hour of operating at a constant current of 200 $\mathrm{mA\,cm^{-2}}$. The anode-side up test performed the worst, failing to produce power after about 30 min of operation. With help of impedance data the authors conclude that anode flooding caused fuel starvation and failure. The vertical cells did not suffer from flooding as natural convection transported the liquid water away.

When the orientation is less severely disturbed, PEMFC performance can still be compromised. Friedrich et al. [161] tested a stack for

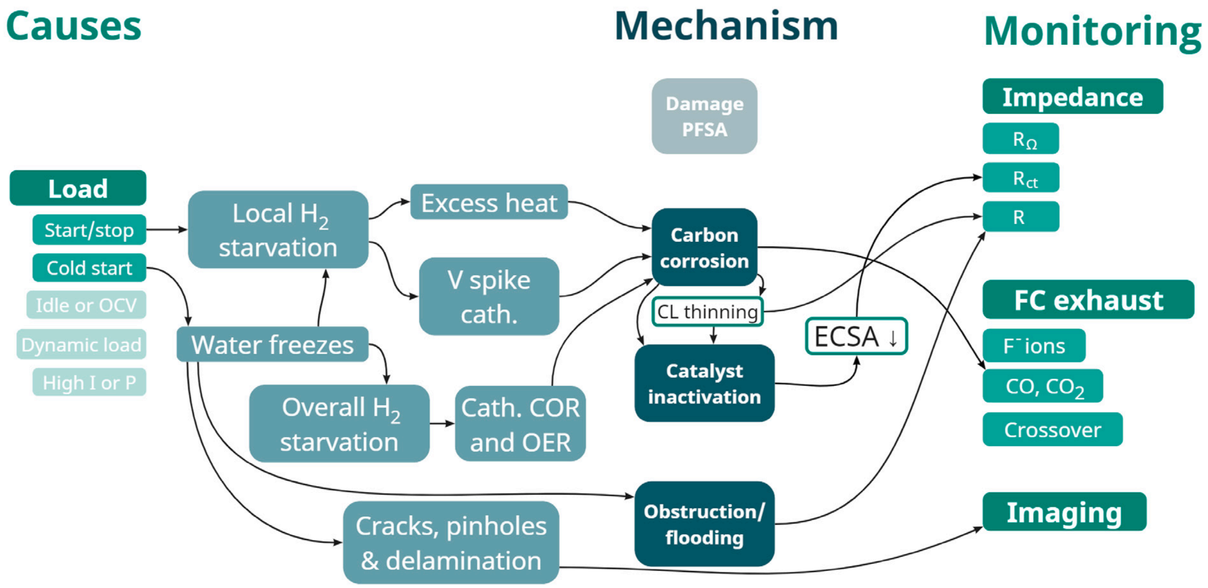

(a) Degradation due to start-up, shut-down and cold start

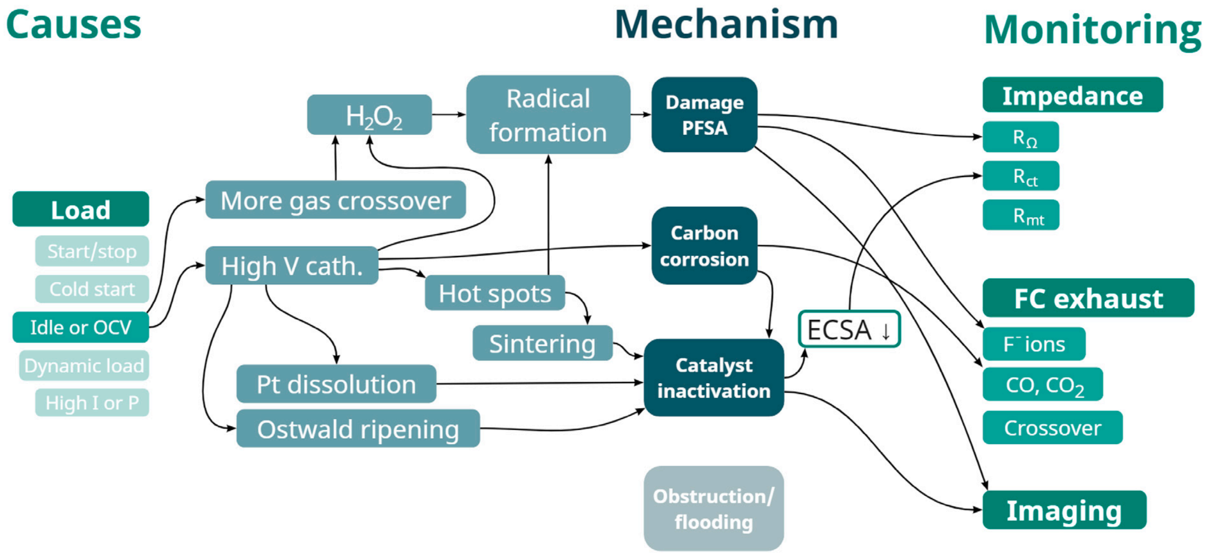

(b) Degradation due to idle or OCV operation

Fig. 6. Schematics of load-induced degradation mechanisms and possible monitoring options. Orange broken lines indicate that the relation has not been reported in the referenced publication, but is still hypothesized to occur. ECSA stands for membrane electrode assembly, CL for catalyst layer, COR for carbon oxidation reaction, OER for oxygen evolution reaction, HER for hydrogen evolution reaction and OCV for open circuit potential. (For interpretation of the references to colour in this figure legend, the reader is referred to the web version of this article.)

aircraft applications, and included a static 30° inclination test in which the air stoichiometry was varied between 1.6 and 2.5. The stack voltage clearly drops when the air is supplied in the low stoichiometry. Even though no additional characterization data is shown, Friedrich et al. suppose water management issues are responsible for the reduction in power output.

The more extensive work by El-Emam et al. [162] also tested a combination of inclination and air flow rates. Interestingly, they considered membrane drying to cause performance reduction. The authors changed both the air flow rate (220 smL/min to 660 smL/min) and orientation of the PEMFC (vertical with upwards reactant flow, via seven different angles to a vertical downwards reactant flow). The overall performance with low air flow rates was best at a 30° downwards angle of the flow channels. The slight inclination downwards probably helped to remove water and prevent cathode flooding. At higher air flow rates of 440 smL/min and above, the vertical position with upward reactant had the highest performance. Here, directing the airflow opposite to gravity pull helped to keep sufficient water in the cell to wet the membrane. This conclusion contrasts the findings of Friedrich et al. [161] discussed above, and shows the delicate balance that fuel cell engineers must strike between membrane wetting and cell flooding, as pointed out in Section 2.4 before.

Different but related research fields considering PEM water electrolysis and solid oxide fuel cells, can also give insight into inclination impacts. A study by Choi et al. [39] investigated the impact of cell orientation on PEM water electrolyzers. Even though the catalysts and

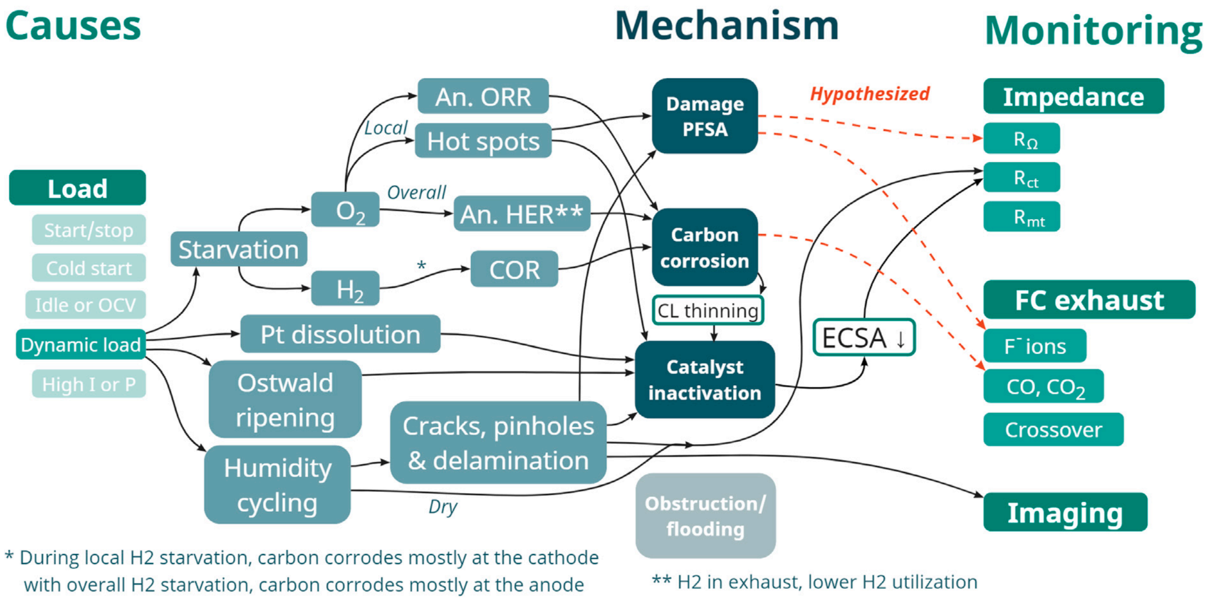

(c) Degradation due to dynamic load operation

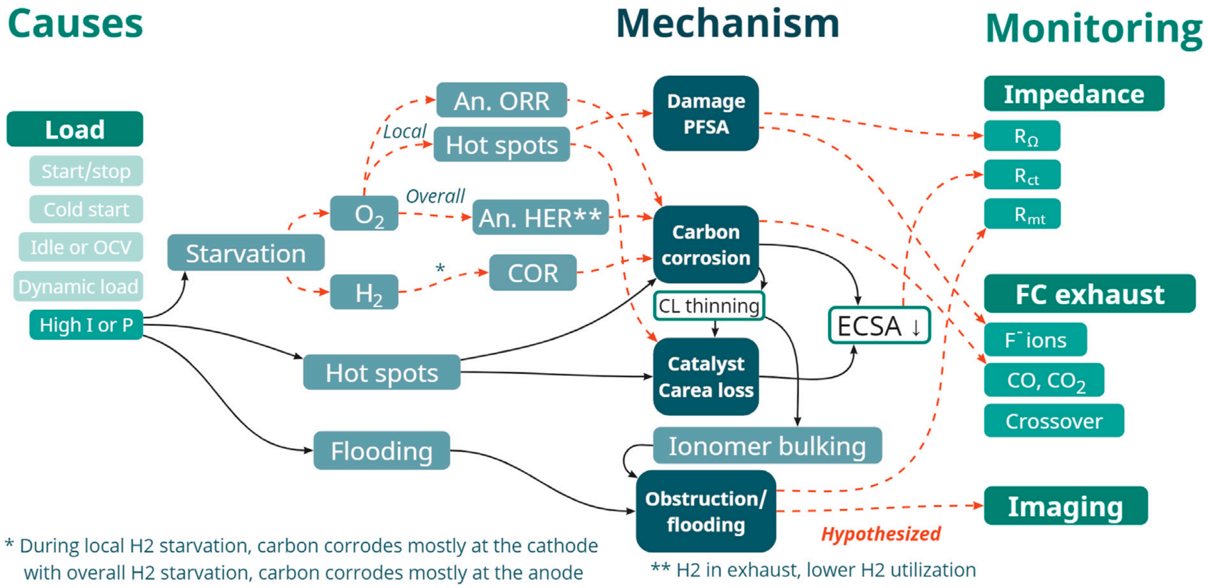

(d) Degradation due to high power operation

Fig. 6. (*continued*).

electrochemistry is different from PEMFCs, the systems are similar with respect to materials used and also deal with two-phase flows. Also in this study, impedance results indicated that mass transfer resistance increased, especially at high current densities at which chemical reaction rates are faster and more water is produced. The performance issues seemed to occur only when a single serpentine flow field was used. When a flow field with five serpentine grooves (a quintuple flow field) was tested, no mass transfer issues occurred. The work by Van Veldhuizen et al. [163] shows that not only the fuel cell system itself, but also the BoP components and control architecture can be impacted by inclined operation. In their dynamic inclination tests the authors found that the solenoid valve plunger experienced forced oscillation resulting in variations in fuel feed, fuel utilization, burner temperature and stack current. Due to built-in safety features in the control system, the periodical exceedance of fuel utilization boundaries resulted in gradual power decrease.

In summary, the limited number of studies on inclination impacts indicate that changing the PEMFC orientation links to water management issues. Various parameters influence the risk of flooding or possibly even membrane drying, including the inclination angle, stoichiometry of the gasses and flow field design. The experiments carried out so far often do not apply elaborate characterization techniques such as impedance spectroscopy or post-mortem analysis to support their hypothesis. Also, to the best of our knowledge, all PEMFC tests have been static, rather than dynamic. Especially for maritime applications this is still an important field to explore, both on stack and system level.

5.2. Vibration

An overview of vibration studies is given in Table 4. The boundaries set by Register [157] are used as reference. The table shows that the frequency, displacement and acceleration characteristics of the vibrations vary, as well as the duration of the simulations and experiments.

Table 4
Table of vibration degradation studies.

Publication	Type	Duration	Vibration details				Degradation
Author (year)			Direction(s)	Frequency [Hz]	Displacement [mm]	Acceleration max. [g]	
Rajalakshmi (2009) [55]	Exp.	90 min	3, XYZ	30 – 200	5	3	Note: PEMFC not operational during test; No degradation signs after test;
Banan (2013) [164]	Model	300 h	3	5 – 40	N/A	4	Delamination impacted by both amplitude and frequency;
El-Emam (2015) [162]	Exp.	Unk	1, vertical	1.33 – 3	600	N/A	At low air flow rates, maximum power density and hydrogen utilization improves when vibration is applied; Low frequency (1.33 Hz) vibration is better than high frequency (3 Hz); High displacement values (6 cm) are harmful;
Banan (2015) [165]	Model	14×10^4 cycles	1, in plane	5 – 40	N/A	4	Note: Both hygrothermal and vibration cycling; Hygrothermal cycles had a stronger negative impact than vibrations; Vibration impact was more significant on delamination, most strongly determined by amplitude;
Hou (2016) [49]	Exp.	250 h	3, XYZ	Unk	Unk	4.6	Hydrogen leakage increased 1.7 times; 5.4% increase in ohmic resistance;
Qiu (2021) [166]	Model	1 s	1, vertical	2	0.2	N/A	Increase in fuel consumption leading to fuel starvation;
Class society reference							
Lloyds (2021) [157]	Exp.	90 min	3, incl. vertical	2 – 100	1.6	4	N/A

Interestingly, some studies find that vibration could improve PEMFC operation while others detect adverse effects.

The previously cited publication by El-Emam et al. [162] also included vibration tests. The amplitude varied between 3 and 6 cm and the frequency changed from 1.33, to 2 and 3 Hz. Fig. 7 shows the most important outcomes. The displacement is relatively high compared to the Lloyds reference, while the frequencies are lower. Nevertheless, their results show an interesting interplay between air flow rate and vibrations. At low air flow rates of 220 smL/min, the low (1.33 Hz) vibration with an amplitude of 3, 4 and 5 cm improved the maximum power density and hydrogen utilization. An amplitude of 3 cm proved to be most beneficial. The authors assume the vibration helps to remove liquid water from the cell and therefore improves mass transport. However, the 6 cm amplitude was almost never beneficial and at higher airflow rates of 440 and 660 nmL/min, vibrations generally had a negative influence. The authors did not suggest why performance reduced at higher vibration amplitudes and frequencies. It would be interesting to get a better insight in the different mechanisms that seem to either improve or reduce power output and PEMFC H_2 utilization.

Rajalakshmi et al. [55] carried out an ex-situ vibration test, exposing a PEMFC stack to vibrations for 1.5 h and monitoring the performance before and after the test. The stack remained intact and both the stack and individual cell voltages did not change. Based on these results, the vibration exposure did not impact the PEMFC stack performance.

Even though the previous studies indicated that vibrations can have a neutral or even positive effect, the other studies referenced here find the opposite result. Hou et al. [49] applied an extreme vibration stress on a PEMFC stack. Their protocol lasted for 250 h, and applied acceleration in the X, Y and Z plane with a maximum of 1.7, 2.0 and 4.7 g respectively (i.e. 16.7, 19.6 and 46.1 m/s^2). Hydrogen leakage, assessed with an anode leak test, was 1.7 times higher than at the start of the test, and cell performance decreased mainly due to a 5.4 % increase in the ohmic resistance. The authors contribute this to changes in contact resistance due to variations in clamping pressure.

While most researchers consider automotive, road-induced vibrations [49,164,165,167], Qiu et al. [166] took ships as use-case for their study. Their simple, single channel PEMFC simulation predicted the concentration of hydrogen in the anode components under a vibration of 0.2 mm and 2 Hz. The outcomes suggest that fuel consumption goes up with vibration intensity, eventually leading to fuel starvation. It remains unclear how the authors define the fuel consumption and the publication lacks more detailed explanation why vibration would lead to changes in H_2 consumption. Moreover, the model is not validated, and it is based on macro scale fluid mechanics without electrochemical foundations. Therefore these results should be investigated in more detail before accepting the outcomes.

The numerical studies by Banan et al. [164,165] included vibration conditions that fall within the Lloyds Register boundaries. With a two-dimensional finite element model they simulate damage propagation due to vibration frequency and amplitude as well as initial delamination state [164]. In the second publication [165] they simulated simultaneous hygrothermal cycles. Both amplitude and frequency impact propagation of cracks and delamination. The effect of acceleration amplitude was non-linear, increasing it from of 1 to 3 g caused an increase in final delamination length. Yet, increasing the acceleration from 3 and 4 g resulted only in a slightly increased delamination length. At acceleration amplitudes below 0.5 g, no damage propagation was observed in the 300 h simulation [164]. When hygrothermal cycles

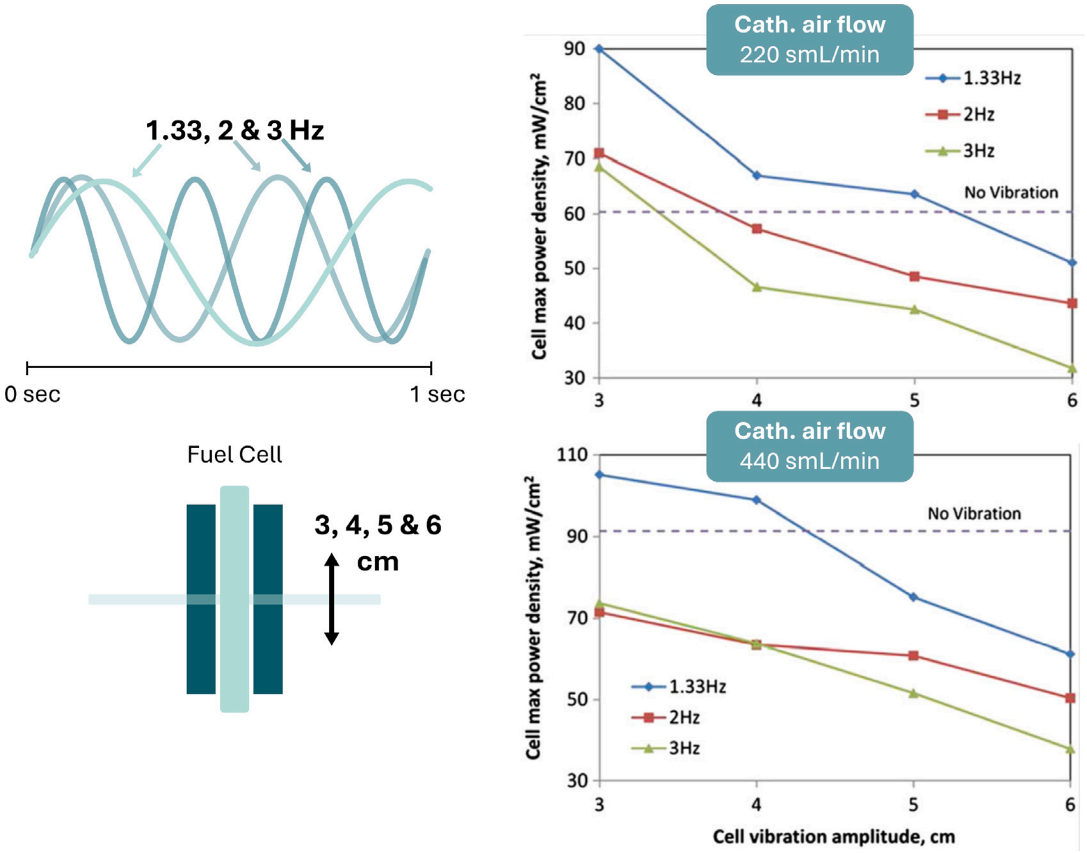

Fig. 7. Schematic representation of vibration experiment by El-Emam et al. [162] and two graphs from their publication of PEMFC power density at different displacements and frequencies. The top graph shows results at a cathode air flow rate of 220 sml/min while the bottom graph includes results at 440 sml/min.

are added to the vibrations, they have a dominating effect on damage propagation. Vibrations seem to have a stronger effect on delamination between the CL and membrane than on propagating membrane cracks [165].

The works cited above indicate that vibration could be both beneficial or damaging, depending on operational parameters such as air and hydrogen flow. Still, the 250 h experiment by Hou et al. [49] does suggest that vibrations could cause serous damage on the long run. It is still unclear whether these conditions are also relevant for maritime applications. Only the work by Qiu et al. [166] was specifically designed to study ship-related vibrations. Their results are interesting, yet the model was not validated with experimental work. In addition, vibrations might also impact the BoP and linked control system, as was the case in the inclination studies by Van Veldhuizen et al. [163]. Clearly, also in this field additional research is required to distinguish if ship vibrations have positive or negative consequences for PEMFC durability.

5.3. Motion induced degradation schematics

This section also concludes with a set of degradation schematics, as seen earlier in Sections 3.8 and 4.7. Section 3.8 includes a more detailed description of how they are set-up. Fig. 8(b) is the only figure with green arrows, showing that aside from damaging, negative impacts, the vibration can also have a positive influence on the PEMFC performance. The extent to which this also holds on the long term is still to be studied. This is in line with the fact that both Figs. 8(a) and 8(b) have more orange broken arrows compared to the other seven overviews, indicating that many of the mechanisms are still hypothesized rather than proven. This highlights the need for further research in this field of motion-based degradation, to improve our knowledge and understanding of the underlying principles. This understanding is a requirement for improving PEMFC operation under vibration and inclination conditions.

6. Insights from schematics

This review aims to provide more insight into PEMFC degradation mechanisms relevant for maritime applications. Even though it is a complex phenomenon, the schematics included at the end of Sections 3–5 aid to demystify the various degradation paths. Earlier work also includes insightful overviews [132,133]. The ones presented here cover a broader range of degradation causes than Thiele et al. [132], who limit themselves to load based causes. By separating the schematics and using some line color and style changes, we aim to make the overview more intuitive than the one from Zhang et al. [133]. More importantly, both other publications focus at automotive, rather than maritime context. In the schematics presented here, important factors such as NaCl degradation and inclination are also included.

The overviews link causes, mechanisms and monitoring options, allowing readers to:

1. Identify and relate monitoring observations to potential causes — e.g. linking fluoride emissions to PFSA damage and its various causes including idle load operation (Fig. 6(b)) or intrusion of Cl^- or metal ions (Figs. 3(a) and 3(b));
2. Oversee various mechanisms related to one cause — e.g. Fig. 6(c) shows how dynamic load operation is linked to a broad cascade of damage mechanisms such as PFSA damage, carbon corrosion,

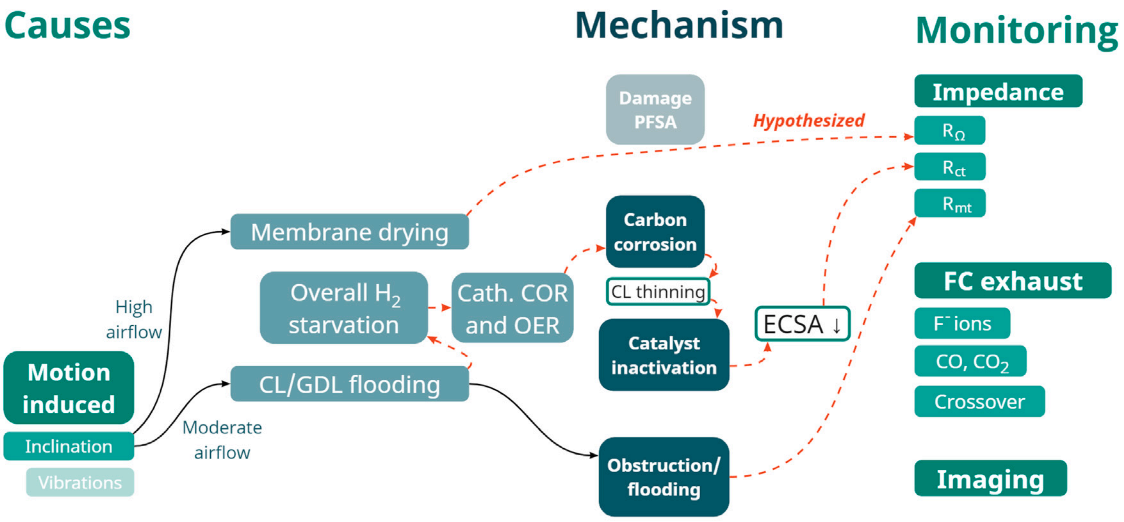

(a) Inclined operation degradation

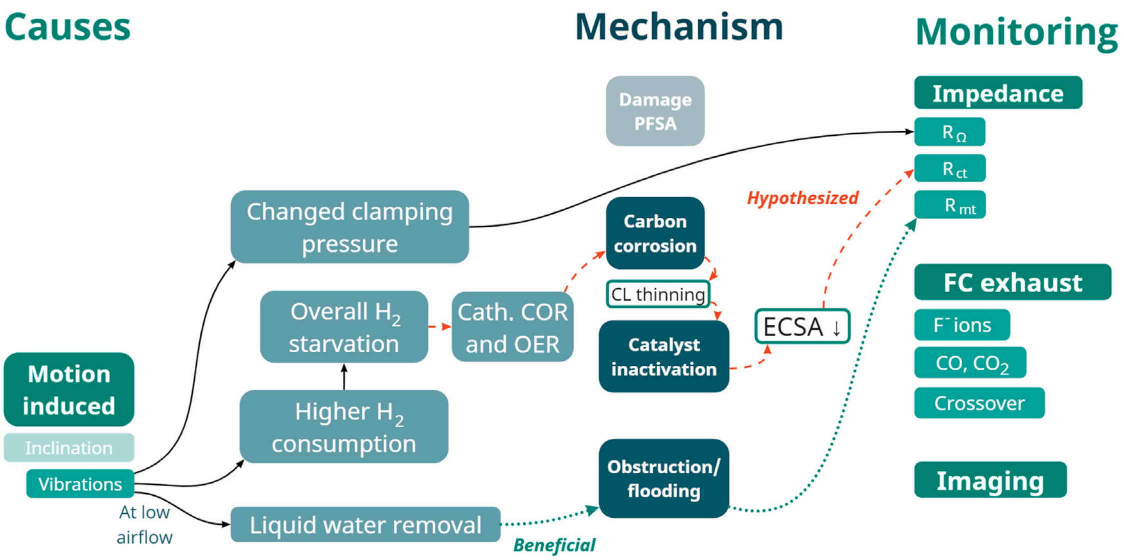

(b) Vibration induced degradation

Fig. 8. Schematics of motion-induced degradation mechanisms and possible monitoring options. Orange broken lines indicate that the relation has not been reported in the referenced publication, but is still hypothesized to occur. Green broken lines indicate that the mechanism can improve PEMFC performance. ECSA stands for membrane electrode assembly, CL for catalyst layer, COR for carbon oxidation reaction and OER for oxygen evolution reaction. (For interpretation of the references to colour in this figure legend, the reader is referred to the web version of this article.)

catalyst inactivation due to loss of support, sintering, platinum dissolution and Ostwald ripening;

3. Compare degradation phenomena at a glance, discriminating between them while also seeing their similarities — e.g. Fig. 3(c) pictures how all different contaminants listed in the figure adsorb to the catalyst, while some also link to other degradation mechanisms such as replacement of H^+ in the membrane;
4. Oversee overall degradation patterns when comparing all nine schematics (Figs. 3(a) to 3(c), 6(a) to 6(d), 8(a) and 8(b)) — e.g. ECSA reduction can occur with any of the degradation triggers. In some cases the reduced availability of catalyst particles only occurs indirectly via carbon corrosion. This is the case for start-up/shut-down, cold starts, inclined operation and PEMFC vibration (Figs. 6(a), 8(a) and 8(b)). All other degradation causes can directly cause catalyst area loss.

These schematic-characteristics facilitate interpretation of experimental work and aid in development of numerical models. This supports the development of maritime PEMFC, for which further research is still required as we will conclude in Section 7. It is worth pointing out that, aside from imaging techniques, the monitoring options are non-invasive, meaning that the analysis does not destroy the fuel cell. They can therefore be applied throughout the use of the fuel cell, regardless if it is a single cell in a lab or a full scale pilot plant.

Because the overviews are a visual summary of the literature cited in this review, it might well be that pathways can be added, or that the orange broken lines (which indicate hypothesized pathways), are proven in existing or future work. Nonetheless, even in the current state the schematics help to improve understanding, visualize relations and spark scientific discussions.

7. Conclusion

This review provides a comprehensive overview of PEMFC degradation specified to the maritime context. We identified the main causes, degradation mechanisms, and monitoring possibilities and summarized them in schematics. In addition, the review revealed several knowledge gaps.

Most PEMFC research focuses on single-cells and on automotive applications. It should broaden its scope by changing the EoL definition and by experimenting on stacks and systems. Rather than using the automotive DOE EoL definition, the EoL could be specified based various parameters such as safety indicators, economic parameters and power requirements. This allows to define application-specific (including maritime-specific) EoL criteria. In addition to the experiments and numerical studies on single cells, PEMFC degradation research should consider stacks or system tests. Especially when PEMFCs are scaled up to meet the high power and energy demands of sea going vessels, the additional complexity of cell-to-cell variation and the alignment and control of the BoP cannot be ignored. Short stack testing provides a compromise, it entails the cell-to-cell and system complexity without increasing experimental costs significantly.

Schematics are derived which categorize the degradation mechanisms as (i) radical damage to the PFSA, (ii) carbon corrosion, (iii) catalyst inactivation, and (iv) reactant blockage. These mechanisms are used to link the causes of degradation (contamination, load, and movement-based stressors) to various damage indicators (impedance measurements, exhaust analysis and imaging techniques). This accessible overview can help scientists and maritime engineers to relate degradation monitoring data to fundamental causes. By doing so, it facilitates the development of more robust PEMFC designs and operational strategies.

The contamination, load, vibration and inclination based degradation studies provide a foundation for maritime PEMFC degradation, but knowledge gaps remain:

(1) Investigate load based degradation for distinct ship types based on representative load profiles to get insight into the combined, interconnected effect of maritime drive cycles;
(2) Determine reference values for air contamination inside ship engine rooms. Specifically air salinity and combustion contaminants (such as NOx, CO, CO_2, and benzene) are relevant to consider in maritime environments;
(3) Determine if PEMFCs can tolerate NaCl, and at what level, by conducting longer term (>50 h) salinity experiments with contamination concentrations that are representative of marine air. Currently, contamination experiments often last shorter, the tested concentrations vary significantly and are probably significantly higher than concentrations in sea air;
(4) Study contamination with H_2-carriers and their residues, especially promising carriers such as sodium borohydride ($NaBH_4$) and dibenzyl toluene ($C_{21}H_{20}$);
(5) Quantify the impact of long term moderate vibration, with amplitudes and frequencies representative of various ship types;
(6) Test the impact of dynamic inclination and analyze the degradation with additional characterization methods such as EIS and post-mortem imaging. Tests should clarify the factors influencing flooding and drying issues.

The outcomes of these research lines will improve power plant designs: maritime drive-cycle degradation research aids in selection of the right power plant components; cathode contamination research can dictate the type of air treatment needed for (sea going) vessels, H_2-carrier degradation research can contribute to ongoing scientific debates on the best way to store H_2 on board of ships; and inclination and vibration studies can give insight into the need for motion compensation in PEMFC systems. All these insights will promote the adaptation and adoption of maritime PEMFCs and by doing so, bring us a step closer to zero-emission shipping.

CRediT authorship contribution statement

Annabel Broer: Writing – original draft, Visualization, Formal analysis, Data curation, Conceptualization. **Henk Polinder:** Writing – review & editing, Supervision, Conceptualization. **Lindert van Biert:** Writing – review & editing, Conceptualization.

Declaration of competing interest

The authors declare that they have no known competing financial interests or personal relationships that could have appeared to influence the work reported in this paper.

Acknowledgments

This work is part of the SH2IPDRIVE project, which is funded by the Netherlands Enterprise Agency (RvO) from subsidy nr. MOB21013.

Appendix A. Supplementary data

Supplementary material related to this article can be found online at https://doi.org/10.1016/j.jpowsour.2025.236678. It contains three clarifying images supporting content of section 2.1, 4.2 and 5.

Data availability

Code available at: https://doi.org/10.4121/c56334c8-31ae-43eb-9b74-e02805c20ed2.

References

[1] International Chamber of Shipping, Shipping and world trade: World seaborne trade, 2018, URL: https://www.ics-shipping.org/shipping-fact/shipping-and-world-trade-world-seaborne-trade/#:~:text=The%20international%20shipping%20industry%20is,would%20simply%20not%20be%20possible.
[2] IMO, Fourth IMO Greenhouse Gas Study, English. Tech. Rep., 2020.
[3] Sirimanne, Review of Maritime Transport - Towards a Green and Just Transition, Tech. Rep., United Nations, Geneva, 2023, ISBN: 978-92-1-002886-8. URL: https://unctad.org/publication/review-maritime-transport-2023.
[4] European Environment Agency and European Maritime Safety Agency, European Maritime Transport Environmental Report 2021, Publications Office of the European Union, Luxenburg, 2021, en. Environmental Report 1. ISBN 978-92-9480-371-9 ISSN 1977-8449 doi:10.2800/3525. URL: https://data.europa.eu/doi/10.2800/3525. (Visited on 29 January 2025).
[5] European Environmental Agency, Contribution of the transport sector to total emissions of the main air pollutants, english, 2019, URL: https://www.eea.europa.eu/data-and-maps/daviz/contribution-of-the-transport-sector-6#tab-chart_4.
[6] IMO, Resolution MEPC.377(80): 2023 IMO Strategy on Reduction of GHG Emissions from Ships, English. Tech. Rep., IMO, 2023.
[7] Artur J. Majewski, An introduction to Fuel Cell, Electrolyser and Hydrogen Technology & Applications, Athens, 2023, English. Lecture. URL: https://www.jess-summerschool.eu/week-1.
[8] L. Van Biert, M. Godjevac, K. Visser, P.V. Aravind, A review of fuel cell systems for maritime applications, J. Power Sources (ISSN: 03787753) 327 (2016) 345–364, http://dx.doi.org/10.1016/j.jpowsour.2016.07.007, URL: https://linkinghub.elsevier.com/retrieve/pii/S0378775316308631. (Visited on 26 July 2022).
[9] IDTechEx, Online summary - Fuel Cell Boats & Ships 2023–2033: PEMFC, SOFC, Hydrogen, Ammonia, LNG, English. Tech. Rep., 2022, URL: https://www.idtechex.com/en/research-report/fuel-cell-boats-and-ships-2023-2033-pemfc-sofc-hydrogen-ammonia-lng/907.
[10] Marco Gianni, Andrea Pietra, Rodolfo Taccani, Outlook of future implementation of PEMFC and SOFC onboard cruise ships, in: U. Desideri, L. Ferrari, J. Yan (Eds.), in: E3S Web of Conferences, vol. 238, 2021, p. 04004, http://dx.doi.org/10.1051/e3sconf/202123804004, URL: https://www.e3s-conferences.org/10.1051/e3sconf/202123804004. (Visited on 27 January 2025).
[11] Ahmed G. Elkafas, Massimo Rivarolo, Eleonora Gadducci, Loredana Magistri, Aristide F. Massardo, Fuel cell systems for maritime: A review of research development, commercial products, applications, and perspectives, Processes (ISSN: 2227-9717) 11 (1) (2022) 97, http://dx.doi.org/10.3390/pr11010097, URL: https://www.mdpi.com/2227-9717/11/1/97. (Visited on 27 January 2025).

[12] Sami Kanerva, Klaus Vänskä, Hansueli Krattiger, Fuel Cells in Commercial Marine Applications, ABB, 2021, Online. URL: https://library.e.abb.com/public/ff09a86b8e2b40c7a390e5ff322b885d/Fuel+cells+in+commercial+marine+applications.pdf?x-sign=lEUru1RTLNGKH8eMqanLGIkTppFIWIPMjjaVv5Crhb7DEjKbb%2FsxPN58mjdgYczd.

[13] Rod Borup, Jeremy Meyers, Bryan Pivovar, Yu Seung Kim, Rangachary Mukundan, Nancy Garland, Deborah Myers, Mahlon Wilson, Fernando Garzon, David Wood, Piotr Zelenay, Karren More, Ken Stroh, Tom Zawodzinski, James Boncella, James E. McGrath, Minoru Inaba, Kenji Miyatake, Michio Hori, Kenichiro Ota, Zempachi Ogumi, Seizo Miyata, Atsushi Nishikata, Zyun Siroma, Yoshiharu Uchimoto, Kazuaki Yasuda, Ken-ichi Kimijima, Norio Iwashita, Scientific aspects of polymer electrolyte fuel cell durability and degradation, Chem. Rev. 107 (10) (2007) 3904–3951, http://dx.doi.org/10.1021/cr050182l, ISSN: 1520-6890. URL: https://pubs.acs.org/doi/10.1021/cr050182l. (Visited on 06 May 2024).

[14] A. Baroutaji, J.G. Carton, M. Sajjia, A.G. Olabi, Materials in PEM fuel cells, in: Materials Science and Materials Engineering, Elsevier, ISBN: 978-0-12-803581-8, 2016, http://dx.doi.org/10.1016/B978-0-12-803581-8.04006-6, URL: https://www.sciencedirect.com/science/article/pii/B9780128035818040066. (Visited on 15 October 2022).

[15] Frank A. De Bruijn, Gaby J.M. Janssen, PEM fuel cell materials: Costs, performance and durability, in: Klaus-Dieter Kreuer (Ed.), Fuel Cells, Springer New York, New York, NY, ISBN: 978-1-4614-5784-8, 2013, pp. 249–303, http://dx.doi.org/10.1007/978-1-4614-5785-5_9, URL: https://link.springer.com/10.1007/978-1-4614-5785-5_9. (Visited on 29 July 2024).

[16] Abhi Parekh, Recent developments of proton exchange membranes for PEMFC: A review, Front. Energy Res. (ISSN: 2296-598X) 10 (2022) 956132, http://dx.doi.org/10.3389/fenrg.2022.956132, URL: https://www.frontiersin.org/articles/10.3389/fenrg.2022.956132/full. (Visited on 29 July 2024).

[17] Fangling Jiang, Fengjuan Zhu, Fan Yang, Xiaohui Yan, Aiming Wu, Liuxuan Luo, Xiaolin Li, Junliang Zhang, Comparative investigation on the activity degradation mechanism of Pt/C and PtCo/C electrocatalysts in PEMFCs during the accelerate degradation process characterized by an in situ X-ray absorption fine structure, ACS Catal. 10 (1) (2020) 604–612, http://dx.doi.org/10.1021/acscatal.9b04598, Number: 1.

[18] Xuan Cheng, Zheng Shi, Nancy Glass, Lu Zhang, Jiujun Zhang, Datong Song, Zhong-Sheng Liu, Haijiang Wang, Jun Shen, A review of PEM hydrogen fuel cell contamination: Impacts, mechanisms, and mitigation, J. Power Sources (ISSN: 03787753) 165 (2) (2007) 739–756, http://dx.doi.org/10.1016/j.jpowsour.2006.12.012, URL: https://linkinghub.elsevier.com/retrieve/pii/S0378775306025304. (Visited on 13 January 2023).

[19] Peng Ren, Pucheng Pei, Yuehua Li, Ziyao Wu, Dongfang Chen, Shangwei Huang, Degradation mechanisms of proton exchange membrane fuel cell under typical automotive operating conditions, Prog. Energy Combust. Sci. 80 (2020) 100859, http://dx.doi.org/10.1016/j.pecs.2020.100859, Publisher: Elsevier Ltd. URL: https://linkinghub.elsevier.com/retrieve/pii/S0360128520300691.

[20] Michael A. Schmid, Tim Wagner, Benjamin Wiedemann, Joachim Scholta, Effects of impurities in the cathode airflow on proton exchange membrane fuel cell stacks, Fuel Cells 22 (6) (2022) 254–270, http://dx.doi.org/10.1002/fuce.202200063, ISSN: 1615-6854. URL: https://onlinelibrary.wiley.com/doi/10.1002/fuce.202200063. (Visited on 12 February 2024).

[21] Jinfeng Wu, Xiao Zi Yuan, Jonathan J. Martin, Haijiang Wang, Jiujun Zhang, Jun Shen, Shaohong Wu, Walter Merida, A review of PEM fuel cell durability: Degradation mechanisms and mitigation strategies, J. Power Sources (ISSN: 03787753) 184 (1) (2008) 104–119, http://dx.doi.org/10.1016/j.jpowsour.2008.06.006, URL: https://linkinghub.elsevier.com/retrieve/pii/S0378775308011968. (Visited on 24 January 2025).

[22] Jianlu Zhang, Huamin Zhang, Jinfeng Wu, Jiujun Zhang, PEM Fuel Cell Testing and Diagnosis, Elsevier, ISBN: 978-0-444-53688-4, 2013, http://dx.doi.org/10.1016/B978-0-444-53688-4.05001-4, URL: https://linkinghub.elsevier.com/retrieve/pii/B9780444536884050014. (Visited on 02 February 2023).

[23] Jiujun Zhang (Ed.), PEM Fuel Cell Electrocatalysts and Catalyst Layers: Fundamentals and Applications, Springer London, London, ISBN: 978-1-84800-935-6, 2008, http://dx.doi.org/10.1007/978-1-84800-936-3, URL: https://link.springer.com/10.1007/978-1-84800-936-3. (Visited on 26 January 2023).

[24] Quentin Meyer, Yachao Zeng, Chuan Zhao, In situ and operando characterization of proton exchange membrane fuel cells, Adv. Mater. 31 (40) (2019) 1–25, http://dx.doi.org/10.1002/adma.201901900, Number: 40.

[25] Y. Nabae, Q. Yuan, S. Nagata, K. Kusaba, T. Aoki, N. Takao, T. Itoh, M. Arao, H. Imai, K. Higashi, T. Sakata, T. Uruga, Y. Iwasawa, In situ X-ray absorption spectroscopy to monitor the degradation of Fe/N/C cathode catalyst in proton exchange membrane fuel cells, J. Electrochem. Soc. 168 (1) (2021) http://dx.doi.org/10.1149/1945-7111/abdc64, Number: 1 Publisher: IOP Publishing.

[26] Shiro Tanaka, Arnaud G. Malan, Investigating design parameters of a perforated metal gas diffusion layer in a polymer electrolyte membrane fuel cell, J. Power Sources (ISSN: 0378-7753) 413 (2019) 198–208, http://dx.doi.org/10.1016/j.jpowsour.2018.12.045, URL: https://www.sciencedirect.com/science/article/pii/S037877531831396X. (Visited on 23 November 2022).

[27] Xianguo Li, Imran Sabir, Review of bipolar plates in PEM fuel cells: Flow-field designs, Int. J. Hydrog. Energy 30 (4) (2005) 359–371, http://dx.doi.org/10.1016/j.ijhydene.2004.09.019, Number: 4.

[28] James Larminie, Andrew Dicks, Fuel Cell Systems Explained, second ed., J. Wiley, Chichester, West Sussex, ISBN: 978-0-470-84857-9, 2003.

[29] Li Qingfeng, LT03 Electrolytes for LT Fuel Cells & Electrolysers, Athens, 2023, URL: https://www.jess-summerschool.eu/week-1.

[30] Andrei A. Kulikovsky, Chapter 1 - Fuel cell basics, in: Analytical Modeling of Fuel Cells, Elsevier, ISBN: 978-0-444-64222-6, 2019, pp. 1–33, http://dx.doi.org/10.1016/B978-0-44-464222-6.00008-3, URL: https://linkinghub.elsevier.com/retrieve/pii/B9780444642226000083. (Visited on 18 August 2022).

[31] Heikki Kumpulainen, Terttu Peltonen, Ulla Koponen, Mikael Bergelin, Matti Valkiainen, Mikael Wasberg, In situ voltammetric characterization of PEM fuel cell catalyst layers, VTT Tiedotteita, Espoo, ISBN: 951-38-5888-X, 2002, p. 28, English. Research Notes 2137.

[32] Shingo Kanazawa, Eiji Tada, A. Nishikata, Tooru Tsuru, EIS and CV characteristics of Pt cathode catalyst in PEMFC, ECS Meet. Abstr. (ISSN: 2151-2043) MA2012-02 (2) (2012) 149, http://dx.doi.org/10.1149/MA2012-02/2/149, URL: https://iopscience.iop.org/article/10.1149/MA2012-02/2/149. (Visited on 07 August 2024).

[33] Narayanamoorthy Bhuvanendran, Sabarinathan Ravichandran, Qian Xu, Thandavarayan Maiyalagan, Huaneng Su, A quick guide to the assessment of key electrochemical performance indicators for the oxygen reduction reaction: A comprehensive review, Int. J. Hydrog. Energy (ISSN: 03603199) 47 (11) (2022) 7113–7138, http://dx.doi.org/10.1016/j.ijhydene.2021.12.072, URL: https://linkinghub.elsevier.com/retrieve/pii/S0360319921047728. (Visited on 06 August 2024).

[34] Noémie Elgrishi, Kelley J. Rountree, Brian D. McCarthy, Eric S. Rountree, Thomas T. Eisenhart, Jillian L. Dempsey, A practical beginner's guide to cyclic voltammetry, J. Chem. Educ. 95 (2) (2018) 197–206, http://dx.doi.org/10.1021/acs.jchemed.7b00361, ISSN: 1938-1328. URL: https://pubs.acs.org/doi/10.1021/acs.jchemed.7b00361. (Visited on 06 August 2024).

[35] P. Lettenmeier, S. Kolb, N. Sata, A. Fallisch, L. Zielke, S. Thiele, A.S. Gago, K.A. Friedrich, Comprehensive investigation of novel poregraded gas diffusion layers for high-performance and cost-effective proton exchange membrane electrolyzers, Energy Environ. Sci. 10 (12) (2017) 2521–2533, http://dx.doi.org/10.1039/c7ee01240c, Number: 12 Publisher: Royal Society of Chemistry.

[36] Zhepeng Tang, Qiu An Huang, Yan Jie Wang, Fangzhou Zhang, Weiheng Li, Aijun Li, Lei Zhang, Jiujun Zhang, Recent progress in the use of electrochemical impedance spectroscopy for the measurement, monitoring, diagnosis and optimization of proton exchange membrane fuel cell performance, J. Power Sources 468 (June) (2020) 228361, http://dx.doi.org/10.1016/j.jpowsour.2020.228361, Number: June Publisher: Elsevier B.V. URL: https://doi.org/10.1016/j.jpowsour.2020.228361.

[37] E. Ejiri, K. Yamada, Experimental study on performance of a banded structure membrane fuel cell, J. Fuel Cell Sci. Technol. 6 (3) (2009) 031001, http://dx.doi.org/10.1115/1.3005385, ISSN:1551-6989. URL: https://asmedigitalcollection.asme.org/electrochemical/article/doi/10.1115/1.3005385/470250/Experimental-Study-on-Performance-of-a-Banded. (Visited on 08 August 2022).

[38] Maximilian Grandi, Kurt Mayer, Matija Gatalo, Gregor Kapun, Francisco Ruiz-Zepeda, Bernhard Marius, Miran Gaberšček, Viktor Hacker, The influence catalyst layer thickness on resistance contributions of PEMFC determined by electrochemical impedance spectroscopy, Energies (ISSN: 1996-1073) 14 (21) (2021) 7299, http://dx.doi.org/10.3390/en14217299, URL: https://www.mdpi.com/1996-1073/14/21/7299. (Visited on 09 May 2024).

[39] Yena Choi, Woojung Lee, Youngseung Na, Effect of gravity and various operating conditions on proton exchange membrane water electrolysis cell performance, Membranes (ISSN: 2077-0375) 11 (11) (2021) 822, http://dx.doi.org/10.3390/membranes11110822, URL: https://www.mdpi.com/2077-0375/11/11/822. (Visited on 31 March 2023).

[40] J.J. Giner-Sanz, E.M. Ortega, V. Pérez-Herranz, Mechanistic equivalent circuit modelling of a commercial polymer electrolyte membrane fuel cell, J. Power Sources (ISSN: 2333-9144) 379 (October 2017) (2018) 328–337, http://dx.doi.org/10.1016/j.jpowsour.2018.01.066.

[41] Yongtaek Lee, Bosung Kim, Yongchan Kim, Xianguo Li, Effects of a microporous layer on the performance degradation of proton exchange membrane fuel cells through repetitive freezing, J. Power Sources (ISSN: 0378-7753) 196 (4) (2011) 1940–1947, http://dx.doi.org/10.1016/j.jpowsour.2010.10.028, URL: https://www.sciencedirect.com/science/article/pii/S0378775310017556. (Visited on 09 August 2022).

[42] Felix N. Büchi, Minoru Inaba, Thomas J. Schmidt (Eds.), Polymer Electrolyte Fuel Cell Durability, Springer New York, New York, NY, ISBN: 978-0-387-85534-9, 2009, http://dx.doi.org/10.1007/978-0-387-85536-3, (Visited on 26 July 2022).

[43] Qianwen Tang, Bing Li, Daijun Yang, Pingwen Ming, Cunman Zhang, Yanbo Wang, Review of hydrogen crossover through the polymer electrolyte membrane, Int. J. Hydrog. Energy (ISSN: 03603199) 46 (42) (2021) 22040–22061, http://dx.doi.org/10.1016/j.ijhydene.2021.04.050, Number: 42. URL: https://linkinghub.elsevier.com/retrieve/pii/S0360319921013550. (Visited on 26 July 2022).

[44] Tatsumi Kitahara, Hironori Nakajima, Gas diffusion media and NaCl contamination of polymer electrolyte fuel cells for marine applications, ECS Trans. 86 (13) (2018) 271–279, http://dx.doi.org/10.1149/08613.0271ecst, ISSN: 1938-6737. Number: 13. URL: https://iopscience.iop.org/article/10.1149/08613.0271ecst. (Visited on 26 July 2022).

[45] Jorben Mus, Challenges Related to the Application of Hydrogen Fuel Cells in Unmanned Aerial Vehicles, Ghent, Belgium, 2024, URL: https://www.ephyc2024.com/.

[46] Tim Lochner, Regina M. Kluge, Johannes Fichtner, Hany A. El-Sayed, Batyr Garlyyev, Aliaksandr S. Bandarenka, Temperature effects in polymer electrolyte membrane fuel cells, ChemElectroChem 7 (17) (2020) 3545–3568, http://dx.doi.org/10.1002/celc.202000588, Number: 17.

[47] Jundika C. Kurnia, Agus P. Sasmito, Tariq Shamim, Advances in proton exchange membrane fuel cell with dead-end anode operation: A review, Appl. Energy (ISSN: 03062619) 252 (2019) 113416, http://dx.doi.org/10.1016/j.apenergy.2019.113416, URL: https://linkinghub.elsevier.com/retrieve/pii/S0306261919310906. (Visited on 13 May 2024).

[48] Jing Yao, Zhen Wu, Bofei Wang, Yuchen Yang, Fusheng Yang, Zaoxiao Zhang, Jianwei Ren, Bo Li, High-stability dead-end anode proton exchange membrane fuel cells by purge optimization, J. Power Sources (ISSN: 03787753) 595 (2024) 234062, http://dx.doi.org/10.1016/j.jpowsour.2024.234062, URL: https://linkinghub.elsevier.com/retrieve/pii/S0378775324000132. (Visited on 13 May 2024).

[49] Yongping Hou, Dong Hao, Jianping Shen, Ping Li, Tao Zhang, Hong Wang, Effect of strengthened road vibration on performance degradation of PEM fuel cell stack, Int. J. Hydrog. Energy (ISSN: 03603199) 41 (9) (2016) 5123–5134, http://dx.doi.org/10.1016/j.ijhydene.2016.01.072, URL: https://linkinghub.elsevier.com/retrieve/pii/S0360319915312477. (Visited on 25 April 2024).

[50] Marie Lamard, Bruno Auvity, Paul Buttin, Sébastien Rosini, Clément Retière, Impact of nacl spray on the durability of PEMFC single cells and stacks in marine environment, J. Electrochem. Soc. 170 (2) (2023) 024504, http://dx.doi.org/10.1149/1945-7111/acb8e0, ISSN: 1945-7111. URL: https://iopscience.iop.org/article/10.1149/1945-7111/acb8e0. (Visited on 21 March 2023).

[51] Marie Lamard, Bruno Auvity, Paul Buttin, Sébastien Rosini, Clément Retière, Multiscale study of PEMFC in marine environment: Impact of a nacl spray on durability, ECS Trans. 109 (9) (2022) 251–263, http://dx.doi.org/10.1149/10909.0251ecst, ISSN: 1938-6737. URL: https://iopscience.iop.org/article/10.1149/10909.0251ecst. (Visited on 10 February 2023).

[52] Pucheng Pei, Xing Yuan, Pengxiang Chao, Xizhong Wang, Analysis on the PEM fuel cells after accelerated life experiment, Int. J. Hydrog. Energy (ISSN: 03603199) 35 (7) (2010) 3147–3151, http://dx.doi.org/10.1016/j.ijhydene.2009.09.103, URL: https://linkinghub.elsevier.com/retrieve/pii/S0360319909015742. (Visited on 04 January 2023).

[53] Tatyana V. Reshetenko, Comprehensive analysis of recovery procedures for SO2-contaminated proton exchange membrane fuel cells, Electrochim. Acta (ISSN: 00134686) 507 (2024) 145168, http://dx.doi.org/10.1016/j.electacta.2024.145168, URL: https://linkinghub.elsevier.com/retrieve/pii/S0013468624014051. (Visited on 24 January 2025).

[54] M.S. Mikkola, T. Rockward, F.A. Uribe, B.S. Pivovar, The effect of NaCl in the cathode air stream on PEMFC performance, Fuel Cells 7 (2) (2007) 153–158, http://dx.doi.org/10.1002/fuce.200600206, ISSN: 1615-6854. URL: https://onlinelibrary.wiley.com/doi/10.1002/fuce.200600206. (Visited on 26 July 2022).

[55] N. Rajalakshmi, S. Pandian, K.S. Dhathathreyan, Vibration tests on a PEM fuel cell stack usable in transportation application, Int. J. Hydrog. Energy (ISSN: 0360-3199) 34 (9) (2009) 3833–3837, http://dx.doi.org/10.1016/j.ijhydene.2009.03.002, URL: https://www.sciencedirect.com/science/article/pii/S0360319909003450. (Visited on 08 August 2022).

[56] R. Mohtadi, W.K. Lee, S. Cowan, J.W. Van Zee, Mahesh Murthy, Effects of hydrogen sulfide on the performance of a PEMFC, Electrochem. Solid-State Lett. (ISSN: 10990062) 6 (12) (2003) A272, http://dx.doi.org/10.1149/1.1621831, URL: https://iopscience.iop.org/article/10.1149/1.1621831. (Visited on 26 January 2023).

[57] Alireza Sadeghi Alavijeh, Ramin M.H. Khorasany, Zachary Nunn, Aronne Habisch, Michael Lauritzen, Erin Rogers, G. Gary Wang, Erik Kjeang, Microstructural and mechanical characterization of catalyst coated membranes subjected to in situ hygrothermal fatigue, J. Electrochem. Soc. 162 (14) (2015) F1461–F1469, http://dx.doi.org/10.1149/2.0471514jes, Number: 14.

[58] S.J.C. Cleghorn, D.K. Mayfield, D.A. Moore, J.C. Moore, G. Rusch, T.W. Sherman, N.T. Sisofo, U. Beuscher, A polymer electrolyte fuel cell life test: 3 years of continuous operation, J. Power Sources (ISSN: 03787753) 158 (1) (2006) 446–454, http://dx.doi.org/10.1016/j.jpowsour.2005.09.062, URL: https://linkinghub.elsevier.com/retrieve/pii/S0378775305013546. (Visited on 02 October 2023).

[59] Zhiguang Hua, Zhixue Zheng, Elodie Pahon, Marie-Cécile Péra, Fei Gao, A review on lifetime prediction of proton exchange membrane fuel cells system, J. Power Sources (ISSN: 03787753) 529 (2022) 231256, http://dx.doi.org/10.1016/j.jpowsour.2022.231256, URL: https://linkinghub.elsevier.com/retrieve/pii/S0378775322002737. (Visited on 22 June 2022).

[60] Huicui Chen, Pucheng Pei, Mancun Song, Lifetime prediction and the economic lifetime of proton exchange membrane fuel cells, Appl. Energy (ISSN: 1872-9118) 142 (2015) 154–163, http://dx.doi.org/10.1016/j.apenergy.2014.12.062, URL: https://linkinghub.elsevier.com/retrieve/pii/S0306261914013191. (Visited on 26 July 2022).

[61] Pucheng Pei, Qianfei Chang, Tang Tang, A quick evaluating method for automotive fuel cell lifetime, Int. J. Hydrog. Energy (ISSN: 03603199) 33 (14) (2008) 3829–3836, http://dx.doi.org/10.1016/j.ijhydene.2008.04.048, URL: https://linkinghub.elsevier.com/retrieve/pii/S036031990800476X. (Visited on 20 February 2023).

[62] Xiaosong Hu, Changfu Zou, Xiaolin Tang, Teng Liu, Lin Hu, Cost-optimal energy management of hybrid electric vehicles using fuel cell/battery health-aware predictive control, IEEE Trans. Power Electron. 35 (1) (2020) 382–392, http://dx.doi.org/10.1109/TPEL.2019.2915675, ISSN: 0885-8993, 1941-0107. URL: https://ieeexplore.ieee.org/document/8709824/. (Visited on 04 January 2023).

[63] Yebeen Kim, Jiwoong Kim, Kyoungdoug Min, Analysis of power consumption on BOP system in a fuel cell electric bus according to the fuel cell load range, Int. J. Automot. Technol. 25 (4) (2024) 701–715, http://dx.doi.org/10.1007/s12239-024-00064-0, ISSN: 1976-3832. URL: https://link.springer.com/10.1007/s12239-024-00064-0. (Visited on 03 January 2023).

[64] Robert Benesch, Tracey Jacksier, Hydrogen and Material Quality Issues for PEM Fuel Cells, IEEE, Chicago, IL, USA, ISBN: 978-0-7803-9280-9, 2005, pp. 481–486, http://dx.doi.org/10.1109/VPPC.2005.1554601, URL: http://ieeexplore.ieee.org/document/1554601/. (Visited on 04 October 2024).

[65] Dharmjeet Madhav, Junru Wang, Rajesh Keloth, Jorben Mus, Frank Buysschaert, Veerle Vandeginste, A review of proton exchange membrane degradation pathways, mechanisms, and mitigation strategies in a fuel cell, Energies (ISSN: 1996-1073) 17 (5) (2024) 998, http://dx.doi.org/10.3390/en17050998, URL: https://www.mdpi.com/1996-1073/17/5/998. (Visited on 08 August 2023).

[66] Hui Li, Shanna Knights, Zheng Shi, John W. Van Zee, Jiujun Zhang, Proton Exchange Membrane Fuel Cells: Contamination and Mitigation StrategiesZheng Shi, Datong Song, Hui Li, Jianlu Zhang, Zhong-Sheng Liu, Jiujun Zhang, first ed., CRC Press, Boca Raton, ISBN: 978-0-429-13268-1, 2010, http://dx.doi.org/10.1201/EBK1439806784, URL: https://books.google.nl/books?hl=nl&lr=&id=cyO6nUKOD9EC&oi=fnd&pg=PA179&dq=Cathode+Contamination+Modeling+By+Zheng+Shi&ots=DTxkism3xs&sig=DN4kFVgjBguqDIaMBu-t_n5L8VA&redir_esc=y#v=onepage&q=VOC&f=false. (Visited on 03 April 2024).

[67] EEA and ESRA, NOx emissions from ships in European seas, 2019, URL: https://www.eea.europa.eu/data-and-maps/figures/nox-emissions-from-ships-in.

[68] Christophe Leroy, Steven Huleu, A common sense approach for h2s release during dredging, Terra et Aqua (139) (2015) 5–10, URL: http://www.xn–igv441h.com/pdf/article-a-common-sense-approach-for-h2s-release-during-dredging-139-1.pdf.

[69] Yinqi Zhao, Yejun Mao, Weixian Zhang, Yanli Tang, Peizhen Wang, Reviews on the effects of contaminations and research methodologies for PEMFC, Int. J. Hydrog. Energy (ISSN: 03603199) 45 (43) (2020) 23174–23200, http://dx.doi.org/10.1016/j.ijhydene.2020.06.145, URL: https://linkinghub.elsevier.com/retrieve/pii/S0360319920323004. (Visited on 07 August 2023).

[70] B. Shabani, M. Hafttananian, Sh. Khamani, A. Ramiar, A.A. Ranjbar, Poisoning of proton exchange membrane fuel cells by contaminants and impurities: Review of mechanisms, effects, and mitigation strategies, J. Power Sources (ISSN: 03787753) 427 (2019) 21–48, http://dx.doi.org/10.1016/j.jpowsour.2019.03.097, URL: https://linkinghub.elsevier.com/retrieve/pii/S0378775319303520. (Visited on 26 August 2022).

[71] Tatyana V. Reshetenko, Jean St-Pierre, Study of the aromatic hydrocarbons poisoning of platinum cathodes on proton exchange membrane fuel cell spatial performance using a segmented cell system, J. Power Sources (ISSN: 03787753) 333 (2016) 237–246, http://dx.doi.org/10.1016/j.jpowsour.2016.09.165, URL: https://linkinghub.elsevier.com/retrieve/pii/S0378775316313647. (Visited on 23 May 2024).

[72] U. Misz, A. Talke, A. Heinzel, G. Konrad, Sensitivity analyses on the impact of air contaminants on automotive fuel cells, Fuel Cells 16 (4) (2016) 444–462, http://dx.doi.org/10.1002/fuce.201500159, ISSN: 1615-6854. URL: https://onlinelibrary.wiley.com/doi/10.1002/fuce.201500159. (Visited on 23 May 2024).

[73] Jon M. Moore, Paul L. Adcock, J. Barry Lakeman, Gary O. Mepsted, The effects of battlefield contaminants on PEMFC performance, 2000.

[74] Annabel Broer, Henk Polinder, Lindert Van Biert, Salinity and Volatile Organic Compounds in Engine Room air of a Sea-Going Vessel, Delft, 2025.

[75] IMPELL Purification Technologies LP, VOC air purifiers & fume extraction systems, Applications (2024) URL: https://ipsystemsusa.com/applications/wave-solder-maintenance/.

[76] Albert Subrenat, Jean-Noël Baléo, Pierre Le Cloirec, Analysis of pressure drops in pleated activated carbon cloth filters, J. Environ. Eng. 126 (6) (2000) 562–568, http://dx.doi.org/10.1061/(ASCE)0733-9372(2000)126:6(562), ISSN: 1943-7870. URL: https://ascelibrary.org/doi/10.1061/%28ASCE%290733-9372%282000%29126%3A6%28562%29. (Visited on 16 September 2024).

[77] Nedstack, PemGen CHP-FCPS-100 Datasheet, Nedstack fuel cell technology B.V., Arnhem, The Netherlands, p. 2, English. Datasheet.

[78] Thor Aarhaug, Hydrogen purity introduction workshop, 2019, URL: https://www.sintef.no/globalassets/projectweb/metrohyve-2/2-1-metrohydraite-aarhaug_hp_v1.pdf.

[79] Erin S. Van Rheenen, Johan T. Padding, Chris Slootweg, Klaas Visser, A review of the potential of hydrogen carriers for zero emission, low signature ship propulsion systems, 2022, http://dx.doi.org/10.24868/10649, URL: https://library.imarest.org/record/10649. (Visited on 13 January 2023).

[80] Hongfei Cheng, John Wang, Chuan Wu, Zhaolin Liu, Electrocatalysts for formic acid-powered PEM fuel cells: Challenges and prospects, Energy Mater. Adv. (ISSN: 2692-7640) 4 (2023) 0067, http://dx.doi.org/10.34133/energymatadv.0067, URL: https://spj.science.org/doi/10.34133/energymatadv.0067. (Visited on 07 August 2024).

[81] Phan Anh Duong, Borim Ryu, Jinwon Jung, Hokeun Kang, Design, modelling, and thermodynamic analysis of a novel marine power system based on methanol solid oxide fuel cells, integrated proton exchange membrane fuel cells, and combined heat and power production, Sustainability (ISSN: 2071-1050) 14 (19) (2022) 12496, http://dx.doi.org/10.3390/su141912496, URL: https://www.mdpi.com/2071-1050/14/19/12496. (Visited on 30 July 2024).

[82] Hayoung Jang, Byongug Jeong, Peilin Zhou, Seungman Ha, Chybyung Park, Dong Nam, Ahmad Rashedi, Parametric trend life cycle assessment for hydrogen fuel cell towards cleaner shipping, J. Clean. Prod. (ISSN: 09596526) 372 (2022) 133777, http://dx.doi.org/10.1016/j.jclepro.2022.133777, URL: https://linkinghub.elsevier.com/retrieve/pii/S0959652622033546. (Visited on 10 February 2023).

[83] B. Lindström, Hydrogen generation by steam reforming of methanol over copper-based catalysts for fuel cell applications, Int. J. Hydrog. Energy (ISSN: 03603199) 26 (9) (2001) 923–933, http://dx.doi.org/10.1016/S0360-3199(01)00034-9, URL: https://linkinghub.elsevier.com/retrieve/pii/S0360319901000349. (Visited on 06 August 2024).

[84] Apoorva M. Ranjekar, Ganapati D. Yadav, Steam reforming of methanol for hydrogen production: A critical analysis of catalysis, processes, and scope, Ind. Eng. Chem. Res. 60 (1) (2021) 89–113, http://dx.doi.org/10.1021/acs.iecr.0c05041, ISSN: 1520-5045. URL: https://pubs.acs.org/doi/10.1021/acs.iecr.0c05041. (Visited on 06 August 2024).

[85] Cheng-Chun Chen, Ming-Shan Jeng, Chih-Hsing Leu, Chang-Chung Yang, Yu-Li Lin, Shun-Chih King, Shu-Yii Wu, Low-level CO in hydrogen-rich gas supplied by a methanol processor for PEMFCs, Chem. Eng. Sci. (ISSN: 00092509) 66 (21) (2011) 5095–5106, http://dx.doi.org/10.1016/j.ces.2011.07.002, URL: https://linkinghub.elsevier.com/retrieve/pii/S0009250911004623. (Visited on 07 August 2024).

[86] Tony Thampan, Rick Rocheleau, Keith Bethune, Douglas Wheeler, Effect of trace contaminants on PEM fuel cell performance, MRS Proc. 885 (2005) 0885–A01–05, http://dx.doi.org/10.1557/PROC-0885-A01-05, ISSN: 1946-4274. URL: http://link.springer.com/10.1557/PROC-0885-A01-05. (Visited on 23 May 2024).

[87] N. Rajalakshmi, T.T. Jayanth, K.S. Dhathathreyan, Effect of carbon dioxide and ammonia on polymer electrolyte membrane fuel cell stack performance, Fuel Cells 3 (4) (2003) 177–180, http://dx.doi.org/10.1002/fuce.200330107, ISSN: 1615-6854. URL: https://onlinelibrary.wiley.com/doi/10.1002/fuce.200330107. (Visited on 07 August 2024).

[88] Velia Fabiola Valdés-López, Tom Mason, Paul R. Shearing, Dan J.L. Brett, Carbon monoxide poisoning and mitigation strategies for polymer electrolyte membrane fuel cells – A review, Prog. Energy Combust. Sci. (ISSN: 03601285) 79 (2020) 100842, http://dx.doi.org/10.1016/j.pecs.2020.100842, URL: https://linkinghub.elsevier.com/retrieve/pii/S036012851930156X. (Visited on 13 January 2023).

[89] James M. Ohi, Nicholas Vanderborgh, Gerald Voecks Consultants, Shabbir Ahmed, Romesh Kumar, Dennis Papadius, Tommy Rockward, Hydrogen Fuel Quality Specifications for Polymer Electrolyte Fuel Cells in Road Vehicles - Report to the Safety, Codes and Standards Program, Tech. Rep., U.S. Department of Energy, 2016, URL: https://www.energy.gov/sites/prod/files/2016/11/f34/fcto_h2_fuel_quality_specs_pem_fc_road_vehicles.pdf.

[90] Zhigang Qi, Chunzhi He, Arthur Kaufman, Effect of CO in the anode fuel on the performance of PEM fuel cell cathode, J. Power Sources (ISSN: 03787753) 111 (2) (2002) 239–247, http://dx.doi.org/10.1016/S0378-7753(02)00300-2, URL: https://linkinghub.elsevier.com/retrieve/pii/S0378775302003002. (Visited on 31 August 2024).

[91] Peter Reithuber, Florian Poimer, Stefan Brandstätter, Eberhard Schutting, Simon Buchberger, Alexander Trattner, Helmut Eichlseder, Experimental investigation of the influence of NO on a PEM fuel cell system and voltage recovery strategies, Energies (ISSN: 1996-1073) 16 (9) (2023) 3720, http://dx.doi.org/10.3390/en16093720, URL: https://www.mdpi.com/1996-1073/16/9/3720. (Visited on 04 May 2023).

[92] Anja Talke, Ulrich Misz, Gerhard Konrad, Angelika Heinzel, Influence of nitrogen compounds on PEMFC: A comparative study, J. Electrochem. Soc. 165 (6) (2018) F3111–F3117, http://dx.doi.org/10.1149/2.0181806jes, ISSN:1945-7111. URL: https://iopscience.iop.org/article/10.1149/2.0181806jes. (Visited on 09 October 2023).

[93] Fenning Jing, Ming Hou, Weiyu Shi, Jie Fu, Hongmei Yu, Pingwen Ming, Baolian Yi, The effect of ambient contamination on PEMFC performance, J. Power Sources (ISSN: 03787753) 166 (1) (2007) 172–176, http://dx.doi.org/10.1016/j.jpowsour.2006.12.103, URL: https://linkinghub.elsevier.com/retrieve/pii/S0378775307001139. (Visited on 26 January 2023).

[94] Xiaofeng Wang, Phillip Baker, Xiaoyu Zhang, Hector F. Garces, Leonard J. Bonville, Ugur Pasaogullari, Trent M. Molter, An experimental overview of the effects of hydrogen impurities on polymer electrolyte membrane fuel cell performance, Int. J. Hydrog. Energy (ISSN: 1879-3487) 39 (34) (2014) 19701–19713, http://dx.doi.org/10.1016/j.ijhydene.2014.09.151, URL: https://linkinghub.elsevier.com/retrieve/pii/S0360319914027463. (Visited on 23 May 2024).

[95] Jean St-Pierre, Yunfeng Zhai, Michael S. Angelo, Effect of selected airborne contaminants on PEMFC performance, J. Electrochem. Soc. 161 (3) (2014) F280–F290, http://dx.doi.org/10.1149/2.057403jes, ISSN: 1945-7111. URL: https://iopscience.iop.org/article/10.1149/2.057403jes. (Visited on 23 May 2024).

[96] Jean St-Pierre, Yunfeng Zhai, Impact of the cathode pt loading on PEMFC contamination by several airborne contaminants, Molecules (ISSN: 1420-3049) 25 (5) (2020) 1060, http://dx.doi.org/10.3390/molecules25051060, URL: https://www.mdpi.com/1420-3049/25/5/1060. (Visited on 22 May 2024).

[97] Gerrit De Leeuw, Edgar L. Andreas, Magdalena D. Anguelova, C.W. Fairall, Ernie R. Lewis, Colin O'Dowd, Michael Schulz, Stephen E. Schwartz, Production flux of sea spray aerosol, Rev. Geophys. (ISSN: 8755-1209) 49 (2) (2011) RG2001, http://dx.doi.org/10.1029/2010RG000349, URL: http://doi.wiley.com/10.1029/2010RG000349. (Visited on 01 May 2023).

[98] Ernie Lewis, R., Stephen E. Schwartz, Sea Salt Aerosol Production: Mechanisms, Methods, Measurements, and Models, Washington, DC, ISBN: 0-87590-417-3, 2004, URL: https://books.google.nl/books?hl=nl&lr=&id=AEIo8ebgw00C&oi=fnd&pg=PR9&dq=Sea+Salt+Aerosol+Production:+Mechanisms,+Methods,+Measurements+and+Models%E2%80%94A+Critical+Review,+Geophys.+Monogr.+Ser.,+vol.+152,+413+pp.,+AGU,+Washington,+D.+C&ots=eP3r_gcRf2&sig=cUdtGSrCfgul-ceZCrXieCIVetI&redir_esc=y#v=onepage&q&f=false.

[99] Lenntech, Composition of seawater, Lenntech Water Treat. Solutions (2023) URL: https://www.lenntech.com/composition-seawater.htm.

[100] Suguru Uemura, Munetoshi Yamazki, Toshihiko Yoshida, Ting-Chu Jao, Shuichiro Hirai, Performance degradation of PEMFC by sea salt aerosol contamination, ECS Trans. 80 (8) (2017) 651–655, http://dx.doi.org/10.1149/08008.0651ecst, ISSN: 9781607688259, Number: 8 Publisher: The Electrochemical Society.

[101] Sunjin Park, Diana Shorova, Hansung Kim, Effect of operating cell voltage on the NaCl poisoning mechanism in polymer electrolyte membrane fuel cells, J. Power Sources (ISSN: 03787753) 538 (2022) 231590, http://dx.doi.org/10.1016/j.jpowsour.2022.231590, URL: https://linkinghub.elsevier.com/retrieve/pii/S0378775322005936. (Visited on 26 July 2022).

[102] B. Viswanath Sasank, N. Rajalakshmi, K.S. Dhathathreyan, Performance analysis of polymer electrolyte membrane (PEM) fuel cell stack operated under marine environmental conditions, J. Mar. Sci. Technol. 21 (3) (2016) 471–478, http://dx.doi.org/10.1007/s00773-016-0369-y, ISSN: 1437-8213. Number: 3. URL: http://link.springer.com/10.1007/s00773-016-0369-y. (Visited on 26 July 2022).

[103] Jin-Long Cui, Zhen-Dong Yao, Yong-Fu Cui, Fu-Peng Cheng, Ting Xiao, Hong-Liang Sun, Ru-Jin Tian, Jun-Cai Sun, Electrochemical properties of tungsten-alloying-modified AISI 430 stainless steel as bipolar plates for PEMFCs used in marine environment, Acta Met. Sin. (Engl. Letters) 29 (10) (2016) 920–927, http://dx.doi.org/10.1007/s40195-016-0464-4, ISSN: 2194-1289. Number: 10. URL: http://link.springer.com/10.1007/s40195-016-0464-4. (Visited on 26 July 2022).

[104] Syed Talat Ali, Qingfeng Li, Chao Pan, Jens Oluf Jensen, Lars Pleth Nielsen, Per Møller, Effect of chloride impurities on the performance and durability of polybenzimidazole-based high temperature proton exchange membrane fuel cells, Int. J. Hydrog. Energy (ISSN: 03603199) 36 (2) (2011) 1628–1636, http://dx.doi.org/10.1016/j.ijhydene.2010.10.076, URL: https://linkinghub.elsevier.com/retrieve/pii/S0360319910021841. (Visited on 27 October 2022).

[105] Hui Li, Haijiang Wang, Weimin Qian, Shengsheng Zhang, Silvia Wessel, Tommy T.H. Cheng, Jun Shen, Shaohong Wu, Chloride contamination effects on proton exchange membrane fuel cell performance and durability, J. Power Sources (ISSN: 03787753) 196 (15) (2011) 6249–6255, http://dx.doi.org/10.1016/j.jpowsour.2011.04.018, URL: https://linkinghub.elsevier.com/retrieve/pii/S0378775311008056. (Visited on 27 October 2022).

[106] Alfred Lam, Hui Li, Shengsheng Zhang, Haijiang Wang, David P. Wilkinson, Silvia Wessel, Tommy T.H. Cheng, Ex situ study of chloride contamination on carbon supported Pt catalyst, J. Power Sources (ISSN: 0378-7753) 205 (2012) 235–238, http://dx.doi.org/10.1016/j.jpowsour.2012.01.063, URL: https://www.sciencedirect.com/science/article/pii/S0378775312001620. (Visited on 01 August 2022).

[107] Dharmjeet Madhav, Changyuan Shao, Jorben Mus, Frank Buysschaert, Veerle Vandeginste, The effect of salty environments on the degradation behavior and mechanical properties of nafion membranes, Energies (ISSN: 1996-1073) 16 (5) (2023) 2256, http://dx.doi.org/10.3390/en16052256, URL: https://www.mdpi.com/1996-1073/16/5/2256. (Visited on 03 April 2023).

[108] Koji Matsuoka, Shigeru Sakamoto, Kunihiro Nakato, Akira Hamada, Yasuhiko Itoh, Degradation of polymer electrolyte fuel cells under the existence of anion species, J. Power Sources (ISSN: 03787753) 179 (2) (2008) 560–565, http://dx.doi.org/10.1016/j.jpowsour.2008.01.027, URL: https://linkinghub.elsevier.com/retrieve/pii/S0378775308000979. (Visited on 27 October 2022).

[109] Hironori Nakajima, Tatsumi Kitahara, Kenta Dan, Electrochemical impedance diagnosis of abnormal operational conditions for reliability of polymer electrolyte fuel cells in marine power application -sea salt contamination-, ECS Trans. 92 (8) (2019) 341–349, http://dx.doi.org/10.1149/09208.0341ecst, ISSN: 1938-6737. URL: https://iopscience.iop.org/article/10.1149/09208.0341ecst. (Visited on 10 February 2023).

[110] T.J. Schmidt, U.A. Paulus, H.A. Gasteiger, R.J. Behm, The oxygen reduction reaction on a Pt/carbon fuel cell catalyst in the presence of chloride anions, J. Electroanal. Chem. (ISSN: 0022-0728) 508 (1–2) (2001) 41–47, http://dx.doi.org/10.1016/S0022-0728(01)00499-5, Number: 1-2.

[111] Andrew J. Steinbach, Clayton V. Hamilton, Mark K. Debe, Impact of micromolar concentrations of externally-provided chloride and sulfide contaminants on PEMFC reversible stability, ECS Trans. 11 (1) (2007) 889–902, http://dx.doi.org/10.1149/1.2781001, ISSN: 1938-6737. URL: https://iopscience.iop.org/article/10.1149/1.2781001. (Visited on 27 October 2022).

[112] Aleš Paulu, Jan Matuštík, Tatiana Trecáková, Vladimír Kočí, Overlooked source of hydrogen: The environmental potential of chlor-alkali by-product, Int. J. Hydrog. Energy (ISSN: 03603199) 49 (2024) 1437–1443, http://dx.doi.org/10.1016/j.ijhydene.2023.10.246, URL: https://linkinghub.elsevier.com/retrieve/pii/S0360319923053946. (Visited on 31 July 2024).

[113] Johan Tallgren, Jari Ihonen, Humidifier characterisation report, 2018, Deliverable 3.1. URL: https://projectsites.vtt.fi/sites/maranda/files/Deliverable_3_1.pdf.

[114] Olga A. Baturina, Albert Epshteyn, Paul A. Northrup, Karen E. Swider-Lyons, Insights into PEMFC performance degradation from HCl in air, J. Electrochem. Soc. (ISSN: 00134651) 158 (10) (2011) B1198, http://dx.doi.org/10.1149/1.3621318, URL: https://iopscience.iop.org/article/10.1149/1.3621318. (Visited on 11 April 2024).

[115] Olga A. Baturina, Albert Epshteyn, Paul Northrup, Karen E. Swider-Lyons, The influence of cell voltage on the performance of a PEM fuel cell in the presence of HCl in air, J. Electrochem. Soc. 161 (4) (2014) F365–F372, http://dx.doi.org/10.1149/2.105403jes, ISSN: 1945-7111. URL: https://iopscience.iop.org/article/10.1149/2.105403jes. (Visited on 17 February 2023).

[116] Zixuan Wang, Chasen Tongsh, Bowen Wang, Zhi Liu, Qing Du, Kui Jiao, Operation characteristics of open-cathode proton exchange membrane fuel cell with different cathode flow fields, Sustain. Energy Technol. Assessments (ISSN: 22131388) 49 (2022) 101681, http://dx.doi.org/10.1016/j.seta.2021.101681, URL: https://linkinghub.elsevier.com/retrieve/pii/S2213138821006950. (Visited on 05 August 2024).

[117] Xiao-Zi Yuan, Hui Li, Yi Yu, Max Jiang, Weimin Qian, Shengsheng Zhang, Haijiang Wang, Silvia Wessel, Tommy T.H. Cheng, Diagnosis of contamination introduced by ammonia at the cathode in a polymer electrolyte membrane fuel cell, Int. J. Hydrog. Energy (ISSN: 03603199) 37 (17) (2012) 12464–12473, http://dx.doi.org/10.1016/j.ijhydene.2012.05.125, URL: https://linkinghub.elsevier.com/retrieve/pii/S0360319912012682. (Visited on 13 January 2023).

[118] Xiaoyu Zhang, Ugur Pasaogullari, Trent Molter, Influence of ammonia on membrane-electrode assemblies in polymer electrolyte fuel cells, Int. J. Hydrog. Energy (2009) http://dx.doi.org/10.1016/j.ijhydene.2009.08.099.

[119] Miklos Czaun, Jotheeswari Kothandaraman, Alain Goeppert, Bo Yang, Samuel Greenberg, Robert B. May, George A. Olah, G.K. Surya Prakash, Iridium-catalyzed continuous hydrogen generation from formic acid and its subsequent utilization in a fuel cell: Toward a carbon neutral chemical energy storage, ACS Catal. (ISSN: 2155-5435, 2155-5435) 6 (11) (2016) 7475–7484, http://dx.doi.org/10.1021/acscatal.6b01605, URL: https://pubs.acs.org/doi/10.1021/acscatal.6b01605. (Visited on 08 August 2024).

[120] Xiaoyu Zhang, Hugo M. Galindo, Hector F. Garces, Philip Baker, Xiaofeng Wang, Ugur Pasaogullari, Steven L. Suib, Trent Molter, Influence of formic acid impurity on proton exchange membrane fuel cell performance, J. Electrochem. Soc. 157 (3) (2010).

[121] Michael J. Kelly, Günter Fafilek, Jürgen O. Besenhard, Hermann Kronberger, Gerhard E. Nauer, Contaminant absorption and conductivity in polymer electrolyte membranes, J. Power Sources (ISSN: 03787753) 145 (2) (2005) 249–252, http://dx.doi.org/10.1016/j.jpowsour.2005.01.064, URL: https://linkinghub.elsevier.com/retrieve/pii/S0378775305003046. (Visited on 22 April 2024).

[122] Steffen Henrik Frensch, Guillaume Serre, Frédéric Fouda-Onana, Henriette Casper Jensen, Morten Lykkegaard Christensen, Samuel Simon Araya, Søren Knudsen Kær, Impact of iron and hydrogen peroxide on membrane degradation for polymer electrolyte membrane water electrolysis: Computational and experimental investigation on fluoride emission, J. Power Sources 420 (February) (2019) 54–62, http://dx.doi.org/10.1016/j.jpowsour.2019.02.076, Number: February.

[123] F. Fouda-Onana, M. Chandesris, V. Médeau, S. Chelghoum, D. Thoby, N. Guillet, Investigation on the degradation of MEAs for PEM water electrolysers part I: Effects of testing conditions on MEA performances and membrane properties, Int. J. Hydrog. Energy 41 (38) (2016) 16627–16636, http://dx.doi.org/10.1016/j.ijhydene.2016.07.125, Number: 38.

[124] Vo Dinh Cong Tinh, Dukjoon Kim, Enhancement of oxidative stability of PEM fuel cell by introduction of HO• radical scavenger in Nafion ionomer, J. Membr. Sci. 613 (May) (2020) 118517, http://dx.doi.org/10.1016/j.memsci.2020.118517, Number: May Publisher: Elsevier B.V..

[125] Grace Amadi, Graham Smith, Edward Brightman, Detection and degradation of pinhole defects in polymer electrolyte fuel cells (A0516), in: A-Session Proceedings 27th EFCF: Low-Temperature Electrolyzers, Fuel Cells and H2 Processing, EFCF, Luzern, Switzerland, 2023, pp. 208–214.

[126] R. Mohtadi, W.-k. Lee, J.W. Van Zee, Assessing durability of cathodes exposed to common air impurities, J. Power Sources (ISSN: 0378-7753) 138 (1) (2004) 216–225, http://dx.doi.org/10.1016/j.jpowsour.2004.06.036, Number: 1. URL: https://www.sciencedirect.com/science/article/pii/S0378775304006913. (Visited on 27 July 2022).

[127] Charles Lorenzo, David Bouquain, Samuel Hibon, Daniel Hissel, Synthesis of degradation mechanisms and of their impacts on degradation rates on proton-exchange membrane fuel cells and lithium-ion nickel–manganese–cobalt batteries in hybrid transport applications, Reliab. Eng. Syst. Saf. (ISSN: 09518320) 212 (2021) 107369, http://dx.doi.org/10.1016/j.ress.2020.107369, URL: https://linkinghub.elsevier.com/retrieve/pii/S0951832020308589. (Visited on 10 October 2023).

[128] Zunyan Hu, Liangfei Xu, Jianqiu Li, Minggao Ouyang, Ziyou Song, Haiyan Huang, A reconstructed fuel cell life-prediction model for a fuel cell hybrid city bus, Energy Convers. Manage. (ISSN: 01968904) 156 (2018) 723–732, http://dx.doi.org/10.1016/j.enconman.2017.11.069, URL: https://linkinghub.elsevier.com/retrieve/pii/S0196890417311214. (Visited on 26 July 2022).

[129] R. Mukundan, G. James, J. Davey, D. Langlois, D. Torraco, W. Yoon, A.Z. Weber, R.L. Borup, Accelerated testing validation, 41, 2011, pp. 613–619, http://dx.doi.org/10.1149/1.3635594, Issue: 1.

[130] R.K. Ahluwalia, X. Wang, J.-K. Peng, V. Konduru, S. Arisetty, N. Ramaswamy, S. Kumaraguru, Achieving 5,000-h and 8,000-h low-PGM electrode durability on automotive drive cycles, J. Electrochem. Soc. 168 (4) (2021) 044518, http://dx.doi.org/10.1149/1945-7111/abf507, ISSN: 1945-7111. Number: 4. URL: https://iopscience.iop.org/article/10.1149/1945-7111/abf507. (Visited on 26 July 2022).

[131] Tim Lochner, Laurens Hallitzky, Markus Perchthaler, Michael Obermaier, Jarek Sabawa, Simon Enz, Aliaksandr S. Bandarenka, Local degradation effects in automotive size membrane electrode assemblies under realistic operating conditions, Appl. Energy 260 (November 2019) (2020) 114291, http://dx.doi.org/10.1016/j.apenergy.2019.114291, Number: November 2019 Publisher: Elsevier.

[132] Paul Thiele, Yue Yang, Steffen Dirkes, Maximilian Wick, Stefan Pischinger, Realistic accelerated stress tests for PEM fuel cells: Test procedure development based on standardized automotive driving cycles, Int. J. Hydrog. Energy (ISSN: 03603199) 52 (2024) 1065–1080, http://dx.doi.org/10.1016/j.ijhydene.2023.08.292, URL: https://linkinghub.elsevier.com/retrieve/pii/S0360319923044853. (Visited on 12 February 2024).

[133] Xinfeng Zhang, Daijun Yang, Minghui Luo, Zuomin Dong, Load profile based empirical model for the lifetime prediction of an automotive PEM fuel cell, Int. J. Hydrog. Energy (ISSN: 03603199) 42 (16) (2017) 11868–11878, http://dx.doi.org/10.1016/j.ijhydene.2017.02.146, URL: https://linkinghub.elsevier.com/retrieve/pii/S0360319917307139. (Visited on 15 April 2024).

[134] C. Dall'Armi, D. Pivetta, R. Taccani, Uncertainty analysis of the optimal health-conscious operation of a hybrid PEMFC coastal ferry, Int. J. Hydrog. Energy (ISSN: 03603199) 47 (21) (2022) 11428–11440, http://dx.doi.org/10.1016/j.ijhydene.2021.10.271, URL: https://linkinghub.elsevier.com/retrieve/pii/S0360319921043810. (Visited on 17 February 2023).

[135] Peng Wu, Richard Bucknall, Hybrid fuel cell and battery propulsion system modelling and multi-objective optimisation for a coastal ferry, Int. J. Hydrog. Energy (ISSN: 03603199) 45 (4) (2020) 3193–3208, http://dx.doi.org/10.1016/j.ijhydene.2019.11.152, URL: https://linkinghub.elsevier.com/retrieve/pii/S0360319919343757. (Visited on 12 April 2024).

[136] Guangjin Wang, Fei Huang, Yi Yu, Sheng Wen, Zhengkai Tu, Degradation behavior of a proton exchange membrane fuel cell stack under dynamic cycles between idling and rated condition, Int. J. Hydrog. Energy (ISSN: 03603199) 43 (9) (2018) 4471–4481, http://dx.doi.org/10.1016/j.ijhydene.2018.01.020, URL: https://linkinghub.elsevier.com/retrieve/pii/S0360319918300557. (Visited on 11 October 2023).

[137] Atsushi Ohma, Shinji Yamamoto, Kazuhiko Shinohara, Membrane degradation mechanism during open-circuit voltage hold test, J. Power Sources (ISSN: 03787753) 182 (1) (2008) 39–47, http://dx.doi.org/10.1016/j.jpowsour.2008.03.078, URL: https://linkinghub.elsevier.com/retrieve/pii/S0378775308006319. (Visited on 15 April 2024).

[138] Ka Hung Wong, Erik Kjeang, Mitigation of chemical membrane degradation in fuel cells: Understanding the effect of cell voltage and iron ion redox cycle, ChemSusChem (ISSN: 18645631) 8 (6) (2015) 1072–1082, http://dx.doi.org/10.1002/cssc.201402957, URL: https://onlinelibrary.wiley.com/doi/10.1002/cssc.201402957. (Visited on 06 February 2023).

[139] Phi Manh Ngo, Hironori Nakajima, Takahiro Karimata, Tomoko Saitou, Kohei Ito, Investigation of in-situ catalytic combustion in polymer-electrolyte-membrane fuel cell during combined chemical and mechanical stress test, J. Power Sources (ISSN: 03787753) 542 (2022) 231803, http://dx.doi.org/10.1016/j.jpowsour.2022.231803, URL: https://linkinghub.elsevier.com/retrieve/pii/S0378775322007935. (Visited on 09 August 2024).

[140] Minoru Inaba, Taro Kinumoto, Masayuki Kiriake, Ryota Umebayashi, Akimasa Tasaka, Zempachi Ogumi, Gas crossover and membrane degradation in polymer electrolyte fuel cells, Electrochim. Acta (ISSN: 00134686) 51 (26) (2006) 5746–5753, http://dx.doi.org/10.1016/j.electacta.2006.03.008, URL: https://linkinghub.elsevier.com/retrieve/pii/S0013468606002271. (Visited on 09 August 2024).

[141] Preethy Parthasarathy, Anil V. Virkar, Electrochemical Ostwald ripening of Pt and Ag catalysts supported on carbon, J. Power Sources (ISSN: 0378-7753) 234 (2013) 82–90, http://dx.doi.org/10.1016/j.jpowsour.2013.01.115, URL: https://www.sciencedirect.com/science/article/pii/S0378775313001729. (Visited on 10 August 2022).

[142] Kazuaki Yasuda, Akira Taniguchi, Tomoki Akita, Tsutomu Ioroi, Zyun Siroma, Platinum dissolution and deposition in the polymer electrolyte membrane of a PEM fuel cell as studied by potential cycling, Phys. Chem. Chem. Phys. 8 (6) (2005) 746–752, http://dx.doi.org/10.1039/B514342J, ISSN: 1463-9084. URL: http://xlink.rsc.org/?DOI=B514342J. (Visited on 07 February 2023).

[143] Kazuaki Yasuda, Akira Taniguchi, Tomoki Akita, Tsutomu Ioroi, Zyun Siroma, Characteristics of a platinum black catalyst layer with regard to platinum dissolution phenomena in a membrane electrode assembly, J. Electrochem. Soc. (ISSN: 00134651) 153 (8) (2006) A1599, http://dx.doi.org/10.1149/1.2210590, URL: https://iopscience.iop.org/article/10.1149/1.2210590. (Visited on 07 February 2023).

[144] Pucheng Pei, Huicui Chen, Main factors affecting the lifetime of proton exchange membrane fuel cells in vehicle applications: A review, Appl. Energy (ISSN: 03062619) 125 (2014) 60–75, http://dx.doi.org/10.1016/j.apenergy.2014.03.048, URL: https://linkinghub.elsevier.com/retrieve/pii/S0306261914002797. (Visited on 03 January 2023).

[145] Tom Fletcher, Rob Thring, Martin Watkinson, An energy management strategy to concurrently optimise fuel consumption & PEM fuel cell lifetime in a hybrid vehicle, Int. J. Hydrog. Energy (ISSN: 03603199) 41 (46) (2016) 21503–21515, http://dx.doi.org/10.1016/j.ijhydene.2016.08.157, URL: https://linkinghub.elsevier.com/retrieve/pii/S0360319916325435. (Visited on 12 October 2022).

[146] Paul T. Yu, Zhongyi Liu, Rohit Makharia, Investigation of carbon corrosion behavior and kinetics in proton exchange membrane fuel cell cathode electrodes, J. Electrochem. Soc. (ISSN: 1945-7111) 160 (6) (2013) F645–F650, http://dx.doi.org/10.1149/2.120306jes, URL: https://iopscience.iop.org/article/10.1149/2.120306jes. (Visited on 05 February 2023).

[147] A.P. Young, J. Stumper, E. Gyenge, Characterizing the structural degradation in a PEMFC cathode catalyst layer: Carbon corrosion, J. Electrochem. Soc. (ISSN: 00134651) 156 (8) (2009) B913, http://dx.doi.org/10.1149/1.3139963, URL: https://iopscience.iop.org/article/10.1149/1.3139963. (Visited on 17 April 2024).

[148] Wensheng He, Guangyu Lin, Trung Van Nguyen, Diagnostic tool to detect electrode flooding in proton-exchange-membrane fuel cells, AIChE J. 49 (12) (2003) 3221–3228, http://dx.doi.org/10.1002/aic.690491221, ISSN: 15475905. URL: https://onlinelibrary.wiley.com/doi/10.1002/aic.690491221. (Visited on 09 October 2023).

[149] Wolfgang Schmittinger, Ardalan Vahidi, A review of the main parameters influencing long-term performance and durability of PEM fuel cells, J. Power Sources (ISSN: 03787753) 180 (1) (2008) 1–14, http://dx.doi.org/10.1016/j.jpowsour.2008.01.070, URL: https://linkinghub.elsevier.com/retrieve/pii/S0378775308001924. (Visited on 18 September 2023).

[150] Jarek P. Sabawa, Aliaksandr S. Bandarenka, Investigation of degradation mechanisms in PEM fuel cells caused by low-temperature cycles, Int. J. Hydrog. Energy (xxxx) (2021) http://dx.doi.org/10.1016/j.ijhydene.2021.02.088, Number: xxxx Publisher: Elsevier Ltd.

[151] Hendrik Schulenburg, Bernhard Schwanitz, Nicolas Linse, Günther G. Scherer, A. Wokaun, Julijana Krbanjevic, Roman Grothausmann, Ingo Manke, 3D imaging of catalyst support corrosion in polymer electrolyte fuel cells, J. Phys. Chem. C 115 (29) (2011) 14236–14243, http://dx.doi.org/10.1021/jp203016u, ISSN: 1932-7455. URL: https://pubs.acs.org/doi/10.1021/jp203016u. (Visited on 27 November 2023).

[152] Kah-Young Song, Hee-Tak Kim, Effect of air purging and dry operation on durability of PEMFC under freeze/thaw cycles, Int. J. Hydrog. Energy (ISSN: 03603199) 36 (19) (2011) 12417–12426, http://dx.doi.org/10.1016/j.ijhydene.2011.06.095, URL: https://linkinghub.elsevier.com/retrieve/pii/S0360319911015679. (Visited on 05 February 2023).

[153] Sang-Yeop Lee, Hyoung-Juhn Kim, EunAe Cho, Kug-Seung Lee, Tae-Hoon Lim, In Chul Hwang, Jong Hyun Jang, Performance degradation and microstructure changes in freeze–thaw cycling for PEMFC MEAs with various initial microstructures, Int. J. Hydrog. Energy (ISSN: 03603199) 35 (23) (2010) 12888–12896, http://dx.doi.org/10.1016/j.ijhydene.2010.08.070, URL: https://linkinghub.elsevier.com/retrieve/pii/S036031991001709X. (Visited on 05 February 2023).

[154] Dominik Bentele, Kerem Aylar, Katja Olsen, Elias Klemm, Sebastian Harald Eberhardt, PEMFC anode durability: Innovative characterization methods and further insights on OER based reversal tolerance, J. Electrochem. Soc. 168 (2) (2021) http://dx.doi.org/10.1149/1945-7111/abe50b, Number: 2 Publisher: IOP Publishing.

[155] A. Taniguchi, T. Akita, K. Yasuda, Y. Miyazaki, Analysis of degradation in PEMFC caused by cell reversal during air starvation, Int. J. Hydrog. Energy (ISSN: 03603199) 33 (9) (2008) 2323–2329, http://dx.doi.org/10.1016/j.ijhydene.2008.02.049, URL: https://linkinghub.elsevier.com/retrieve/pii/S0360319908002267. (Visited on 06 February 2023).

[156] M. Bodner, A. Schenk, D. Salaberger, M. Rami, C. Hochenauer, V. Hacker, Air starvation induced degradation in polymer electrolyte fuel cells, Fuel Cells 17 (1) (2017) 18–26, http://dx.doi.org/10.1002/fuce.201600132, ISSN: 1615-6854. URL: https://onlinelibrary.wiley.com/doi/10.1002/fuce.201600132. (Visited on 03 May 2024).

[157] Lloyd's Register, Performance and Environmental Test Specification for the following Environmentally Tested Products used in Marine Applications, (1) Loyd's Register, London, 2021, p. 27.

[158] J. S. Carlton, D. Vlasic, Lloyd's Register, Ship Vibration and Noise: Some Topical Aspects, London, UK, 2005.

[159] Apostolos Grammatikopoulos, Complexe Belastingen En Trilllingen (Complex Loads and Vibrations), Delft University of Technology, 2024, URL: https://brightspace-cc.tudelft.nl/course/23848/mt3433-complexe-belastingen-en-trillingen-202324-q3.

[160] Marco Biot, Francesco De Lorenzo, Noise and Vibrations on Board Cruise Ships: Are New standards Effective?, Ischia (Naples), 2007.

[161] Kaspar Andreas Friedrich, Josef Kallo, Johannes Schirmer, Gerrit Schmitthals, Fuel cell systems for aircraft application, ECS Trans. 25 (1) (2009) 193–202, http://dx.doi.org/10.1149/1.3210571, ISSN: 1938-6737. URL: https://iopscience.iop.org/article/10.1149/1.3210571. (Visited on 16 February 2023).

[162] Salah H. El-Emam, Ahmed A. Mousa, Mahmoud M. Awad, Effects of stack orientation and vibration on the performance of PEM fuel cell, Int. J. Energy Res. 39 (2015) 75–83, http://dx.doi.org/10.1002/er.3217, URL: https://onlinelibrary.wiley.com/doi/epdf/10.1002/er.3217.

[163] B.N. Van Veldhuizen, E. Zera, L. Van Biert, S. Modena, K. Visser, P.V. Aravind, Experimental evaluation of a solid oxide fuel cell system exposed to inclinations and accelerations by ship motions, J. Power Sources (ISSN: 03787753) 585 (2023) 233634, http://dx.doi.org/10.1016/j.jpowsour.2023.233634, URL: https://linkinghub.elsevier.com/retrieve/pii/S0378775323010108. (Visited on 07 October 2024).

[164] Roshanak Banan, Aimy Bazylak, Jean Zu, Effect of mechanical vibrations on damage propagation in polymer electrolyte membrane fuel cells, Int. J. Hydrog. Energy (ISSN: 0360-3199) 38 (34) (2013) 14764–14772, http://dx.doi.org/10.1016/j.ijhydene.2013.08.136, URL: https://www.sciencedirect.com/science/article/pii/S0360319913021812. (Visited on 08 August 2022).

[165] Roshanak Banan, Aimy Bazylak, Jean Zu, Combined effects of environmental vibrations and hygrothermal fatigue on mechanical damage in PEM fuel cells, Int. J. Hydrog. Energy (ISSN: 0360-3199) 40 (4) (2015) 1911–1922, http://dx.doi.org/10.1016/j.ijhydene.2014.11.125, URL: https://www.sciencedirect.com/science/article/pii/S0360319914032595. (Visited on 08 August 2022).

[166] Yang Qiu, Xiaofei Wen, Shengnan Zhou, Zetao Chen, Construction and application of prediction spectrum between PEMFC's performances and ship vibration, in: Journal of Physics: Conference Series, vol. 2044, Nanning, China, 2021, 012119, http://dx.doi.org/10.1088/1742-6596/2044/1/012119, Number: 1. URL: https://iopscience.iop.org/article/10.1088/1742-6596/2044/1/012119. (Visited on 26 July 2022).

[167] Ahmet Çalık, Sefa Yıldırım, Erdi Tosun, Estimation of crack propagation in polymer electrolyte membrane fuel cell under vibration conditions, Int. J. Hydrog. Energy (ISSN: 0360-3199) 42 (36) (2017) 23347–23351, http://dx.doi.org/10.1016/j.ijhydene.2017.02.119, URL: https://www.sciencedirect.com/science/article/pii/S0360319917306304. (Visited on 08 August 2022).